

# Establishment and calibration of consensus process model for nitrous oxide dynamics in water quality engineering

**Domingo-Felez, Carlos**

*Publication date:*
2017

*Document Version*
Publisher's PDF, also known as Version of record

# Establishment and calibration of consensus process model for nitrous oxide dynamics in water quality engineering

Carlos Domingo-Félez

PhD Thesis
June 2017

DTU Environment
Department of Environmental Engineering
Technical University of Denmark

**Carlos Domingo-Félez**

**Establishment and calibration of consensus process model for nitrous oxide dynamics in water quality engineering**

PhD Thesis, June 2017



Address: DTU Environment
Department of Environmental Engineering
Technical University of Denmark
Bygningstorvet, building 113
2800 Kgs. Lyngby
Denmark

Phone reception: +45 4525 1600
Fax: +45 4593 2850

Homepage: http://www.env.dtu.dk
E-mail: reception@env.dtu.dk
Printed by: GraphicCo
June 2017

# Preface

This thesis is based on the work carried out at the Department of Environmental Engineering at the Technical University of Denmark from January 2014 to April 2017. This thesis was prepared as part of the LaGas project (http://www.lagas.dk ). The research was performed under the main supervision of Professor Barth F. Smets (DTU Environment) and co-supervision of Associate Professor Benedek Gy. Plósz (DTU Environment) and Associate Professor Gürkan Sin (DTU Chemical and Biochemical Engineering).

The thesis is organized in two parts: the first part puts into context the findings of the PhD in an introductive review; the second part consists of the papers listed below. These will be referred to in the text by their paper number written with the Roman numerals **I-V**.

**I** **Domingo-Félez, C.**, Pellicer-Nàcher, C., Petersen, M. S., Jensen, M. M., Plósz, B. G., Smets, B.F. 2017. Heterotrophs are key contributors to nitrous oxide production in activated sludge under low C-to-N ratios during nitrification – Batch experiments and modeling. *Biotechnology and Bioengineering*, **114**, 132-140.

**II** **Domingo-Félez, C.**, Smets, B.F. 2016. A consilience model to describe N2O production during biological N removal. *Environmental Science: Water Research and Technology*, **6**, 923-930.

**III** **Domingo-Félez, C.**, Calderó-Pascual, M., Sin, G., Plósz, B. G., Smets, B.F. 2017. Calibration of the comprehensive NDHA-N2O dynamics model for nitrifier-enriched biomass using targeted respirometric assays. *Submitted*

**IV** **Domingo-Félez, C.**, Smets, B.F. 2017. Application of the NDHA model to describe N2O dynamics in activated sludge mixed culture biomass. *Manuscript in preparation*.

**V** **Domingo-Félez, C.**, Smets, B.F. 2017. Modelling electron competition in a mixed denitrifying microbial community with different carbon sources through an electric circuit analogy. *Manuscript in preparation*.

In addition, the following authored or co-authored publications, not included in this thesis, were also concluded during this PhD study:

- **Domingo-Félez, C.**, Mutlu, A. G., Jensen, M. M., Smets, B. F. (2014). Aeration strategies to mitigate nitrous oxide emissions from single-stage nitritation/anammox reactors. *Environmental Science and Technology*. **(48**) 15: 8679-8687.

- Ma, Y., **Domingo-Félez, C.**, Plósz, B. G., Smets, B. F. (*2017*). Suppression of nitrite-oxidizing bacteria in intermittently membrane-aerated biofilms: a model-based explanation. DOI: 10.1021/acs.est.7b00463. *Accepted in Environmental Science and Technology*.

- Su, Q., Ma, C., **Domingo-Félez, C.**, Kiil, A.S., Thamdrup, B., Jensen, M.M., Smets, B. F. (*2017*). Low nitrous oxide production through nitrifier-denitrification in intermittent-feed high-rate high performance nitritation reactors. *Under revision for Water Research*.

- Blum, J. M., Su, Q., Ma, Y., Valverde-Pérez, B., **Domingo-Félez, C.**, Jensen, M. M, Smets, B. F. (*2017*). The pH dependency of N-converting enzymatic processes, pathways and microbes: effect on net-N2O production. *Submitted*.

This PhD study also contributed to international conferences with the following proceeding papers:

- **Domingo-Félez, C.**, Smets, B. F. Critical assessment of a novel $N_2O$ model. N2O Expert Meeting and Workshop. Bochum (Germany). 21$^{st}$ – 22$^{nd}$ September 2016. Oral presentation.
- **Domingo-Félez, C.**, Valverde-Pérez, B., Plósz, B. G., Sin, G., Smets, B. F. Towards an optimal experimental design for N2O model calibration during biological nitrogen removal. 5$^{th}$ IWA/WEF Wastewater Treatment Modelling Seminar (WWTmod2016). Annecy (France). 2$^{nd}$- 6$^{th}$ April 2016. Poster presentation.
- **Domingo-Félez, C.**, Pellicer-Nàcher, C., Petersen, M. S., González-Combarros, R., Jensen, M. M., Sin, G., Smets, B. F. Challenges encountered calibrating $N_2O$ dynamics from mixed cultures. International Conference on Nitrogen (ICON4). Edmonton (Canada). University of Alberta. June 29$^{th}$-July 2$^{nd}$ 2015. Poster presentation.

- **Domingo-Félez, C.**, Plósz, B. G., Sin, G., Smets, B. F. $N_2O$ and NO dynamics in AOB-enriched and mixed-culture biomass: Experimental Observations and Model Calibration. Fifth International Conference on Nitrification and Related Processes (ICoN5). Vienna (Austria). 23-27 July 2017. Accepted Abstract.
- Ma, Y., **Domingo-Félez, C.**, Plósz, B. G., Smets, B. F. Suppression of nitrite-oxidizing bacteria in intermittently aerated biofilm reactors: a model-based explanation. IWA Microbial Ecology in Water Engineering & Biofilms. 4-7th September 2016. Copenhagen (Denmark). Poster presentation.
- Smets, B. F., Pellicer-Nàcher, C., **Domingo-Félez, C.**, Jensen, M. M., Ramin, E., Plósz, B. G., Sin, G., Gernaey, K., V., Modelling $N_2O$ dynamics in the engineered cycle: Evaluation of alternate model structures. Spa (Belgium). 4th IWA/WEF Wastewater Treatment Modelling Seminar. 30 March – 2 April 2014. Poster presentation. Proceedings p. 343-346.
- **Domingo-Félez, C.**, Calderó-Pascual, M., Sin, G., Plósz, B. G., Smets, B. F. Calibration of the NDHA $N_2O$ model via respirometric assays. Frontiers International Conference on Wastewater Treatment. 21-24th May, Palermo (Italy). Poster flash presentation.
- Ma, Y., **Domingo-Félez, C.**, Smets, B. F. $N_2O$ Production in Membrane-aerated Nitrifying Biofilms: Experimentation and Modelling. Frontiers International Conference on Wastewater Treatment. 21-24th May, Palermo (Italy). Poster flash presentation.
- Ma, Y., **Domingo-Félez, C.**, Piscedda, A., Smets, B. F. Investigating Intermittent Aeration in Membrane-Aerated Nitrifying Biofilm Reactors. IWA 10th International Conference on Biofilm Reactors on, Dublin (Ireland) 9-12th May 2017. Oral presentation.
- Morset, M., Valverde-Pérez, B., Blum, J. M., **Domingo-Félez, C.**, Mauricio-Iglesias, M., Smets, B. F. $N_2O$ emissions from a single-stage partial nitritation/anammox granule-based reactor – a model based assessment. IWA 10th International Conference on Biofilm Reactors on, Dublin (Ireland) 9-12th May 2017. Poster presentation.
- Ekström, S., **Domingo-Félez, C.**, Jensen, M. M., Gustavsson, D. J. I., Persson , F., Jansen J. L. C., Smets, B. F. Influence of aeration strategy on $N_2O$ emissions from a pilot-scale mainstream anammox process. NORDIWA 2015 – 14th Nordic Wastewater Conference (November, 2015, Bergen, Norway). Oral presentation.

# Acknowledgements

First, I would like to thank Professor Barth F. Smets for giving me the opportunity to conduct this research and being part of the LaGas project. Also for always being available and offering a hand to climb out of the *well of details*. Thanks to my co-supervisors Associate Professor Benedek Gy Plósz and Associate Professor Gürkan Sin for their help when it was needed and for letting me see things from another perspective. Thanks to everyone involved in the LaGas project, a good example of how to tackle a problem with different approaches.

To everyone in the Metlab group for the very nice work atmosphere. What started as a six-months Erasmus has become a six years long experience. Specially thanks to Carles and Gizem for your enthusiasm and hard work that helped me before I started this PhD. To those who were here when I arrived, or graduated and left, or stayed, or will graduate soon, thanks for the good times inside and outside DTU: Uli, Arda, Katerina, Arnaud, Marlene, Lene, Sara, Marta, Vaibhav, Bas, Jane, Qingxian, Yunjie, Jan, Borja, Alex, Dorka, Fabio, Elena, Elham, Katerina…

To *my* students: Ilias, Rosana, Anne-Sofie, María, Andrea and Martin, thanks for your hard work and for dealing with my, sometimes, excessive rambling about $N_2O$. Thanks also to the students during the TA hours with whom I also learnt and to Mathias and Marlene for the much appreciated help with the Danish translation.

To the cake club, for showing that sometimes a small effort pays off when you need it. To the Friday bar for the much needed breaks, especially when it was not Friday (Carson, Pauly, Flo, Klaus, Pedram, Camilla, Bentje, etc.) and to the rest of friends from Zaragoza, Muniesa, RI, etc.

And of course to my family for their constant support, my parents Dora and Simón, my brother Alberto, my aunt María-José, my grandparents Joaquina, Mariano, Joaquina and Bienvenido.

Be curious and doubt.

# Summary

Research on biological nitrogen removal (BNR) in wastewater treatment plants (WWTP) has historically focused on achieving good effluent quality, with more recent attention to energy savings and carbon dioxide ($CO_2$) footprints. Novel processes and operating conditions are being implemented that enhance cost and energy efficiency in BNR, while maintaining effluent quality. Now, increasing attention is placed on direct emissions of nitrous oxide ($N_2O$) as by-product of BNR; $N_2O$ is a greenhouse gas (GHG) with a high warming potential and also an ozone depleting chemical compound.

Several $N_2O$ production pathways have been identified from pure culture studies, while mechanisms are still being unravelled. Heterotrophic bacteria (HB) and ammonium oxidizing bacteria (AOB) are well known to produce $N_2O$. However, the effect of environmental factors on $N_2O$ production is not yet well understood. Current process modelling efforts aim to reproduce experimental data with mathematical equations, structuring our understanding of the system. Various mechanistic models with different structures describing $N_2O$ production have been proposed, but no consensus exists between researchers. Hence, the existing plant-wide GHG models still lack a complete biological process model that can be integrated in a methodology that assesses $N_2O$ emissions and their impact on overall plant performance.

A mathematical model structure that describes $N_2O$ production during biological nitrogen removal is proposed. Two autotrophic and one heterotrophic biological pathways are coupled with abiotic processes. The model stoichiometry and process rates synthesize a comprehensive literature review on the metabolism of microbes involved in nitrogen removal. The proposed model can describe all relevant NO and $N_2O$ production pathways with fewer parameters than present in other proposed models.

A novel experimental design based on the developed model and on extant respirometric techniques is introduced. Monitoring dissolved oxygen and $N_2O$ allowed the isolation of individual processes and the estimation of parameters associated to oxygen consumption (endogenous activity, nitrite and ammonium oxidation) and $N_2O$ production (NN, ND and HD pathway contributions).

To estimate parameters of the $N_2O$ model a rigorous procedure is presented as a case study. The calibrated model predicts the NO and $N_2O$ dynamics at varying ammonium, nitrite and dissolved oxygen levels in two independent

systems: (a) an AOB-enriched biomass and (b) activated sludge (AS) mixed liquor biomass. A total of ten (a) and seventeen (b) parameters are identified with high accuracy (coefficients of variation < 25%). The critical validation of the model response and the estimated parameter values represent a novel and rigorous tool for $N_2O$ modelling studies. For the first time, uncertainty associated with parameter estimation from $N_2O$ models is reported, this procedure is recommended to be included with best-fit simulations.

Additionally, modelling electron competition in heterotrophic processes is explored via an analogy to current intensity through resistors in electric circuits. While further model validation is required, this approach captured the electron competition during denitrification for four different carbon sources.

Overall, a combination of modelling and experimental efforts to study $N_2O$ dynamics was successfully implemented. Results represent a step forward in the development of consensus process model for $N_2O$ emissions in WQE processes.

# Dansk sammenfatning

Forskning i biologisk kvælstoffjernelse på spildevandsrensningsanlæg har historisk fokuseret på at opnå en god udledningskvalitet, mens opmærksomheden de seneste år er blevet rettet mod energibesparelser og $CO_2$-udslip. Nye processer og driftsforhold, der nedsætter omkostninger og øger energieffektiviteten for biologisk kvælstoffjernelse implementeres samtidig med at udledningskvaliteten fastholdes. Senest er der kommet øget opmærksomhed på direkte emissioner af dinitrogenoxid (N2O), også kaldt lattergas, som er et biprodukt af biologisk kvælstoffjernelse. Lattergas er en drivhusgas med et højt drivhusgaspotentiale og en ozonnedbrydende kemisk forbindelse.

Flere bakterielle processer for lattergasproduktion er blevet identificeret ved hjælp af studier af rene kulturer, mens mekanismerne bag lattergasproduktionen stadig undersøges. Både heterotrofe denitrificerende bakterier og ammoniak-oxiderende bakterier producerer lattergas. Men man ved endnu meget lidt om hvilke faktorer, der regulerer lattergasproduktionen. Igangværende forskning inden for procesmodellering forsøger at reproducere eksperimentelle data med matematiske ligninger og derved strukturere vores forståelse af systemet. Forskellige mekanistiske modeller med forskellige strukturer der beskriver lattergasproduktion har tidligere været foreslået, men der er ingen konsensus imellem forskere. Derfor mangler de eksisterende drivhusgasemissionsmodeller for hele renseanlægget stadig en komplet biologisk procesmodel, som kan integreres på en måde der giver mulighed for at vurdere lattergasemissioner og indvirkningen af disse på den samlede anlægspræstation.

Her foreslås en matematisk modelstruktur, der beskriver lattergasproduktionen under biologisk kvælstoffjernelse. To autotrofe og en heterotrof biologisk reaktionsvej er koblet sammen med abiotiske processer. Modellens støkiometri og reaktionsrater udspringer fra et omfattende litteraturstudie i de mikroorganismers metabolisme, der er involveret i fjernelse af nitrogen. Modellen kan beskrive alle relevante kvælstofoxid- og lattergas-produktionsveje med færre parametre end i tidligere publicerede modeller.

I afhandlingen introduceres også et nyt eksperimentelt design baseret på den udviklede model og på eksisterende respirometriske teknikker. Målinger af opløst oxygen og lattergas gjorde det muligt at isolere individuelle processer og estimering af parametre forbundet med iltforbrug (endogen aktivitet, ni-

trit- og ammonium-oxidation) og lattergasproduktion (bidrag fra NN-, ND- og HD-productionsveje).

For at estimere parametre i lattergas modellerne, fremlægges en stringent procedure som et case study. Den kalibrerede model forudsiger dynamikken af kvæfstofoxid- og lattergas-akkumulering ved forskellige niveauer af ammonium-, nitrit- og opløst oxygen i to uafhængige systemer: (a) en beriget ammoniak-oxiderende biomasse og (b) aktiveret slam biomasse. I alt blev ti (a) og sytten (b) parametre identificeret med høj nøjagtighed (variationskoefficienter <25%). Den kritiske validering af modeludkastet og de estimerede parameterværdier repræsenterer et nyt og stringent redskab til lattergas modelleringsstudier. For første gang rapporteres usikkerheden i forbindelse med parametervurdering fra lattergas-modeller. Det anbefales at tilføje denne fremgangsmetode til best-fit simuleringsprocedurer.

Derudover undersøges modellering af konkurrencen om elektroner imellem de heterotrofe processer analogt til strøm-intensiteten gennem modstande i elektriske kredsløb. Mens yderligere validering af modellen er påkrævet, fangede fremgangsmåden den elektronkonkurrence, der forekommer når denitrificerende bakterier oxiderer fire forskellige kulstofkilder.

Samlet set blev en kombination af modellering og forsøg med formålet at studere N2O-dynamik succesfuldt gennemført. Resultaterne er et skridt fremad i udviklingen af en konsensus procesmodel for lattergasemissioner i ingeniørmæssige vandkvalitets-processer.

# Table of contents

# Abbreviations

| | |
|---|---|
| ACF | Autocorrelation function |
| AMO | Ammonia monooxygenase |
| AOB | Aerobic ammonia oxidizing bacteria |
| AS | Activated sludge |
| ASM | Activated sludge model |
| BNR | Biological nitrogen removal |
| COD | Chemical oxygen demand |
| CV | Coefficient of variation |
| FIM | Fisher information matrix |
| GHG | Greenhouse gas |
| GSA | Global sensitivity analysis |
| HAO | Hydroxylamine oxydoreductase |
| HB | Heterotrophic bacteria |
| HD | Heterotrophic denitrification |
| ICE | Indirect coupling of electrons |
| LHS | Latin hypercube sampling |
| LSA | Local sensitivity analysis |
| MLR | Multiple linear regression |
| NAR | Nitrate reductase |
| ND | Nitrifier denitrification |
| NIR | Nitrite reductase |
| NN | Nitrifier nitrification |
| NOB | Aerobic nitrite oxidizing bacteria |
| NOR | Nitric oxide reductase |
| NOS | Nitrous oxide reductase |
| RMSE | Root mean squared error |
| SMN | Stoichiometric metabolic network |
| SRC | Standardized regression coefficient |
| VSS | Volatile suspended solids |
| WQE | Water quality engineering |
| WWTP | Wastewater treatment plant |
| DO | Dissolved oxygen |
| $HNO_2$ | Free nitrous acid |
| $NH_2OH$ | Hydroxylamine |
| $NH_3$ | Ammonia |
| $NH_4^+$ | Ammonium |
| $N_2$ | Dinitrogen gas |
| NO | Nitric oxide |
| $N_2O$ | Nitrous oxide |
| $NO_2^-$ | Nitrite |
| $NO_3^-$ | Nitrate |
| $NO_x^-$ | Nitrogen oxides |
| $O_2$ | Molecular oxygen |

# 1 Introduction

## 1.1 Background and motivation of the study

Nitrous oxide ($N_2O$) is a stratospheric ozone depleter and a greenhouse gas (GHG), recently identified as the most important threat to the ozone layer of the 21st century (Ravishankara *et al.*, 2009). The global warming potential of $N_2O$ is 300 times higher than that of $CO_2$ due to its long residence time in the atmosphere (Stocker *et al.*, 2013).

In the anthropogenic water cycle $N_2O$ emissions can contribute up to 26% of the GHG footprint (Desloover *et al.*, 2012), and specifically during sewage treatment accounts for 3.2% of the total $N_2O$ global emission rates (Mosier *et al.*, 1999). The objective of wastewater treatment is of sanitary purposes, reducing the number of pathogens present in wastewater. However, still 47% of wastewater produced in manufacturing and domestic sectors is untreated (Stocker *et al.*, 2013). Hence, global $N_2O$ emissions may be enhanced by the increasing wastewater treatment loadings.

The carbon footprint of full-scale wastewater treatment plants (WWTPs) consists of direct emissions of GHG (e.g. methane, nitrous oxide), energy consumption, use of chemicals, etc. The study of Scandinavian municipal WWTPs indicated that the most important contributions corresponded to the direct GHG emissions and energy categories (Gustavsson and Tumlin, 2013). Overall, while energy neutral and energy self-sufficient WWTPs exist (Yan *et al.*, 2017), carbon neutral WWTPs are still lacking in the literature (Gustavsson and Tumlin, 2013).

A high variability in $N_2O$ emissions exists and emission factors are not representative for individual process configurations (Ahn *et al.*, 2010). The impact assessment of $N_2O$ emissions from the nitrogenous liquid waste should be thus addressed at a local level.

Intensive on-site measurements together with accurate measurement protocols have been reported as an alternative to estimate $N_2O$ emissions (Chandran, 2011). Mechanistic models have also been suggested to predict $N_2O$ emissions from plant-wide systems and incorporated during control strategies (Snip *et al.*, 2014). However, poor knowledge of key processes driving $N_2O$ production and lack of consensus on how to model the producing pathways has impeded the implementation of plant-wide GHG models (Desloover *et al.*, 2012). Models have increased their predictive capabilities,

but convergence towards a consilience $N_2O$ model has not been achieved yet (Mannina *et al.*, 2016).

Compared to full-scale systems, the differences in formation mechanisms and kinetics between biomass cultures can be studied in lab-scale reactors or targeted experiments as they offer more controlled environments. Model development can also benefit from recent advances on microbial metabolism and analytical measurements (e.g. pure culture studies, quantification of microbial communities, isotopic portioning, microelectrodes, etc.). Therefore, a better understanding of the biological factors that control $N_2O$ production and consumption will improve the mathematical prediction of new $N_2O$ process models.

Additionally, the high parameter variability of reported $N_2O$ models highlights possible model limitations to address regulation of multiple pathways, microbial population switches, or hydrodynamic heterogeneities (Manser *et al.*, 2005; Spérandio *et al.*, 2016). The confidence of model predictions is critical when comparing the performance of $N_2O$ models during the development of mitigation strategies as the carbon footprint is highly sensitive to $N_2O$ emissions (Gustavsson and Tumlin, 2013). Moreover, as an end-product of nitrogen removal $N_2O$ predictions are greatly affected by the uncertainty of primary N-substrates (e.g. $NH_4^+$, $NO_2^-$, etc.). The quality of the calibration results is commonly addressed in environmental models (Bennett *et al.*, 2013) but has not been studied for $N_2O$ emissions. Hence, rigorous methods for $N_2O$ model response evaluation will benefit model discrimination procedures, and improve mitigation strategies (Belia *et al.*, 2009).

## 1.2 Aim of the thesis

This thesis is embedded in a project (LaGas) that focuses on untangling the factors driving $N_2O$ production from wastewater treatment. LaGas is a multi-disciplinary project in which this thesis aims to contribute by building and validating a consensus mechanistic process model for $N_2O$ dynamics for water quality engineering use. This thesis represents the modelling link between lab-scale stable isotope techniques and intensive full-scale measuring campaigns.

In this thesis, a state-of-the-art overview of the pathways driving $N_2O$ production during BNR is exposed, current $N_2O$ modelling approaches are discussed and a consilience model is proposed. An overview of the research approach followed in this thesis is shown in **Figure 1.1**.

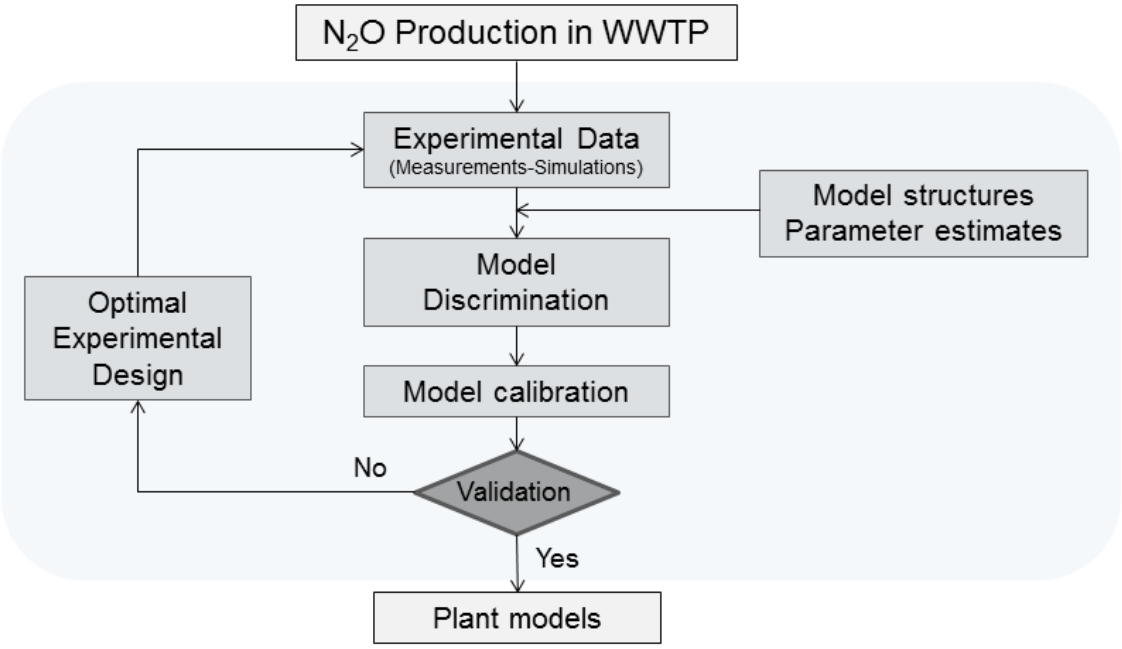


**Figure 1.1.** Overview of the research approach in this thesis.

The objectives of the thesis are:

• Critically review $N_2O$ models to evaluate the prediction accuracy and assess structural limitations. (**Paper I**).

• Develop a consilience $N_2O$ model structure capable of describing the known biological and abiotic pathways relevant for water quality engineering processes (**Paper II**).

• Design of lab-scale experiments to accurately obtain parameters describing $N_2O$ production (**Paper III** and **IV**).

• Validate the estimated model parameters by assessing the model response and the parameter values (**Paper III** and **IV**).

• Analyse the predictive capabilities and precision of validated process models (**Paper III, IV** and **V**).

• Explore a modelling approach that describes electron competition; specifically applied for heterotrophic processes (**Paper V**).

# 2 Nitrous oxide production during biological nitrogen removal

## 2.1 Biological nitrogen removing organisms

The microbiome of wastewater treatment plants is a complex community comprised mostly of bacteria, and to a lesser extent, archaea. A large assumption is that all sewage treatment microbial communities will have roughly similar community compositions. The number of bacteria in activated sludge is estimated to be in the range of 1–10 x $10^{12}$/g VSS (Nielsen and Nielsen, 2002), 80% of which are typically active. Chemoorganoheterotrophs are the most abundant populations in activated sludge, belonging to Alpha-, Beta-, Gamma-, Delta- and Actinobacteria. These microbes are capable of nitrogen removal, iron reduction, sulfate reduction, phosphate and glycogen accumulation, among other functions. In the next sections the microbial communities involved in nitrogen removal as well as the biochemical processes they mediate will be discussed in more detail (**Figure 2.1**).

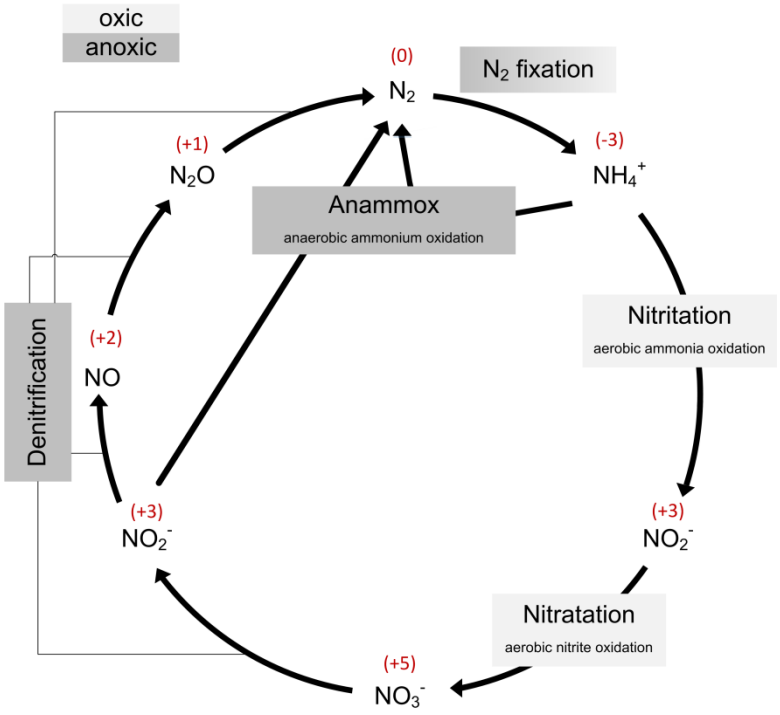


**Figure 2.1.** Simplified nitrogen cycle and relevant biological transformations.

### 2.1.1 Aerobic ammonia oxidizing bacteria

Aerobic ammonia oxidizing bacteria (AOB) are chemolithoautotrophic Proteobacteria (i.e., they use inorganic energy sources). AOB obtain energy from the oxidation of ammonia ($NH_3$) to nitrite ($NO_2^-$) with molecular oxygen ($O_2$) as electron acceptor (**2.1**). The oxidation of $NH_3$ with oxygen to hydroxylamine ($NH_2OH$) is an endergonic process catalysed by the ammonia monooxygenase (AMO) (**2.2**) (Sayavedra-Soto *et al.*, 1996). This step requires two electrons, supplied by the subsequent $NH_2OH$ oxidation to $NO_2^-$, catalysed by the enzyme hydroxylamine oxidoreductase (HAO) (Böttcher and Koops, 1994; de Bruijn *et al.*, 1995) (**Figure 2.2**). $NH_2OH$ oxidation releases four electrons, two sustain $NH_3$ oxidation and the other two are utilized for anabolic processes (**2.3**) (Vajrala *et al.*, 2013). While carbon dioxide ($CO_2$) is the preferred carbon source incorporated during growth, the metabolism of AOB is more versatile and they can also incorporate and obtain energy from small organic substrates (Daims and Wagner, 2010).

$$NH_3 + 0.0496CO_2 + 1.44O_2 \rightarrow 0.01C_5H_7O_2N + 0.99NO_2^- + 0.97H_2O + 0.99H^+ \quad (\mathbf{2.1})$$

$$NH_3 + O_2 + 2H^+ + 2e^- \xrightarrow{AMO} NH_2OH + H_2O \quad (\mathbf{2.2})$$

$$NH_2OH + H_2O + 2e^- \xrightarrow{HAO} HNO_2 + 4H^+ + 4e^- \quad (\mathbf{2.3})$$

In addition, AOB have a denitrifying functionality where $NO_2^-$ can be used as electron acceptor at low dissolved oxygen (DO) conditions. $NH_2OH$ oxidation provides the electrons for the sequential $NO_2^-$ reduction to nitrous oxide ($N_2O$) via nitric oxide (NO) (Poth and Focht, 1985). This process is encoded by a set of $NO_2^-$- and NO-reducing enzymes (NIR, NOR) and is termed nitrifier denitrification (ND). AOB can also produce $N_2O$ from the incomplete oxidation of $NH_2OH$ to $HNO_2$ via NO, or its reduced form HNO (Hooper and Terry, 1979). This process is referred to as nitrifier nitrification (NN) (Zhu *et al.*, 2013) associated $N_2O$ production. The enzymology of AOB suggests the presence of alternate $N_2O$ producing pathways such as one mediated by CYT554 which possesses a NO reducing catalytic units similar to the NOR cluster (Upadhyay *et al.*, 2006; Kozlowski *et al.*, 2014). Recently, a direct enzymatic conversion of $NH_2OH$ to $N_2O$ mediated by CYTP460 was also demonstrated (Caranto *et al.*, 2016). DO differently affects the transcription and expression of NIR and NOR enzymes. NO production, regulated by NirK, would be favoured under anoxic conditions (Kester, 1997; Perez-

Garcia *et al.*, 2014), while NorB activity would be upregulated under oxic conditions (Yu and Chandran, 2010).

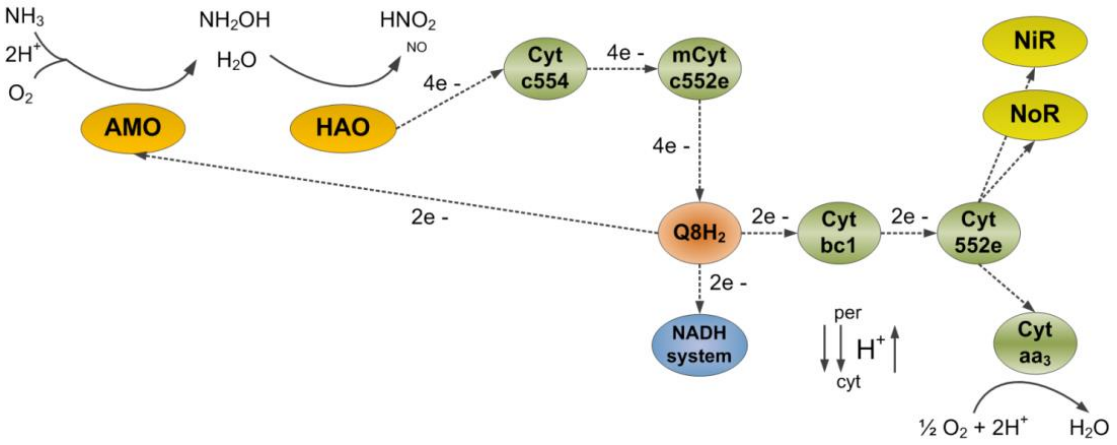


**Figure 2.2.** Simplified $NH_3$ oxidation to $HNO_2$ by AOB, main intermediates, electron flow and enzymatic sites.

The majority of AOB species belong to the Betaproteobacteria class (*Nitrosomonas*, *Nitrosospira*) while two known species belong to the Gammaproteobacteria (*Nitrosococcus halophilus* and *N. oceani*). Different sub-lineages of the genus *Nitrosomonas* are frequently detected by 16S rRNA and amoA sequence analysis in wastewater treatment plants (Nielsen *et al.*, 2010; Purkhold *et al.*, 2000). *Nitrosomonas europaea*, or *Nitrosomonas eutropha* adapt to higher ammonia concentrations compared to *Nitrosomonas oligotropha*. Diversity varies between systems, with some being dominated by one species and others, where ammonium concentrations vary over a wide range, by several species (Daims and Wagner, 2010).

Ecologically, *Nitrosomonas* cells have a higher specific growth rate than *Nitrosospira* species and a lower substrate affinity, suggesting a better adaptation to systems with high substrate as wastewater treatment plants (Schramm *et al.*, 1999; Terada *et al.*, 2013). The $NH_4^+$ and $NH_2OH$ aerobic oxidation by AOB pure cultures (*N. europaea*, *N. communis*, and *N. multiformis* among others) revealed different physiological responses of NO and $N_2O$ production (Kozlowski *et al.*, 2016).

### 2.1.2 Aerobic nitrite oxidizing bacteria

Some nitrite oxidizing bacteria (NOB) belong to the Alphaproteobacteria class (e.g. *Nitrobacter* spp,), the Betaproteobacteria (e.g. *Nitrotoga* spp.) oth-

ers to the Nitrospira phylum (e.g. *Nitrospira* spp.) and recently some Chloroflexi (e.g. *Nitrolanceta* spp.) were discovered (Sorokin *et al.*, 2012). They are also more physiologically diverse than AOB, not all NOB being chemolithoautotrophs (Madigan *et al.*, 2010). NOB obtain energy from the oxidation of $NO_2^-$ to nitrate ($NO_3^-$) catalysed by nitrite oxidoreductase (NXR) using water as oxygen source (**2.4**). Molecular oxygen is reduced with the electrons released during $NO_2^-$ oxidation in a cytochrome *aa3*-type terminal oxidase (Daims and Wagner, 2010). NOB genera *Nitrobacter* and *Nitrospira* can also grow mixotrophically on small organic compounds in the absence of $NO_2^-$.

$$NO_2^- + H_2O \xrightarrow{NXR} NO_3^- + 2H^+ + 2e^- \qquad (\mathbf{2.4})$$

Four genera comprise the best studied NOB: *Nitrobacter*, *Nitrospira*, *Nitrococcus*, and *Nitrospina*. In wastewater treatment operations *Nitrobacter*-like bacteria were considered the dominating species, but recent microbial characterization of activated sludge systems and biofilms showed a wider distribution of *Nitrospira* (Nielsen *et al.*, 2010) and in some cases *Nitrotoga* seems dominant (Lücker *et al.*, 2015).

From pure culture studies *Nitrobacter* spp. are considered r-strategist, being outcompeted by *Nitrospira* spp. at low substrate concentrations, K-strategists (Nowka *et al.*, 2014). Coexistence of *Nitrobacter* and *Nitrospira* has been observed in highly-loaded nitrifying reactors, but *Nitrospira* seems to outcompete *Nitrobacter* at low-load activated sludge systems (**Paper IV**).

$N_2O$ is not part of the metabolism of NOB, but they possess a NirK gene responsible for $NO_2^-$ reduction to NO (Perez-Garcia *et al.*, 2016a). Hence, indirectly, NOB play an important role on $N_2O$ emissions from wastewater treatment operations. Indeed, by consuming $NO_2^-$, a possible substrate for $N_2O$ production by AOB, NOB can act as an indirect $N_2O$ mitigator in nitrifying systems.

### 2.1.3 Denitrifying bacteria

Denitrifying bacteria are commonly heterotrophs which at low oxygen tension can use nitrate, nitrite, nitric oxide and nitrous oxide as electron acceptors in their respiratory metabolism (**2.5**). Most denitrifiers can also respire organic carbon with oxygen as electron acceptor. Denitrifiers of the Betaproteobacteria class belong to the genera *Curvibacter*, *Thaurea*, *Azoarcus*, *Zoo-*

*gloea* and *Accumulibacter* (Daims and Wagner, 2010). In addition, chemolitotrophic denitrifers exist, that use compounds such as elemental sulfur, sulphide, or hydrogen as electron donor (Berks *et al.*, 1995); they will not be discussed here as they would not dominate typical water quality engineering systems.

$$NO_3^- + 1.08CH_2OH + 0.24H_2CO_3 \rightarrow 0.056C_5H_7O_2N + 0.47N_2 + 1.68H_2O + HCO_3^- \quad (\mathbf{2.5})$$

$$NO_3^- \xrightarrow{NAR} NO_2^- \xrightarrow{NIR} NO \xrightarrow{NOR} N_2O \xrightarrow{NOS} N_2 \quad (\mathbf{2.6})$$

The four-step reduction is carried out by the NAR, NIR, NOR and NOS enzymes (**2.6**); NAR is a membrane-bound enzyme while NIR, NOR and NOS are located in the periplasm (Berks *et al.*, 1995) (**Figure 2.3**). Heterotrophic denitrifiers possess a highly modular microbiome with very different distribution of denitrifying genes (Graf *et al.*, 2014). Co-occurrence of NAR, NIR and NOR enzymes without NOS would yield a net $N_2O$ producer, while non-denitrifier $N_2O$ reducers carrying an atypical *nosZ* gene have been identified and may act as $N_2O$ sinks (Jones *et al.*, 2014). Moreover, the reduction of $N_2O$ also occurs in some non-denitrifying bacteria (Domeignoz-Horta *et al.*, 2016). The potential of an heterotrophic community to serve as $N_2O$ source or sink may be governed by the diversity and relative abundance of the *nosZ* gene with respect to *nar*, *nir* and *nor* genes (Sanford *et al.*, 2012; Jones *et al.*, 2014). In WWTP removing phosphorus and nitrogen biologically some Phosphate-Accumulating Organisms (PAO) also act as denitrifiers (Ekama and Wentzel, 1999).

The electrons released from carbon oxidation are distributed through the respiratory electron transport chain, to the ubiquinol pool and circulated to two branches: nitrate reductase and cytochrome *c* (Richardson *et al.*, 2009). Both branches have been shown to compete for a limited flow of electrons from NADH and succinate dehydrogenases (Kucera *et al.*, 1983). Similarly, nitrite and nitrous oxide reductases compete for electrons from the reduced cytochrome c (Alefounder *et al.*, 1983). Thus, the reduction rate of individual nitrogen oxide are influenced by the presence of other terminal acceptors (Kucera *et al.*, 1983). The reversible inhibitory effect of DO on $NO_x^-$ reduction is similar for each step (Alefounder *et al.*, 1983; Richardson *et al.*, 2009). $N_2O$ reduction is the most sensitive step towards DO, and under low DO $N_2O$ accumulation is promoted compared to the other N-species (Wild *et al.*, 1994). The activity of enzymes encoded by the *nir*, *nor* and *nosZ* genes,

located in the periplasm, are pH-dependent, with different optima for each denitrification step (Thomsen *et al.*, 1994).

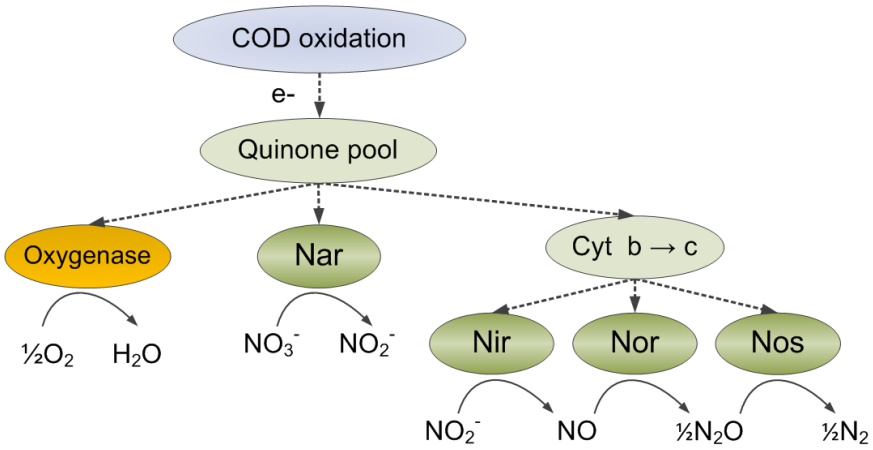


**Figure 2.3.** Diagram of canonical electron transport system in denitrification.

External carbon sources such as methanol, ethanol or acetate are commonly added to wastewater to enhance denitrification and improve nitrogen removal (Mokhayeri *et al.*, 2009). The denitrification rates and yield vary significantly based on the carbon source used, which has been proposed as the controlling factor for the community function and structure (Lu *et al.*, 2014). The metabolic pathways to oxidize each carbon source are different (Madigan *et al.*, 2010), and thus, dosage of a specific carbon source can shape the microbial community (Hallin *et al.*, 2006). Acetate-fed enriched for members of the *Comamonadaceae* and *Rhodocyclaceae* family, while methanol-fed enriched for members of the *Methylophilaceae* (Osaka *et al.*, 2006). Methanol oxidizers typically represent a small fraction of the complex denitrifying guild in wastewater treatment plants but increase after an adaptation period (Ginige *et al.*, 2004; Lu *et al.*, 2014).

### 2.1.4 Anaerobic ammonium oxidizing bacteria

Theoretical calculations predicted the existence lithotrophs that could oxidize $NH_4^+$ to $N_2$ with $NO_3^-$ or $O_2$ as electron acceptors (Broda, 1977). Anaerobic ammonium oxidizing, "anammox" bacteria, are chemolithoautotrophs that obtain energy from the anaerobic oxidation of $NH_4^+$ with $NO_2^-$ as electron acceptor and fix inorganic carbon (**2.7**) (Strous and Heijnen, 1998).

$$NH_4^+ + 1.32NO_2^- + 0.066HCO_3^- + 0.13H^+ \rightarrow 1.02N_2 + 0.26NO_3^- + 0.066CH_2O_{0.5}O_{0.15} + 2.03H_2O \quad (\mathbf{2.7})$$

Anammox bacteria comprise five genera *Ca. Anammoxoglobus*, *Ca. Brocadia*, *Ca. Jettenia*, *Ca. Kuenenia*, and *Ca. Scalindua*, all belonging to the *Planctomycetes* phylum. Previously considered as slow growers (doubling time of 10-15 days), it was recently shown to grow much faster (2.1 – 3.9 days) (Zhang *et al.*, 2017). $N_2O$ is not part of the metabolism of Anammox bacteria, but intermediates of $N_2O$ production pathways such as $NO_2^-$ and NO, are part of the metabolism of Anammox. Hence, as well as NOB, Anammox play an important role on $N_2O$ emissions from wastewater treatment operations.

### 2.1.5 Recent discoveries in the nitrogen cycle

Thermodynamic calculations predicted the existence of complete nitrifying organisms, capable of oxidizing ammonium into nitrate (Costa *et al.*, 2006). Recently, "comammox" organisms (completely ammonium oxidizers) have been discovered, reshaping our understanding of the nitrogen cycle (van Kessel *et al.*, 2015; Daims *et al.*, 2015; Palomo *et al.*, 2016). The abundance of comammox in wastewater treatment plants is significantly lower than AOB, and thus, this study will solely focus on AOB as aerobic ammonium oxidizers (Chao *et al.*, 2016).

### 2.1.6 Abiotic reactions

Earlier studies on abiotic $N_2O$ production have highlighted the importance of two chemical reactions driven by $NH_2OH$ (Heil *et al.*, 2014) that can occur at relevant rates under wastewater treatment conditions.

$$4NH_2OH \rightarrow N_2O + 2NH_3 + 3H_2O \quad (\mathbf{2.8})$$

$$NH_2OH + HNO_2 \rightarrow N_2O + 2H_2O \quad (\mathbf{2.9})$$

$NH_2OH$ can decompose to $N_2O$ at high pH (**2.8**, (Feelisch and Stamler, 1996); its acidic form $NH_3OH^+$ is more stable (Liu *et al.*, 2014) (pKa = 5.9, 25 C)). In the second reaction, an N-N linkage is formed by N-nitrosation of $NH_2OH$, a nucleophile, with a nitrosating agent, $HNO_2$, at low pH (Spott *et al.*, 2011) (**2.9**, (Döring and Gehlen, 1961)). Thus, independently from the main driving process (e.g., nitrification or denitrification) and the environmental condi-

tions (e.g., aerobic or anaerobic), biotically-driven (because it requires $NH_2OH$) abiotic $N_2O$ production is possible in WWTP.

Previously considered as low, $NH_2OH$ concentrations from highly N-loaded wastewaters can be higher than expected (0.03-0.11 mgN/L) (Soler-Jofra *et al.*, 2016), highlighting a possible underestimation of the abiotic $N_2O$ production (Harper *et al.*, 2015). For example, a nitritating reactor for reject water (high AOB activity and $NO_2^-$ accumulation) estimated a 1.1% abiotic emission factor driven by $NH_4^+$ oxidation (Soler-Jofra *et al.*, 2016).

Nitrate or nitrite reduction coupled with Fe(II) oxidation was also proposed as abiotic contributor to NO and $N_2O$ production under anoxia at high nitrite levels in wastewater treatment systems (**2.10**, **2.11**) (Kampschreur *et al.*, 2011).

$$NO_2^- + Fe^{2+} + 2H^+ \rightarrow NO + Fe^{3+} + H_2O \qquad \textbf{(2.10)}$$

$$NO + Fe^{2+} + 1H^+ \rightarrow Fe^{3+} + 0.5N_2O + 0.5H_2O \qquad \textbf{(2.11)}$$

The observations hinted to a role for iron oxidation coupled to nitrite reduction from mixed liquor because of its considerable iron reducing activity. However, the presence or absence of Fe(II) or Fe(III) did not affect aerobic abiotic $N_2O$ production (Terada *et al.*, 2017; Soler-Jofra *et al.*, 2016). For more details on abiotic $N_2O$ production the reader is referred to (Zhu-Barker *et al.*, 2015).

## 2.2 Nitrogen removal in wastewater treatment and nitrous oxide emissions

Sewage treatment contributes to 3.2% of the anthropogenic $N_2O$ emissions, but can triplicate if manure, landfill leacheates and industrial nitrogenous effluents are included (Desloover *et al.*, 2012). The carbon footprint of a WWTP is highly sensitive to $N_2O$ emissions (Gustavsson and Tumlin, 2013), where an $N_2O$ emission factor of 1% increases the carbon footprint by 50% (Monteith *et al.*, 2005), reaching up to 83% of the operational $CO_2$ footprint of a Biological Nitrogen Removal (BNR) plant (Desloover *et al.*, 2011).

All of the BNR processes include an aerobic zone in which biological nitrification occurs. Some anoxic volume or time must also be included to provide biological denitrification to complete the objective of total nitrogen removal. Biological nitrification/denitrification is the most common treatment in WWTP due to its high efficiency, stability and reliability. Energy savings are linked to economic savings, and hence, processes that reduce the high use of energy in aeration are considered as attractive alternatives to actual BNR processes. Short-cut nitritation-denitritation, the combination of nitritation and anammox in single or two-stage systems are such alternatives with lower energy demands (Joss *et al.*, 2011). However, a trade-off seems to exist between aeration costs and reduced $N_2O$ emissions (Ahn *et al.*, 2011).

$N_2O$ mitigation strategies have been proposed based on intensive measurement campaigns (Desloover *et al.*, 2012; Foley *et al.*, 2010), but $N_2O$ emissions are highly variable even for similar processes (0.001 – 25.3% $N_2O$ emitted/N-load). A ranking of BNR technologies based on the potential $N_2O$ risk cannot be established because of the yet unknown high variability of reported $N_2O$ emissions (Desloover *et al.*, 2012; Kampschreur *et al.*, 2008a). Key variables such as low dissolved oxygen or high nitrite accumulation have been identified as potential hotspots for $N_2O$ emissions in BNR processes (Sun *et al.*, 2015; Kampschreur *et al.*, 2009b).

## 2.3 Regulation of nitrous oxide production in wastewater treatment

In nitrogen removing systems $N_2O$ production has been associated to several variables and operational parameters. Suggestions on how to fine-tune these variables has been applied to manage $N_2O$ emissions using a black-box approach (**Figure 2.4**) (Brotto *et al.*, 2015; Kampschreur *et al.*, 2009a; Park *et al.*, 2000). These methods rely on obtaining a better understanding of $N_2O$ emissions by means of correlation analysis: what variables trigger $N_2O$ emissions?

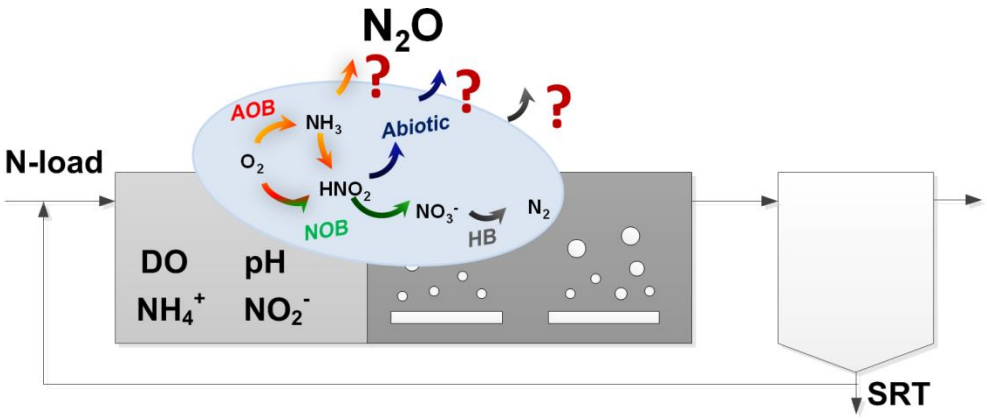


**Figure 2.4.** Nitrous oxide emission during biological nitrogen removal.

The $NH_4^+$ load and influent $NH_4^+$ concentration have been correlated to $N_2O$ emissions from aerobic zones operating at high dissolved oxygen (DO) concentrations (Lotito *et al.*, 2012; Ni *et al.*, 2013b). At low DO $NH_4^+$ is oxidized at a lower rate but a higher fraction is converted to $N_2O$ (Burgess *et al.*, 2002; Li and Wu, 2014) (**Figure 2.5**). The aeration strategy, i.e. aeration rate and frequency of aeration, also impact $N_2O$ emission (Yu *et al.*, 2010; Domingo-Félez *et al.*, 2014; Kampschreur *et al.*, 2008a).

$NO_2^-$ accumulation has also lead to higher $N_2O$ emissions in N-removing systems (Wang *et al.*, 2016b; Kampschreur *et al.*, 2008b) (**Paper I**). As the direct precursor of $N_2O$ in most of the biological pathways, NO has shown the highest correlations with $N_2O$ (Kampschreur *et al.*, 2008b; Wang *et al.*, 2016b; Domingo-Félez *et al.*, 2014).

pH levels have two distinct effects on $N_2O$ production. First, on the enzymatic level, maximum activities have been described as pH-dependent (Park *et al.*, 2007) (**Figure 2.5**). Second, the availability of the true substrates for

AOB and NOB are assumed to be $NH_3$ and $HNO_2$ respectively; the actual concentrations of these species are in a pH-dependent equilibrium with their ionized counterparts $NH_4^+$ and $NO_2^-$ (Udert *et al.*, 2005) ($pKa_{HNO2}$ = 3.25, $pKa_{NH4+}$ = 9.25, 25 C (Lide, 2009)). Acidification enhanced the $N_2O$ yield of *Nitrosospira*-dominated community, suggested due to the hybrid $N_2O$-forming reaction of $NH_2OH$ and $HNO_2$ (Frame *et al.*, 2017).

Inorganic carbon (IC) is fixed to form cellular carbon during AOB growth. At limiting IC availability, $NH_3$ is oxidized at a lower rate due to increased cellular maintenance energy demand, which decreases the overall $N_2O$ produced (Jiang *et al.*, 2015). However, under the same $NH_3$ oxidation rates, IC-limitation increases the fraction of $N_2O$ produced (Mellbye *et al.*, 2016). Depending on the nitrogen removal system, wastewaters can have varying IC levels.

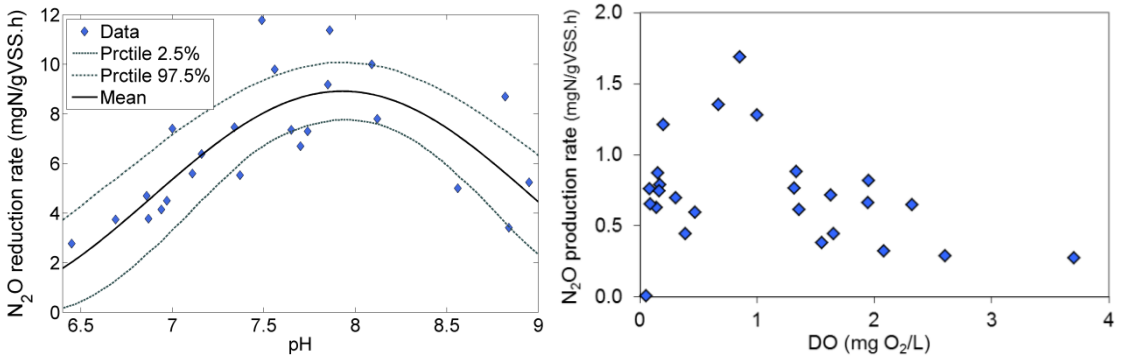


**Figure 2.5.** Left: Nitrous oxide consumption dependency on pH (**Paper IV**). Right: Net production rates at varying dissolved oxygen concentrations from mixed liquor biomass. (Unpublished data).

The heterotrophically-oxidized organic content of conventional urban wastewater typically produces excess IC for autotrophic growth, but high N-strength wastewaters with a lower C/N ratio, may result in IC limited AOB growth (Panwivia *et al.*, 2014).

Operational parameters and wastewater characteristics have also shown to affect $N_2O$ emissions. A limited flow of electron donors (COD) due to a low carbon-to-nitrogen ratio of the incoming wastewater can also slow down $NO_x^-$ reduction rates. Therefore, $N_2O$ production can be enhanced by a lower $N_2O$ reduction rate compared to previous steps because of the lower electron affinity. Consequently, side stream processes, characterized by a high N and low COD content, are potential hotspots for heterotrophic $N_2O$ production (Kampschreur *et al.*, 2009b; Yang *et al.*, 2009; Hu *et al.*, 2013). Additionally,

$N_2O$ consumption is the most sensitive denitrification step to the presence of DO and thus, $N_2O$ can be released in the presence of low DO concentrations (Richardson *et al.*, 2009).

Other operational parameters such as the solids retention time (SRT) have shown increasing $N_2O$ emission factors for low SRT values (Li and Wu, 2014; Lotito *et al.*, 2012). Seasonal variations of $N_2O$ emissions have been observed and associated to temperature changes that affect the microbial populations involved in nitrogen removal (Wang *et al.*, 2014, 2016b).

In biofilms the spatial distribution of microbial communities and mass transfer limitations are linked by chemical gradients (Manser *et al.*, 2005; Picioreanu *et al.*, 2016). Biofilms showed a lower emission factor compared to suspended-growth systems with smaller particle size (Park *et al.*, 2000). For example, in partial nitritation/anammox suspended granules, anammox are located in the inner anoxic layers, acting as a $NO_2^-$ sinks and thus, reducing the risk of $N_2O$ production. Other parameters affecting $N_2O$ production in suspended and biofilm wastewater treatment operations have been recently reviewed (Todt and Dörsch, 2016; Massara et al., 2017).

# 3 Modelling nitrous oxide emissions during WQE

## 3.1 Modelling biological nutrient removal

Models are simplifications of reality that describe, through mathematical equations, a system of interest. The purpose of the model also defines the scope and detail that model predictions should achieve. For example, in wastewater treatment applications models have been used to develop control strategies, to evaluate new plant designs or to support management decisions (Henze *et al.*, 2008). The modelling objectives tend to align with regulatory discharge wastewater characteristics (e.g. particulate, organic carbon, and nutrient content of effluents).

A wastewater treatment process model typically comprises a variety of different components: influent characterisation model, hydraulic process model, sedimentation model and reaction model (**Figure 3.1**).

Specifically, the reaction model integrates the hydrodynamic mixing model and the biological model. The first one considers the model components and flow through the reactor volume, ideally as a Completely-Stirred Tank Reactor (CSTR), Plug-Flow Reactor (PFR), or a combination of ideal reactors. The focus of this thesis is on the biological model that describes the conversions of state variables.

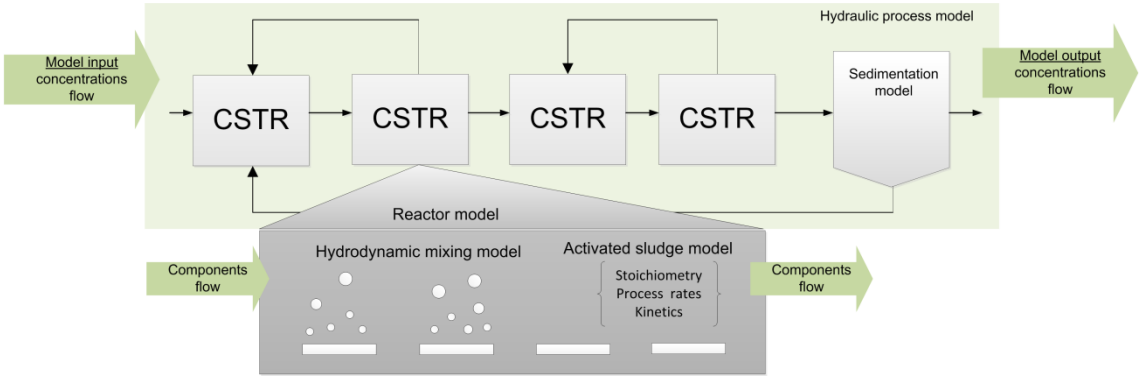


**Figure 3.1.** Representation of a complete wastewater treatment plant model (Modified from (Meijer, 2004)).

## 3.2 ASM-based models for nutrient removal

The increasing metabolic understanding of nutrient removal can be described with mathematical equations and has been successfully used to predict the fate of C, N and P in wastewater treatment operations (Henze *et al.*, 2000). The Activated Sludge Model (ASM) No. 1, No.2, and No. 2d are grey-box models where different microbial guilds present in the activated sludge and their specific functionality are incorporated in a so-called population-based model. ASM1, 2, and 2d consider the microbes as a black box and do not take into account intracellular processes. However, new ASM-based extensions incorporate metabolic process descriptions that result in bigger and more complex models (Snip *et al.*, 2014).

A generic mathematical model (e.g. ASM-based) can be described by the following equations:

$$\frac{d\underline{x}}{dt} = f(t, \underline{x}, \underline{u}, \underline{\theta})$$

$$\underline{x}(t_0) = \underline{x}_0$$

$$\underline{y} = g(\underline{x}(t))$$

Where $t$ is time, $\underline{x}$ are the state variables ($\underline{x}_0$ the initial states), $\underline{u}$ the input variables, $\underline{\theta}$ the input parameters and $\underline{y}$ the output variables. Underscored symbols correspond to vector variables. The partial differential equation describes the substrate utilization and dynamic accumulation. The general rate expression for compound $S_i$ that is affected by multiple processes $P_j$ is described by $\rho_j$ (**Table 3.1**).

**Table 3.1.** Stoichiometric matrix for a two-process and three-component model.

| Processes $P_j$ ↓<br>Components $S_i$ → | $S_1$ | $S_2$ | $X_1$ | Process Rate ($\rho_j$) |
|---|---|---|---|---|
| $P_1$ | $\nu_{1,1}$ | $\nu_{1,2}$ | $\nu_{1,3}$ | $f(\theta_1, \theta_2, S_1, S_2, X_1)$ |
| $P_2$ | $\nu_{2,1}$ | | $\nu_{2,3}$ | $f(\theta_3, X_1)$ |
| Parameters: Kinetic $(\theta_1, \theta_2, \theta_3)$<br>Stoichiometric $\nu_{j,i}$ | Dissolved substrate 1 (-) | Dissolved substrate 2 (-) | Particulate biomass 1 (-) | Observed transformation rate<br>$r_i = \sum_j \rho_j \cdot \nu_{j,i}$ |

The process rate is described by model components and kinetic parameters. The mass balance for a compound corresponds to the observed transformation rate $r_i$, and the rates are coupled through conservation relations (stoichiometry).

## 3.3 Nitrous oxide models

Mathematical models can be useful tools to predict $N_2O$ emissions and thus, help develop mitigation strategies to reduce the carbon footprint of wastewater treatment operations. $N_2O$ models are developed as extensions from existing models for N-removal. Additional state variables, process rates and parameters increase the complexity of $N_2O$ models conventional N-removal models.

Models vary based on the number of processes and/or variables considered in $N_2O$ production and the relationships of their mathematical rates (Liu *et al.*, 2016; Perez-Garcia *et al.*, 2014; Pocquet *et al.*, 2016).

In empirical models $N_2O$ emissions and nitrogen removal rates are fit to operational factors (e.g. pH value, temperature, feeding and aeration strategy, etc.) via multiple linear regression models (MLR) (Leix *et al.*, 2017; Liu *et al.*, 2016). The specific effects and combined influences are then used to find conditions for $N_2O$ mitigation.

Of increasing complexity, Stoichiometric Metabolic Network (SMN) models make use of the increasing knowledge on metabolic engineering to describe microbial interactions (Perez-Garcia *et al.*, 2016b). $N_2O$ production from nitrification by *N. europaea* at steady state was described with a SMN model containing 44 metabolites and 49 stoichiometric reactions (Perez-Garcia *et al.*, 2014). For wastewater treatment purposes ASM-based models are widely used, and many $N_2O$ extensions have been proposed (Ni *et al.*, 2011, 2014; Pocquet *et al.*, 2016; Guo and Vanrolleghem, 2014; Hiatt and Grady, 2008). The ASM-based models differ on the biological description and the number of $N_2O$ pathways, which are always significantly lower than for SMN models (6-7 metabolites, 5-6 reactions) (**Paper II**). Control strategies based on $N_2O$ predictions are being developed for the reduction of $N_2O$ emissions (Boiocchi *et al.*, 2016).

### 3.3.1 Autotrophic models

Initially, single-pathway models were proposed describing/capturing either the NN or ND pathway. The main differences between models regards the stoichiometric coefficients, the number of substrates considered, the identity

of the electron donor, and the inclusion or absence of substrate inhibition. Initial models described NO and $N_2O$ production as directly dependent on $NH_4^+$, DO and $NO_2^-$ levels (Kampschreur *et al.*, 2007; Schreiber, 2009). In subsequent models $NH_2OH$ was considered an intermediate of $NH_3$ oxidation, allowing the NN pathway to be modelled as a fraction of $NH_2OH$ oxidation to $NO_2^-$, either via NOH (Law *et al.*, 2012) or via NO (Ni *et al.*, 2013a) (**Figure 3.2, A**). In the ND pathway $NH_2OH$ acts as electron donor for the consecutive reduction of $NO_2^-$ to $N_2O$ via NO (Ni *et al.*, 2011) (**Figure 3.2, B**). However, $N_2O$ dynamics cannot be captured with single-pathway models, and recent models combining the NN and ND pathways provide better descriptions of $N_2O$ production than single-pathway models (Ni *et al.*, 2014; Pocquet *et al.*, 2016; Ding *et al.*, 2016) (**Figure 3.2, C, D, E**).

In a novel approach, global cellular oxidation (electron generating) and reduction (electron consuming) reactions are linked by a common pool of electron carriers, represented by one model component. This model aggregates all intracellular electron carriers such as cytochromes and ubiquinone into one component that cannot be directly quantified (Kim *et al.*, 2010). Oxidative and reductive processes are therefore uncoupled and competition is described with specific kinetic parameters (Ni *et al.*, 2014).

The two-pathway AOB models are adequate in predicting a shift in NN and ND contributions to total $N_2O$ production at different DO and $NO_2^-$ concentrations. However, these models would not describe the increased NO emissions at low DO and high $NO_2^-$ levels observed in several nitrifying systems (Chandran *et al.*, 2011; Kester, 1997; Rodriguez-Caballero and Pijuan, 2013).

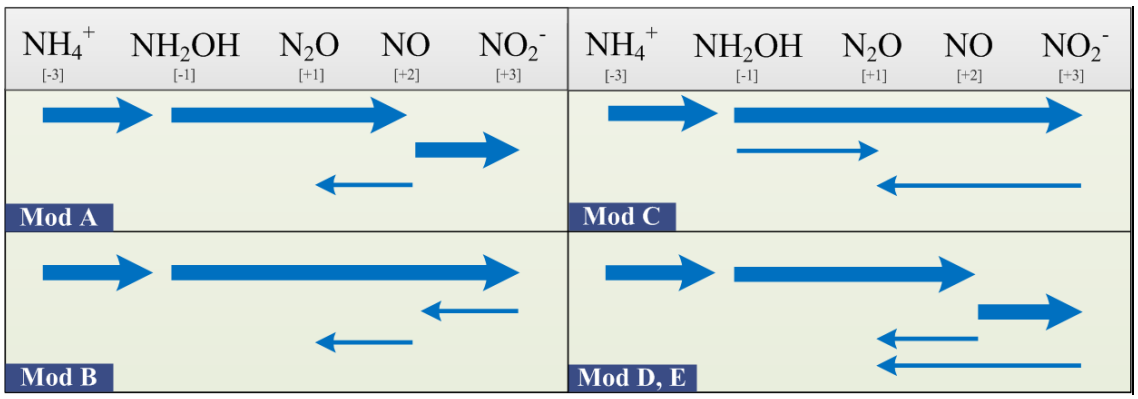


**Figure 3.2.** Comparison of the reactions involved in autotrophic models for $N_2O$ production. The arrow widths represent typical reaction rates. Mod A (Ni *et al.*, 2013b), Mod B (Ni *et al.*, 2011), Mod C (Ding *et al.*, 2016), Mod D (Pocquet *et al.*, 2016), Mode E (Ni *et al.*, 2014).

### 3.3.2 Heterotrophic denitrification models

The first kinetic model describing heterotrophic denitrification was based on pure cultures and described each denitrification step according to the Michaelis-Menten equation (Betlach and Tiedje, 1981). This approach considers every reduction rate independent from each other and has been widely used (Schulthess *et al.*, 1995; Hiatt and Grady, 2008). Wild *et al.*, (1994) explicitly calculated the concentration of enzymes to describe the delay in denitrification and $N_2O$ accumulation after aerobic growth, which was recently updated to the four steps (Zheng and Doskey, 2015). However, these models are limited to the assumption that carbon oxidation supplies all the electrons necessary for the four denitrification steps. Hence, only nitrogenous species limit denitrification rates under excess organic carbon conditions (Pan *et al.*, 2015).

Differently, branched models reflect the modularity of the electron transport chain (Richardson *et al.*, 2009). Grant and Pattey, (1999) developed a model where a maximum electron supply is distributed among electron acceptors, with preference given to the most oxidized compounds in a feed-back redox control ('*inhibition by product via respiratory chain'*). A different approach considered a double branch with common electron mobile carriers and described the accumulation of intermediates, but was not validated experimentally (Thomsen *et al.*, 1994). Almeida *et al.* (1997) proposed an analogy between an electric circuit and the electron flow through the cell membrane. The model was validated with experimental results from two pure culture studies where $NO_2^-$ (*Pseudomonas fluorescens*), and $NO_2^-$ and $N_2O$ (*Paracoccus denitrificans*) accumulated. The indirect coupling of electrons approach (ICE) calculates the concentration of internal electron carriers, uncoupling the carbon oxidation and denitrification processes at the cost of higher complexity (Pan *et al.*, 2013).

Even though the indirect approach has been heralded as superior as it can potentially describe all experimental observations (Pan *et al.*, 2015) more information about reaction kinetics is required. The direct approach can predict COD and nitrogen removal for systems with low intermediates accumulation ($NO_2^-$, $N_2O$) (Ni and Yuan, 2015) but might be inadequate for systems with high accumulation levels.

**Heterotrophic denitrification: competitive electron distribution**

The direct approach first developed by (Betlach and Tiedje, 1981) for denitrification is widely used in ASM-based models and hence will be used here. However, other approaches exist, such as the indirect modelling of carbon and nitrogen removal (Thomsen *et al.*, 1994; Pan *et al.*, 2013; Almeida *et al.*, 1997). The modelling approach presented by (Almeida *et al.*, 1997) is explored here.

A model describing 4-step denitrification and aerobic organic carbon removal is developed based on the analogy between electron competition during denitrification and electron distribution in electric circuits (**Figure 3.3, M1**).

A potential (E) is created by the presence of an electron donor/acceptor pair. The reaction rate is kinetically analogous to the current intensity ($i_i$) through a resistor. The resistance depends on the concentration of the substrate (Monod kinetics, $K_{S,i}$) and a minimum resistance (**3.1**) at substrate ($S_i$) limiting conditions the resistance ($r_i$) is infinite and no current flows, while at excess substrate the resistance becomes minimal, with value ($R_i$).

$$r_i = R_i \cdot \frac{(S_i + K_{S,i})}{S_i} \qquad \left[E \cdot \frac{mgN}{gVSS} \cdot h\right] \qquad (\mathbf{3.1})$$

Following the conservation of potential (**3.2**) and conservation of charge (**3.3**), the current through any resistor can be calculated. Thus, for any branched model the electron distribution from common pools (e.g. quinones, cytochromes) to several electron acceptors can be calculated.

$$E = E_{COD} + E_{NOx} \qquad (\mathbf{3.2})$$

$$i_{COD} = \sum i_{NOX} \qquad (\mathbf{3.3})$$

$$Rate_{NIR} = E_{tot} / \left[ r_{COD} \cdot \left( r_{NIR} \cdot \left( \frac{1}{r_{AER}} + \frac{1}{r_{NAR}} + \frac{1}{r_{NIR}} + \frac{1}{r_{NOR}} + \frac{1}{r_{NOS}} \right) + r_{NIR} \right) \right] \cdot X_{HB} \quad (\mathbf{3.4})$$

Compared to the original model structure by (Almeida *et al.*, 1997) two new electron distribution analogies considering additional processes are implemented: a one-branch model where all the reduction steps compete for electrons from a common source, and a two-branch model that resembles more precisely the intracellular electron distribution at a cost of an additional parameter (**Figure 3.3**). The model uses fewer parameters compared to existing state-of-the art denitrification models (Pan *et al.*, 2013). Model fitting is performed with data obtained from batch experiments with mixed denitrifying

communities for a combination of nitrogen oxides and for four different carbon sources in excess: methanol, ethanol, acetate and a carbon mixture.

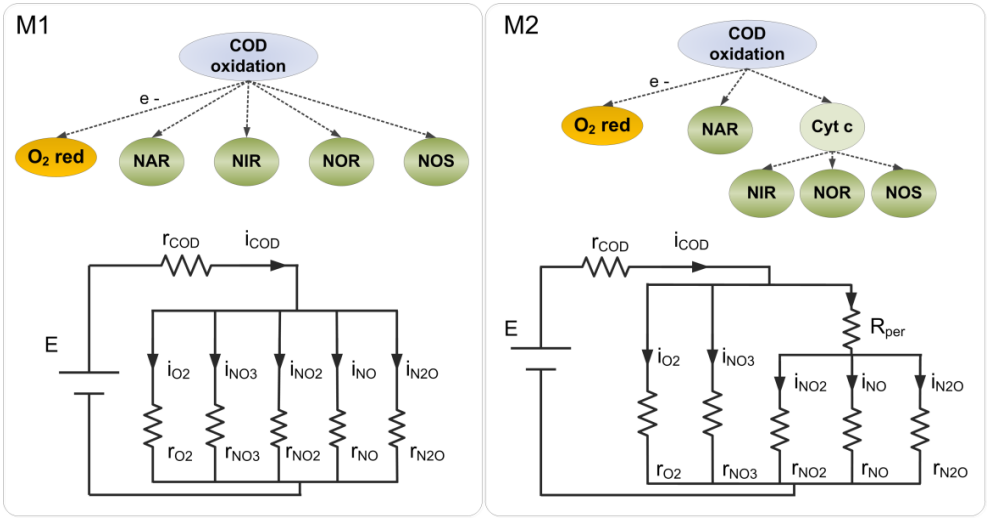


**Figure 3.3.** Simplified electron distribution in heterotrophic respiration and corresponding electric circuit analogy: one-branch model (M1), two-branch model (M2). (**Paper V**).

The model successfully describes the competition for electrons during batch experiments at excess substrate concentrations for a combination of nitrogen oxides (**Figure 3.4**). The total electron consumption rate predicted was not additive as non-competitive models suggest (Hiatt and Grady, 2008), and was distributed differently among the four denitrification steps (**Figure 3.4**).

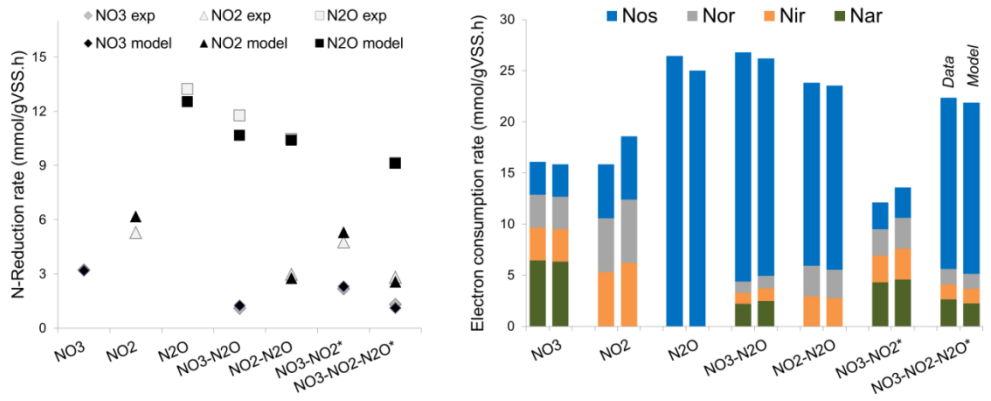


**Figure 3.4.** Left: Experimental (grey) and simulated (black) denitrification rates. Right: Electron consumption rates by $NO_3^-$ reduction (Nar – green), $NO_2^-$ reduction (Nir – orange), NO reduction (Nor – grey) and $N_2O$ reduction (Nos – blue) in Methanol-fed denitrifying experiments. Experimental (left bar) and modelling results (right bar). (* not used during calibration). (**Paper V**).

Among the four carbon sources evaluated calibration results indicate faster specific denitrification rates for methanol compared to any of the other carbon sources ($R_{NAR/NIR/NOS,MeOH} < R_{NAR/NIR/NOS,Acet,EtOH,C\text{-}mix}$) (**Table 3.2**).

**Table 3.2.** Best-fit parameters for denitrification batches: Methanol, Acetate, Ethanol, C-mix. (**Paper V**).

| | Methanol | Acetate | Ethanol | C-mix |
|---|---|---|---|---|
| $R_{NAR}$ | 5.6 | 11.8 | 8.2 | 8.9 |
| $R_{NIR}$ | 5.0 | 9.2 | 44.3 | 25.9 |
| $R_{NOS}$ | 0.6 | 15.0 | 7.6 | 11.1 |

In the scenarios evaluated in this study - excess electron donor (methanol) and electron acceptor - a simpler model such as M1 performs better than the ASM-ICE model. Further evaluation under a wider range of operation conditions (e.g. different carbon loadings) will benefit model discrimination between M1 and ASM-ICE. Overall, a different modelling approach for denitrification was explored but further validation is required.

## 3.4 NDHA model

An ASM-based model structure that describes $N_2O$ production during biological nitrogen removal is proposed. The model builds on existing structures for nitrogen removal and expands the number of processes to describe $N_2O$ dynamics. The model intends to answer the limitations of existing $N_2O$ models. For example, a better understanding of the AOB pathways would help identify operating conditions affecting $N_2O$ production and improve the accuracy of $N_2O$ predictions (Mannina *et al.*, 2016).

Theoretically, the model describes all relevant NO and $N_2O$ production pathways with fewer parameters than other proposed models. The NDHA model comprises the three known biological pathways (NDHA) as well as abiotic production (NDHA) (**Figure 3.5**, **Table 3.3**).

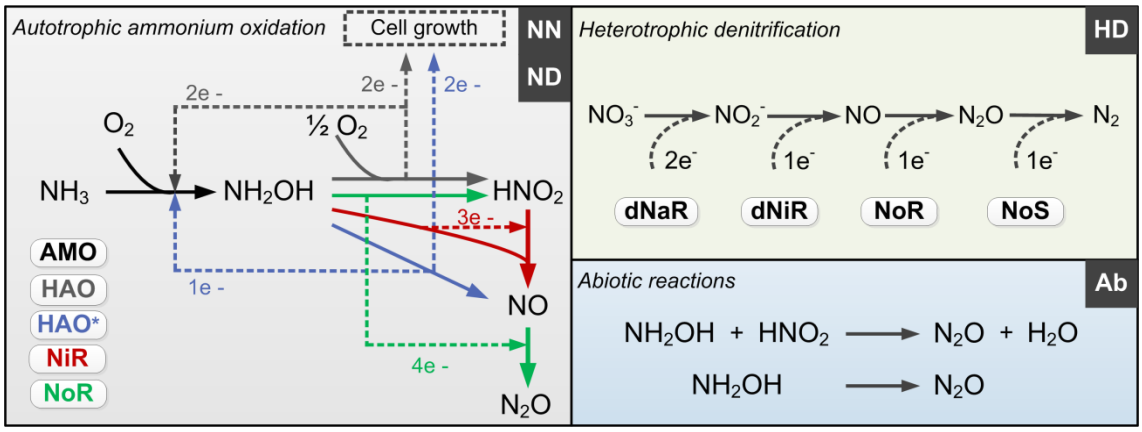


**Figure 3.5.** Diagram of the proposed $N_2O$-producing mechanisms occurring during N-removal: nitrifier nitrification, nitrifier denitrification, heterotrophic denitrification and abiotic pathways (NDHA). (Adapted from **Paper II**).

**Nitrifier Nitrification (NN):** The first process considers $NH_3$ oxidation to $NH_2OH$ (P1). $NH_2OH$ can be oxidized incompletely to $NO_{NN}$ (P2) or completely to $HNO_2$ in the presence of DO (P3). The effect of IC limitation on $NH_3$ oxidation is described by a Monod dependency (Guisasola *et al.*, 2007). The NN process is indirectly dependent on the $NH_3$ oxidation rate, reducing the DO dependency only to P1. The fraction of $NH_2OH$ oxidized via the NN pathway is described by the factor $\varepsilon_{AOB}$.

**P1. AMO** $\quad NH_3 + O_2 \rightarrow NH_2OH$

$$\mu_{AMO}^{AOB} \cdot \frac{S_{O2}}{S_{O2} + K_{O2\_AMO}^{AOB}} \cdot \frac{S_{NH3}}{S_{NH3} + K_{NH3}^{AOB}} \cdot \frac{S_{IC}}{S_{IC} + K_{IC}^{AOB}} \cdot X_{AOB}$$

**P2. HAO*** $NH_2OH \rightarrow NO_{NN}$

$$\mu_{HAO}^{AOB} \cdot \varepsilon_{AOB} \cdot \frac{S_{NH2OH}}{S_{NH2OH} + K_{NH2OH}^{AOB}} \cdot \frac{S_{IC}}{S_{IC} + K_{IC}^{AOB}} \cdot X_{AOB}$$

**P3. HAO** $NH_2OH + 0.5\ O_2 \rightarrow HNO_2 + H_2O$

$$\mu_{HAO}^{AOB} \cdot (1-\varepsilon_{AOB}) \cdot \frac{S_{O2}}{S_{O2} + K_{O2\_HAO}^{AOB}} \cdot \frac{S_{NH2OH}}{S_{NH2OH} + K_{NH2OH}^{AOB}} \cdot \frac{S_{IC}}{S_{IC} + K_{IC}^{AOB}} \cdot X_{AOB}$$

**Nitrifier Denitrification (ND):** In the ND pathway $HNO_2$ denitrification to $NO_{ND}$ is negatively affected by DO (P4). Different from other two-pathway AOB models $N_2O$ production from its precursor (NO) is described by one process (P5) as there is no evidence of different NO reduction mechanisms within individual cells (Upadhyay *et al.*, 2006). The NN and ND pathways are differentiated by two NO-producing processes with different DO and $HNO_2$ dependencies. These dependencies govern the shift between pathways (Chandran *et al.*, 2011; Kozlowski *et al.*, 2014). $N_2O_{NN}$ production is enhanced at high $NH_3$ and DO levels while $N_2O_{ND}$ increases at low DO and high $HNO_2$ levels.

The $NO/N_2O$ ratio can be used to help elucidate the individual contribution of each pathway during model calibration (Pocquet *et al.*, 2016). An advantage of the proposed model is uncoupling the NN- and ND-driven NO production, which allows for a more biologically congruent estimate of $NO/N_2O$.

**P4. NIR** $3\ HNO_2 + NH_2OH \rightarrow 4\ NO_{ND}$

$$\mu_{HAO}^{AOB} \cdot \eta_{NIR} \cdot \frac{K_{i\_O2}^{AOB}}{S_{O2} + K_{i\_O2}^{AOB}} \cdot \frac{S_{NH2OH}}{S_{NH2OH} + K_{NH2OH\_ND}^{AOB}} \cdot \frac{S_{HNO2}}{S_{HNO2} + K_{HNO2}^{AOB}} \cdot X_{AOB}$$

**P5. NOR** $2\ (NO_{ND} + NO_{NN}) + NH_2OH \rightarrow 1.5\ N_2O$

$$\mu_{HAO}^{AOB} \cdot \eta_{NOR} \cdot \frac{S_{NH2OH}}{S_{NH2OH} + K_{NH2OH\_ND}^{AOB}} \cdot \frac{S_{NO}}{S_{NO} + K_{NO\_ND}^{AOB}} \cdot X_{AOB}$$

**Heterotrophic denitrification (HD):**

Because of the wide applicability of the direct approach a four-step complete denitrification is used following the ASM-N model (Hiatt and Grady, 2008). The indirect coupling approach was not considered because of its limited application (only one full-scale study has been reported (Wang *et al.*, 2016a)), and hence limited information about reaction kinetics. Moreover, the ASM-N model has also been extended coupled with phosphorus removal (Liu *et al.*,

2015). In the four-step denitrification model individual reaction kinetics (pH-dependent), inhibition and substrate affinities are considered for every step as recently suggested for systems with low intermediates accumulation (Ni and Yuan, 2015).

**P8-11. HD** $NO_{X,oxidized} + COD \rightarrow NO_{X,reduced}$

$$\mu_{i\,(pH)}^{HB} \cdot \frac{K_{i\_O2\_NOx,i}^{HB}}{S_{O2} + K_{i\_O2\_NOx,i}^{HB}} \cdot \frac{S_S}{S_S + K_{S\_NOx,i}^{HB}} \cdot \frac{S_{NH4}}{S_{NH4} + K_{NH4}^{HB}} \cdot \frac{S_{NOx,i}}{S_{NOx,i} + K_{NOx,i}^{HB}} \cdot X_{HB}$$

Heterotrophic consumption and autotrophic production of $N_2O$ can occur simultaneously, at different rates, throughout wastewater treatment operations. Ignoring heterotrophic $N_2O$ consumption can underestimate the autotrophic production. Thus, an $N_2O$ model should always include compatible structures for both the autotrophic and heterotrophic pathways (**Paper I**).

**Abiotic (Ab)**: Two biologically-driven abiotic $N_2O$ production processes are considered (P7). Nitrification produces $NH_2OH$, which is oxidized to $HNO_2$, while also forming HNO (Igarashi *et al.*, 1997). HNO dimerizes via $H_2N_2O_2$ to $N_2O$ and $H_2O$. Nitrosation of $NH_2OH$ with $HNO_2$ has also been postulated as a relevant reaction in partial nitrification reactors (Soler-Jofra *et al.*, 2016). Reactions rates are modelled with pH dependent second order kinetics. A model combined for the first time the abiotic reaction between $NH_2OH$ and $HNO_2$ together with the ND pathway (Harper *et al.*, 2015). Nitritation reactors with high $NH_4^+$ removal rates or low pH that lead to higher $NH_2OH$ and $HNO_2$ accumulations could thus be relevant sources of simultaneous abiotic and biotic $N_2O$ production.

**P. Abiotic** $NH_2OH \rightarrow N_2O$

$NH_2OH + HNO_2 \rightarrow N_2O$

$$\left(k_{Abiotic\_1} \cdot S_{NH2OH} \cdot f(pH)\right);\ \left(k_{Abiotic\_2} \cdot S_{NH2OH} \cdot S_{HNO2}\right)$$

Model predictions for every pathway are pH-dependent, either due to substrate speciation or to an enzymatic effect on the maximum growth rate. Aerobic growth of nitrite oxidizing bacteria on $HNO_2$ and heterotrophs on soluble COD are also included.

In the NDHA model the assumption that there is no ND-associated NO production is resolved and $NO_{ND}$ is produced from $HNO_2$ reduction as experimentally observed (Rodriguez-Caballero and Pijuan, 2013; Chandran *et al.*, 2011; Kester, 1997; Wang *et al.*, 2016b; Domingo-Félez *et al.*, 2014).

Whether the source of NO is $NH_2OH$ oxidation or $HNO_2$ reduction will determine the contribution of each autotrophic pathway to $N_2O$ production, NN or ND respectively (**Figure 3.6**). Although oxidation and reduction processes are not uncoupled in the NDHA model, the competition for electrons is represented by $NH_2OH$, the common electron donor: $HNO_2$, NO and DO compete for $NH_2OH$ instead of reduced electron carriers.

The same net $N_2O$ production rate can result from different individual $N_2O$ production/consumption rates. Thus, together with total $N_2O$ production, correctly predicting the individual contribution of each pathway is key for $N_2O$ models. For example, the mitigation strategy of an autotrophic system with a small $N_2O$ sink capacity will differ from that of mixed liquor with a higher $N_2O$ consuming capacity.

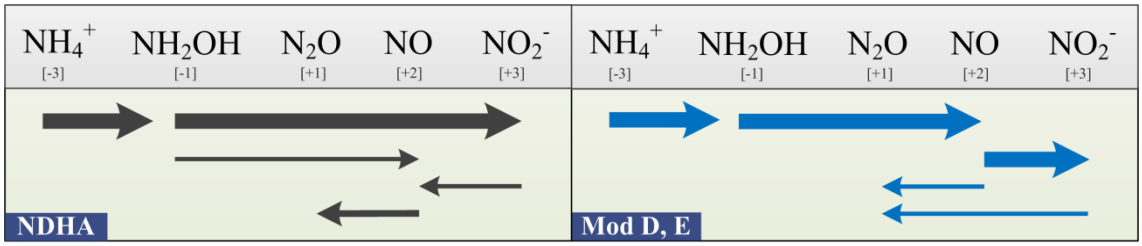


**Figure 3.6.** Schematic comparison of the reactions involved in two-pathway autotrophic models for $N_2O$ production. Arrow widths represent typical reaction rates. Model D (Pocquet *et al.*, 2016), Model E (Ni *et al.*, 2014). (Adapted from **Paper II**).

**Table 3.3.** Gujer matrix for the NDHA model (**Paper IV**):

| Component ▸ Process ▼ | | 1 $S_S$ | 2 $S_{O2}$ | 3 $S_{NH3}$ | 4 $S_{NH2OH}$ | 5 $S_{HNO2}$ | 6 $S_{NO3}$ | 7 $S_{NO}$ | 8 $S_{N2O}$ | 9 $S_{N2}$ | 11 $X_{B,AOB}$ | 12 $X_{B,NOB}$ | 13 $X_{B,H}$ | 14 $X_S$ | 15 $X_I$ |
|---|---|---|---|---|---|---|---|---|---|---|---|---|---|---|---|
| ***AOB growth*** | | | | | | | | | | | | | | | |
| Aerobic_AMO | 1 | | -1.14 | -1 | 1 | | | | | | | | | | |
| Aerobic_HAO* | 2 | | | $-i_{NXB}$ | $-\frac{1}{Y_{AOB}}$ | | | $\frac{1}{Y_{AOB}}$ | | | 1 | | | | |
| Aerobic_HAO | 3 | | $-\left(\frac{2.29-Y_{AOB}}{Y_{AOB}}\right)$ | $-i_{NXB}$ | $-\frac{1}{Y_{AOB}}$ | $\frac{1}{Y_{AOB}}$ | | | | | 1 | | | | |
| Anox_A_NIR | 4 | | | | -1 | -3 | | 4 | | | | | | | |
| Anox_A_NOR | 5 | | | | -1 | | | -2 | 3 | | | | | | |
| ***NOB growth*** | | | | | | | | | | | | | | | |
| Aer_NOB_growth | 6 | | $-\left(\frac{1.14-Y_{NOB}}{Y_{NOB}}\right)$ | $-i_{NXB}$ | | $-\frac{1}{Y_{NOB}}$ | $\frac{1}{Y_{NOB}}$ | | | | | 1 | | | |
| ***HB growth*** | | | | | | | | | | | | | | | |
| Aerobic_H_growth | 7 | $-\frac{1}{Y_{HB}}$ | $-\left(\frac{1-Y_{HB}}{Y_{HB}}\right)$ | $-i_{NXB}$ | | | | | | | | | 1 | | |
| Anox_H_NAR | 8 | $-\frac{1}{Y_{HB}}$ | | $-i_{NXB}$ | | $\left(\frac{1-Y_{HB}}{1.14\cdot Y_{HB}}\right)$ | $-\left(\frac{1-Y_{HB}}{1.14\cdot Y_{HB}}\right)$ | | | | | | 1 | | |
| Anox_H_NIR | 9 | $-\frac{1}{Y_{HB}}$ | | $-i_{NXB}$ | | $-\left(\frac{1-Y_{HB}}{0.57\cdot Y_{HB}}\right)$ | | $\left(\frac{1-Y_{HB}}{0.57\cdot Y_{HB}}\right)$ | | | | | 1 | | |
| Anox_H_NOR | 10 | $-\frac{1}{Y_{HB}}$ | | $-i_{NXB}$ | | | | $-\left(\frac{1-Y_{HB}}{0.57\cdot Y_{HB}}\right)$ | $\left(\frac{1-Y_{HB}}{0.57\cdot Y_{HB}}\right)$ | | | | 1 | | |
| Anox_H_NOS | 11 | $-\frac{1}{Y_{HB}}$ | | $-i_{NXB}$ | | | | | $-\left(\frac{1-Y_{HB}}{0.57\cdot Y_{HB}}\right)$ | $\left(\frac{1-Y_{HB}}{0.57\cdot Y_{HB}}\right)$ | | | 1 | | |
| ***Lysis*** | | | | | | | | | | | | | | | |
| AOB | 12 | | | $i_{NXB}$-$f_I$.$i_{NXI}$-(1-$f_I$).$i_{NXS}$ | | | | | | | -1 | | | 1-$f_{XI}$ | $f_{XI}$ |
| NOB | 13 | | | $i_{NXB}$-$f_I$.$i_{NXI}$-(1-$f_I$).$i_{NXS}$ | | | | | | | | -1 | | 1-$f_{XI}$ | $f_{XI}$ |
| HB | 14 | | | $i_{NXB}$-$f_I$.$i_{NXI}$-(1-$f_I$).$i_{NXS}$ | | | | | | | | | -1 | 1-$f_{XI}$ | $f_{XI}$ |
| ***Hydrolysis*** | | | | | | | | | | | | | | | |
| Aerobic | 15 | 1 | | $i_{NXS}$ | | | | | | | | | | -1 | |
| Anoxic | 16 | 1 | | $i_{NXS}$ | | | | | | | | | | -1 | |
| Anaerobic | 17 | 1 | | $i_{NXS}$ | | | | | | | | | | -1 | |

| Process ▼ | | Process Rate ($g \cdot m^{-3} \cdot min^{-1}$) |
|---|---|---|
| ***AOB growth*** | | |
| Aerobic_AMO | 1 | $\mu_{AMO}^{AOB} \cdot \frac{S_{O2}}{S_{O2} + K_{O2\_AMO}^{AOB}} \cdot \frac{S_{NH3}}{S_{NH3} + K_{NH3}^{AOB} + S_{NH3}^2 / K_{i\_NH3}^{AOB}} \cdot \frac{K_{i\_HNO2}^{AOB}}{S_{HNO2} + K_{i\_HNO2}^{AOB}} \cdot X_{AOB}$ |
| Aerobic_HAO* | 2 | $\mu_{HAO}^{AOB} \cdot \varepsilon_{AOB} \cdot \frac{S_{NH2OH}}{S_{NH2OH} + K_{NH2OH}^{AOB}} \cdot X_{AOB}$ |
| Aerobic_HAO | 3 | $\mu_{HAO}^{AOB} \cdot (1 - \varepsilon_{AOB}) \cdot \frac{S_{O2}}{S_{O2} + K_{O2\_HAO}^{AOB}} \cdot \frac{S_{NH2OH}}{S_{NH2OH} + K_{NH2OH}^{AOB}} \cdot X_{AOB}$ |
| Anox_A_NIR | 4 | $\mu_{HAO}^{AOB} \cdot \eta_{NIR} \cdot \frac{K_{i\_O2}^{AOB}}{S_{O2} + K_{i\_O2}^{AOB}} \cdot \frac{S_{NH2OH}}{S_{NH2OH} + K_{NH2OH\_ND}^{AOB}} \cdot \frac{S_{HNO2}}{S_{HNO2} + K_{HNO2}^{AOB}} \cdot X_{AOB}$ |
| Anox_A_NOR | 5 | $\mu_{HAO}^{AOB} \cdot \eta_{NOR} \cdot \frac{S_{NH2OH}}{S_{NH2OH} + K_{NH2OH\_ND}^{AOB}} \cdot \frac{S_{NO}}{S_{NO} + K_{NO\_ND}^{AOB}} \cdot X_{AOB}$ |
| ***NOB growth*** | | |
| Aer_NOB_growth | 6 | $\mu_{NOB} \cdot \frac{S_{O2}}{S_{O2} + K_{O2}^{NOB}} \cdot \frac{S_{HNO2}}{S_{HNO2} + K_{HNO2}^{NOB} + S_{HNO2}^2 / K_{i\_HNO2}^{NOB}} \cdot \frac{K_{i\_NH3}^{NOB}}{S_{NH3} + K_{i\_NH3}^{NOB}} \cdot X_{NOB}$ |
| ***HB growth*** | | |
| Aerobic_HB_growth | 7 | $\mu_{HB} \cdot \frac{S_{O2}}{S_{O2} + K_{O2}^{HB}} \cdot \frac{S_{NH4}}{S_{NH4} + K_{NH4}^{HB}} \cdot \frac{S_S}{S_S + K_S^{HB}} \cdot X_{HB}$ |
| Anox_HB_NAR | 8 | $\mu_{NAR}^{HB} \cdot \eta_{HD} \cdot \frac{K_{i\_O2\_NAR}^{HB}}{S_{O2} + K_{i\_O2\_NAR}^{HB}} \cdot \frac{S_S}{S_S + K_{S\_NAR}^{HB}} \cdot \frac{S_{NH4}}{S_{NH4} + K_{NH4}^{HB}} \cdot \frac{S_{NO3}}{S_{NO3} + K_{NO3}^{HB}} \cdot X_{HB}$ |
| Anox_HB_NIR | 9 | $\mu_{NIR}^{HB} \cdot \eta_{HD} \cdot \frac{K_{i\_O2\_NIR}^{HB}}{S_{O2} + K_{i\_O2\_NIR}^{HB}} \cdot \frac{K_{i\_NO2\_NIR}^{HB}}{S_{NO} + K_{i\_NO2\_NIR}^{HB}} \cdot \frac{S_S}{S_S + K_{S\_NIR}^{HB}} \cdot \frac{S_{NH4}}{S_{NH4} + K_{NH4}^{HB}} \cdot \frac{S_{NO2}}{S_{NO2} + K_{NO2}^{HB}} \cdot X_{HB}$ |
| Anox_HB_NOR | 10 | $\mu_{NOR}^{HB} \cdot \eta_{HD} \cdot \frac{K_{i\_O2\_NOR}^{HB}}{S_{O2} + K_{i\_O2\_NOR}^{HB}} \cdot \frac{K_{i\_NO2\_NOR}^{HB}}{S_{NO} + K_{i\_NO2\_NOR}^{HB}} \cdot \frac{S_S}{S_S + K_{S\_NOR}^{HB}} \cdot \frac{S_{NH4}}{S_{NH4} + K_{NH4}^{HB}} \cdot \frac{S_{NO}}{S_{NO} + K_{NO}^{HB}} \cdot X_{HB}$ |
| Anox_HB_NOS | 11 | $\mu_{NOS}^{HB} \cdot f(pH) \cdot \eta_{HD} \cdot \frac{K_{i\_O2\_NOS}^{HB}}{S_{O2} + K_{i\_O2\_NOS}^{HB}} \cdot \frac{K_{i\_NO2\_NOS}^{HB}}{S_{NO} + K_{i\_NO2\_NOS}^{HB}} \cdot \frac{S_S}{S_S + K_{S\_NOS}^{HB}} \cdot \frac{S_{NH4}}{S_{NH4} + K_{NH4}^{HB}} \cdot \frac{S_{N2O}}{S_{N2O} + K_{N2O}^{HB}} \cdot X_{HB}$ |
| ***Lysis*** | | |
| AOB | 12 | $b_{AOB} \cdot \left( \frac{S_{O2}}{S_{O2} + K_{O2\_b}} + \eta_{b,anox} \cdot \frac{K_{O2\_b}}{K_{O2\_b} + S_{O2}} \cdot \frac{S_{NOx}}{K_{NO3}^{HB} + S_{NOx}} + \eta_{b,anaer} \cdot \frac{K_{O2\_b}}{K_{O2\_b} + S_{O2}} \cdot \frac{K_{NO3}^{HB}}{K_{NO3}^{HB} + S_{NOx}} \right) \cdot X_{AOB}$ |
| NOB | 13 | $b_{NOB} \cdot (...) \cdot X_{NOB}$ |
| HB | 14 | $b_{HB} \cdot (...) \cdot X_{HB}$ |
| ***Hydrolysis*** | | |
| Aerobic | 15 | $k_H \cdot \frac{X_S / X_{BH}}{K_X + X_S / X_{BH}} \cdot \frac{S_{O2}}{K_{O2}^{HB} + S_{O2}} \cdot X_{HB}$ |
| Anoxic | 16 | $k_H \cdot \eta_{ANOX} \cdot \frac{X_S / X_{BH}}{K_X + X_S / X_{BH}} \cdot \frac{K_{O2}^{HB}}{K_{O2}^{HB} + S_{O2}} \cdot \frac{S_{NOx-}}{K_{NO3}^{HB} + S_{NOx-}} \cdot X_{HB}$ |
| Anaerobic | 17 | $k_H \cdot \eta_{AN} \cdot \frac{X_S / X_{BH}}{K_X + X_S / X_{BH}} \cdot \frac{K_{O2}^{HB}}{K_{O2}^{HB} + S_{O2}} \cdot \frac{K_{NO3}^{HB}}{K_{NO3}^{HB} + S_{NOx-}} \cdot X_{HB}$ |

# 4 Experimental design and parameter estimation

## 4.1 Monitoring nitrous oxide production for model calibration

$N_2O$ is highly soluble in water, over 20 times more than $O_2$ at 20 C, leading to potentially high $N_2O$ bulk concentrations. Yet, at ambient atmospheric $N_2O$ gas concentration (330 ppb, (Stocker *et al.*, 2013)) the equilibrium aqueous concentration is 0.27 μgN/L. The biological production is in equilibrium with physico-chemical processes such as abiotic reactions and physical stripping due to liquid-gas partitioning.

In wastewater treatment applications $N_2O$ can be monitored in both liquid and gas phase. Gas phase measurements are preferred over liquid as $N_2O$ emissions can be directly calculated. However, under low stripping conditions (e.g. mechanical mixing and no aeration) no information is obtained. Liquid phase $N_2O$ measurements are correlated with $N_2O$ emissions via a volumetric mass transfer coefficient ($k_La_{N2O}$ [$d^{-1}$]) that can be experimentally determined (Domingo-Félez *et al.*, 2014). Hence, liquid $N_2O$ measurements provide qualitatively richer information on the net production dynamics compared to gas phase measurements.

**Reactor configurations**

Datasets for $N_2O$ model calibration need to capture the range of operating conditions in which the model will be used. This information can be either directly obtained from the daily reactor performance (Ding *et al.*, 2016) or by conducting targeted experiments (Yang *et al.*, 2009).

Long-term measuring campaigns from full-scale systems provide valuable information on diurnal and seasonal variations (Daelman *et al.*, 2013; Wang *et al.*, 2016b; Spérandio *et al.*, 2016). The hydrodynamic model is, however, as important as the biological model, which increases the model complexity (Ye *et al.*, 2014). The reactor configuration (i.e. SBR, CSTR) and operating conditions (i.e. feeding and aeration strategies) will also impact the information content of the dataset. In a SBR cycle the system undergoes a wide range of concentrations provide compared to a CSTR, where the information content depends on the influent characteristics (Pocquet *et al.*, 2016; Ni *et al.*, 2013b).

Lab-scale systems allow for more controlled environments and more degrees of freedom in the experimental design. However, limitations exist on the representability of lab-scale data on full-scale data (Sin *et al.*, 2005). For example, transient phases or mass transfer limitations can hamper the transferability of information from the lab-scale to the full-scale.

**Datasets**

$N_2O$ models are extensions of existing model structures describing nitrogen transformations. Consequently, the calibration of $N_2O$ models requires datasets of the primary substrates (i.e. DO, $NH_4^+$, $NO_2^-$ , etc.) and additional $N_2O$ measurements (liquid and mass transfer coefficients, or gas phase). The number, the amount and the quality the dataset will pose a direct impact on the calibration results (Brockmann *et al.*, 2008; Dochain and Vanrolleghem, 2001). Quantification of $N_2O$ production intermediates such as NO is not common despite its potential role in model discrimination studies because of its low bulk accumulation (Kampschreur *et al.*, 2008b; Yu *et al.*, 2010; Wang *et al.*, 2016b; Pocquet *et al.*, 2016). Similarly, $NH_2OH$ is rarely quantified and the liquid accumulation is reported low (< 0.1mgN/L) (Yu and Chandran, 2010; Soler-Jofra *et al.*, 2016).

**Respirometry**

Respirometry is an experimental protocol for estimating metabolic rates by measuring consumption of oxygen (or potentially other terminal electron acceptor). The acquisition of DO data relies on high frequency and high sensitive liquid oxygen measurements, allowing automated and continuous measurements (**Figure 4.1**). The burden of chemical-specific analyses (e.g. $NH_4^+$, $NO_2^-$) associated to substrate depletion tests is alleviated (Chandran *et al.*, 2008). Respirometric tests are best for the determination of extant kinetic parameters, which are representative of the existing condition of the biomass (Ellis *et al.*, 1996), and have been applied to characterize aerobic degradation processes in activated sludge (Vanrolleghem *et al.*, 1999). Aerobic carbon degradation (Gernaey et al., 2002) and nitrification processes have been interpreted and optimized via respirometry (Chandran and Smets, 2005). The $N_2O$ and NO response of several pure cultures of AOB during $NH_3$ and $NH_2OH$ oxidation has also been determined via microrespirometric assays (Kozlowski *et al.*, 2016).

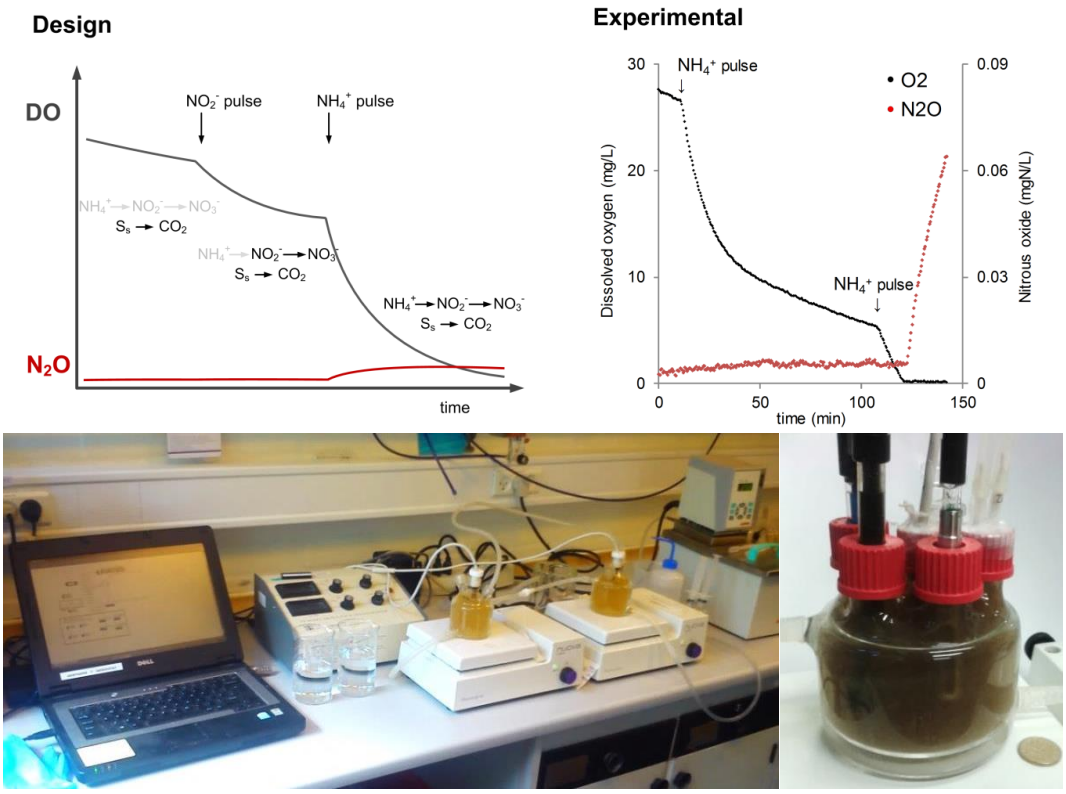


**Figure 4.1.** Top: Schematic of a respirometric assay to estimate nitrification kinetics: left, design; right, experimental DO and liquid $N_2O$ concentrations for two consecutive $NH_4^+$ pulses. Bottom: Experimental setup used for respirometric assays. (**Paper III, IV**).

## Experimental design

In the initial experimental design of this study the regulation of $N_2O$ production – effect of DO, $NO_x^-$, etc. – allows evaluating the performance of existing $N_2O$ model structures (**Figure 4.1**). Mostly, parameters associated to $N_2O$ production are estimated and the capabilities of model structure are assessed based on best-fit simulations (**Paper I**) (Ni *et al.*, 2013c; Ding *et al.*, 2016). However, the experimental design indicates that $N_2O$ emissions are also sensitive to parameters indirectly related to $N_2O$ production (e.g. $\mu_{NOB}$, $k_H$). Hence, the following experimental design aims at obtaining accurate parameter estimates that will reduce the uncertainty of $N_2O$ emissions.

Specific respirometric assays are designed to estimate parameters from the NDHA model structure. Parameter estimates should reflect *in situ* microbial activity (extant) and minimize Monod parameter correlation. Designs consider a low initial substrate-to-initial biomass concentration ($S_0/X_0$) but sufficiently high initial substrate-to-substrate affinity ($S_0/K_S$) (Huang *et al.*, 2014).

During respirometric assays the electron donor consumption (e.g. $NH_4^+$) is measured indirectly by tracking electron acceptor depletion (DO). Simultaneously, the set up can monitor online other variables of interest (e.g. $N_2O$, NO, pH). Datasets for the NDHA model calibration are obtained from respirometric assays and, for those under anoxic conditions, substrate depletion experiments (**Table 4.1**).

**Table 4.1.** Experimental design for respirometric assays (shaded corresponds to anoxic experiments)

| Spikes | Targeted processes | $N_2O$ pathways |
|---|---|---|
| $NH_4^+$ | $NH_4^+$ removal by AOB | NN, ND |
| $NH_2OH$ | $NH_2OH$ removal by AOB | NN, ND |
| $NO_2^-$ | $NO_2^-$ removal by NOB | HD |
| $NH_4^+$, $NH_2OH$, $NO_2^-$ | AOB-driven $N_2O$ production | NN, ND |
| $N_2O$, $NO_2^-$ | HB-driven $N_2O$ production | HD |

A lab-scale respirometer (400-mL) was designed to continuously monitor DO consumption rates. The vessel geometry allows the continuous monitoring of DO, pH, NO and $N_2O$, and the collection of grab samples (**Figure 4.1**). Parallel assays are performed at 25°C in jacketed glass vessels completely filled with biomass and sealed with the insertion of the following sensors: Clark-type polarographic DO electrode, liquid NO, liquid $N_2O$ and pH. In the respirometric assays two types of biomass representative of wastewater treatment systems are studied in Respirom_PN, Respirom_ML:

**Mixed liquor -** Mixed liquor derived from a full-scale phase-isolated activated sludge wastewater treatment plant (700,000 PE Lynetten, Copenhagen, Denmark). Quantitative polymerase chain reaction (qPCR) was used to enumerate the quantities of AOB, *Nitrobacter spp.* and *Nitrospira spp.*, targeting the 16S gene (*Nitrospira spp.* 92 ± 3% relative abundance in comparison to 8 ± 3% of *Nitrobacter spp*., and AOB:NOB = 3:1). Details on the qPCR protocol can be found in (Terada *et al.*, 2010).

**Nitritating enrichment -** A lab-scale nitrifying sequencing batch reactor (5 L) enrichment from an AS mixed liquor sample with $NH_4^+$ as the only nutrient was maintained at oxygen-limited conditions. $NH_4^+$ removal was 82 ± 14%, and nitritation efficiency ($NO_2^-/NH_4^+{}_{removed}$) at 85 ± 24%. The biomass composition, based on 16 rRNA targeted qPCR analysis had a dominance of AOB over NOB (30:1). Among NOB species, and differently from the mixed liquor biomass, *Nitrobacter spp.* dominates over *Nitrospira spp*. (≈ 700:1).

Differences in relative abundance of NOB species are in accordance with their substrate affinity, where *Nitrobacter spp.* dominate over *Nitrospira spp.* in high $NO_2^-$ environments ($NO_2^-$ > 100 and < 1 mgN/L in nitritating enrichment and mixed liquor respectively) (Nowka *et al.*, 2014).

| | Respirom_PN | Respirom_ML | Respirom_ML_aer | | Batch_HD* |
|---|---|---|---|---|---|
| Aeration mode | Preaerated → anoxia | Preaerated → anoxia | Continuous | Continuous | - |
| Substrate addition | Pulse | Pulse | Pulse | Pulse (excess) | Pulse (excess) |
| Biomass | AOB-enriched | Mixed Liquor | Mixed Liquor | Mixed Liquor | Mixed denitrifying |
| Reactor volume | 400 mL | 400 mL | 400 mL | 3 L | 330 mL |
| Used in | Paper III | Paper IV | | Paper I | Paper V |

* from Ribera-Guardia *et al.* (2014)

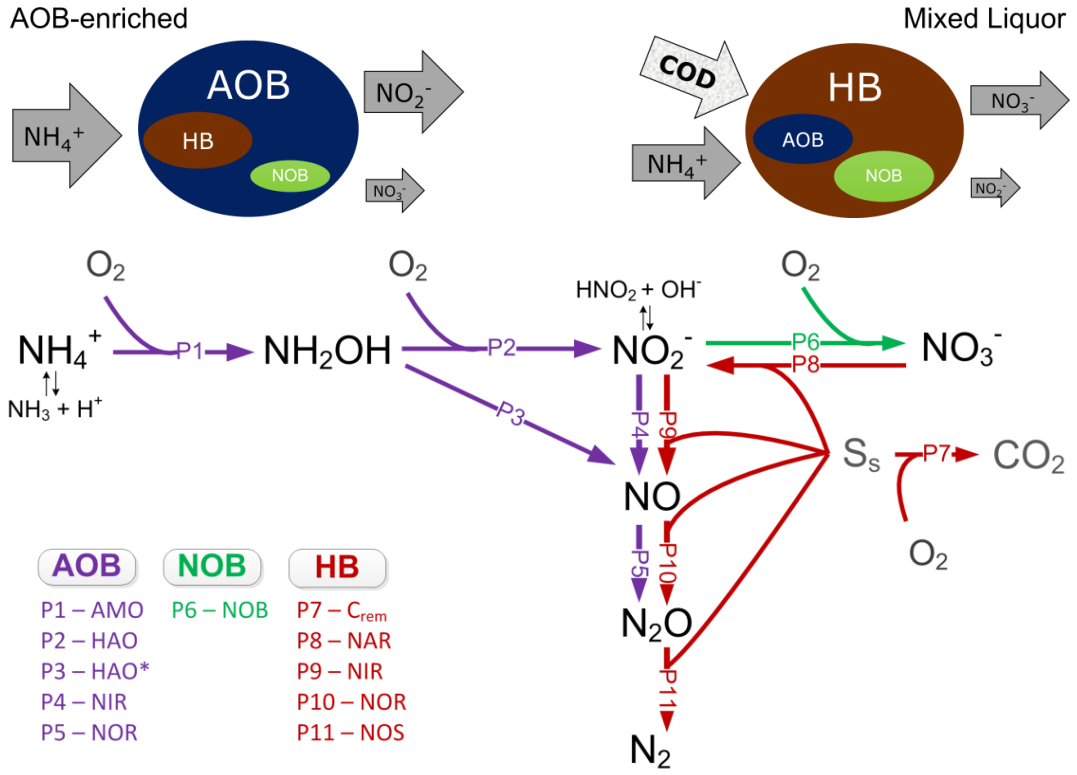


**Figure 4.2.** Top: Characteristics of the experimental designs used. Middle: Diagram of the microbial composition for the two different biomasses studied. Bottom: Main substrates and processes from a nitrogen removing community (**Paper I, III, IV, V**).

The kinetics of the oxidation of the primary N-substrates ($NH_4^+$ and $NO_2^-$) are individually and step-wise measured via extant respirometry at varying DO concentrations (Chandran and Smets, 2005). The purpose is to predict the fate of the primary N-substrates based on the specific oxygen-consuming rate. If a model captures accurately the relevant oxygen-consuming processes, then DO and the primary N-substrates are predicted accurately too. By sequentially adding substrate pulses from oxidized to reduced form (endogenous →

$NO_2^- \rightarrow NH_2OH \rightarrow NH_4^+$), based on the NDHA model structure the individual rates can be isolated (**Figure 4.2**, P1-P11). In all experiments, even prior to any substrate spikes, oxygen consumption is always positive and proportional to the biomass concentration due to endogenous respiration.

Based on the overall good fit of model predictions and experimental data the NDHA model describes the dynamics of the measured DO and N-species for the AOB-enriched and mixed liquor biomass ($R^2 > 0.99$ and 0.94 respectively) (**Figure 4.3**). Best-fit parameter estimates are estimated at high accuracy: coefficients of variation are below 7% for the AOB-enriched and below 25% for the mixed liquor and the collinearity indices below 15, as suggested for identifiable subsets (Brun *et al.*, 2002) (**Table 4.2**). The high correlation observed between $\mu_{AOB.AMO}$-$K_{AOB.NH3}$ and $\mu_{NOB}$-$K_{NOB.HNO2}$ ($\rho > 0.80$ ) typically occurs for Monod-type kinetics but it does not affect their identifiability.

In sum, the respirometric experimental design can be used to precisely identify and calibrate the primary substrate dynamics of the NDHA model based on the DO profiles.

**Table 4.2.** Estimated NDHA model parameters from DO datasets (estimated at 20 C) (**Paper III, IV**).

| **Respirom_PN** | | |
|---|---|---|
| **Parameter** | **Unit** | **Value** |
| $\mu_{AOB.AMO}$ | $d^{-1}$ | 0.49 ± 0.01 |
| $\mu_{NOB}$ | $d^{-1}$ | 0.67 ± 0.07 |
| $k_H$ | $d^{-1}$ | 2.01 ± 0.02 |
| $K_{AOB.NH3}$ | mgN/L | 0.12 ± 0.005 |
| $K_{AOB.O2.AMO}$ | mgO2/L | 0.23 ± 0.02 |

| **Respirom_ML** | | |
|---|---|---|
| **Parameter** | **Unit** | **Value** |
| $\mu_{AOB.AMO}$ | $d^{-1}$ | 0.49 ± 0.01 |
| $\mu_{NOB}$ | $d^{-1}$ | 1.04 ± 0.05 |
| $\mu_{HB}$ | $d^{-1}$ | 5.15 ± 0.11 |
| $K_{AOB.NH3}$ | µgN/L | 7.00 ± 1.17 |
| $K_{NOB.HNO2}$ | µgN/L | 0.027 ± 0.006 |

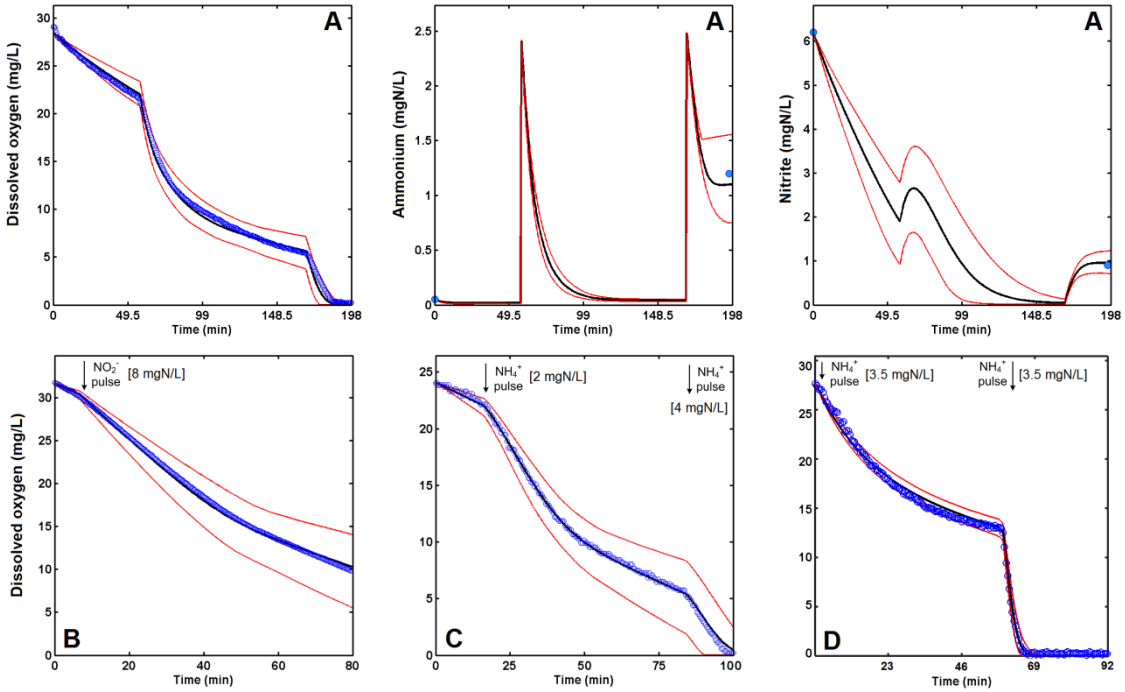


**Figure 4.3.** Experimental DO, $NH_4^+$ and $NO_2^-$ (blue markers) and model predictions (black line best-fit, red lines 95% CI) for the DO calibration from respirometric assays. (A) DO, $NH_4^+$ and $NO_2^-$ concentrations. (B), (C), (D), DO concentrations after pulse additions (D: pH changed from 7 to 8 before the second $NH_4^+$ pulse). Respirom_PN (A, D), Respirom_ML (B, C). (**Paper III, IV**).

## Abiotic $N_2O$ production

To study the effect of $HNO_2$, $NH_2OH$ and pH on abiotic $N_2O$ production a factorial experimental design is constructed (**Table 4.3**). Results show that in the absence of $NO_2^-$, $NH_2OH$-driven abiotic $N_2O$ production only occurs at very high pH (≥ 8.7) (**Figure 4.4**). Coupling $HNO_2$ and $NH_2OH$ produces $N_2O$ at high pH (≥ 8) and high $NH_2OH$ (≥ 0.5 mgN/L). Therefore high $NO_2^-$ and $NH_2OH$ concentrations are necessary, outside the range of typical wastewater systems (pH > 8.4, $NO_2^-$ > 500 mgN/L, $NH_2OH$ ≥ 0.5 mgN/L).

**Table 4.3.** Factorial experimental design to study abiotic $N_2O$ production. (Unpublished data).

| | | | | | |
|---|---|---|---|---|---|
| $HNO_2$ (µgN/L) | 0 | 0.2 | 2 | 20 | 100 |
| $NH_2OH$ (mgN/L) | 0 | 0.05 | 0.2 | 0.5 | 2 |
| pH | 6.5 | 7.25 | 8 | 8.7 | 9.4 |

Overall, the substrate concentrations necessary to produce $N_2O$ abiotically are outside the range of the experiments design to calibrate the NDHA model: high pH, $NO_2^-$ and $NH_2OH$.

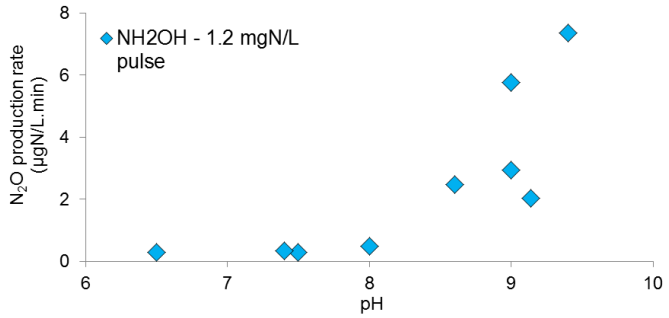


**Figure 4.4.** Abiotic $N_2O$ production rates for $NH_2OH$ pulses (1.2 mgN/L) at varying pH. (Unpublished data).

## 4.2 Parameter estimation and model evaluation

The objective of the experimental studies is to obtain informative $N_2O$ datasets that allows the estimation of parameters associated to $N_2O$ production with the NDHA model. The ability of the results obtained from lab-scale experimentation to predict full-scale processes remains to be validated.

Systematic calibration protocols for activated sludge models are applied to wastewater treatment operations. Numerous experimental methodologies and calibration approaches exist with varying degrees of automatization and requirements (e.g. influent fractionation, parameter subset selection, parameter estimation procedure, etc.) (Corominas et al., 2011; Mannina et al., 2011; Sin et al., 2008). Deterministic methods have been commonly used, but with increasing computational power Bayesian methodologies are being proposed to activated sludge models (Sharifi *et al.*, 2014; Martin and Ayesa, 2010).

However, $N_2O$ modelling studies still lack fundamental process understanding and have not been integrated in calibration protocols yet. While some $N_2O$ models have reported a calibration framework (Guo and Vanrolleghem, 2014), in most $N_2O$ models the parameter estimation procedures are often ill-described, with little information about each step. For example, the parameter subset selection procedure is sometimes not addressed.

$N_2O$ modelling efforts currently focus on evaluating the capabilities of model structures to describe $N_2O$ production with best-fit simulations (Ni *et al.*, 2013c; Spérandio *et al.*, 2016) (**Paper I**). However, the quality of the $N_2O$ calibration results has not been analysed further in-depth as occurs for other environmental models (Bennett *et al.*, 2013). Hence, more rigorous tools for model response evaluation will become more important to discriminate between $N_2O$ models, especially for models with similar best-fit predictions (Lang *et al.*, 2017).

The focus of this study is on the parameter estimation procedure and validation of the model response and the estimated parameter values (**Figure 4.5**). The methods presented represent a rigorous tool that will benefit $N_2O$ model discrimination procedures.

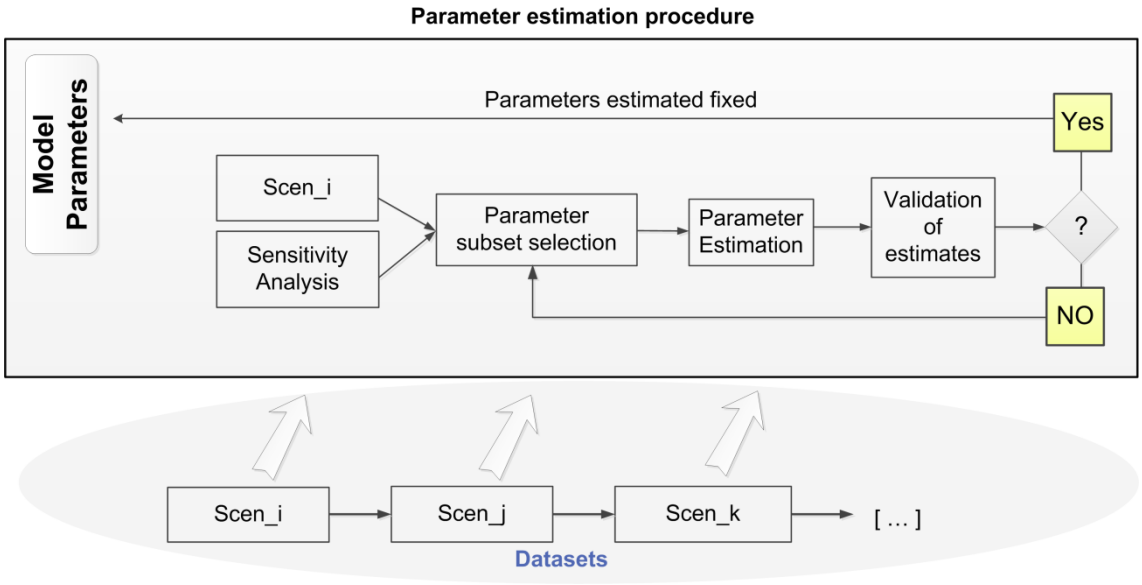


**Figure 4.5.** Parameter estimation procedure. (**Paper III, IV**).

### Parameter subset selection

The objective of this step is to select the parameters to be estimated from a given scenario. Sensitivity analysis techniques identify those parameters where a change in value leads to a large variation in model output. High sensitivity is a necessary, but not sufficient, condition for a parameter to be identified (Dochain and Vanrolleghem, 2001). Local sensitivity analysis (LSA) analyses the model response to individual parameter changes and have been applied to $N_2O$ model calibrations (Pocquet *et al.*, 2016; Spérandio *et al.*, 2016). The drawback of LSA rankings is that results depend on the parameter values and do not capture parameter interactions, for which global sensitivity analysis is required (GSA) (Brun *et al.*, 2001; Sweetapple *et al.*, 2013). For GHG emissions, GSA methods are preferred over LSA despite the higher computational costs (Sweetapple *et al.*, 2013; Boiocchi *et al.*, 2017; Mannina and Cosenza, 2015). GSA is beneficial to identify sensitive parameters, but more importantly, to identify what parameters cannot be estimated to fix their values. Hence, the Standardized Regression Coefficient (SRC) method is used to identify non-sensitive parameters and fix them to their default value (**Figure 4.6**). Dynamic and averaged results are combined as a screening method to manually select the top sensitive parameters that are considered for estimation (Machado *et al.*, 2009). Among these parameters subsets of different size and combination of parameters are considered. Metrics such as RDE (Machado *et al.*, 2009) and modE are used to quantify the information con-

tent of a dataset and elucidate what parameter subset should be estimated (**Paper III**).

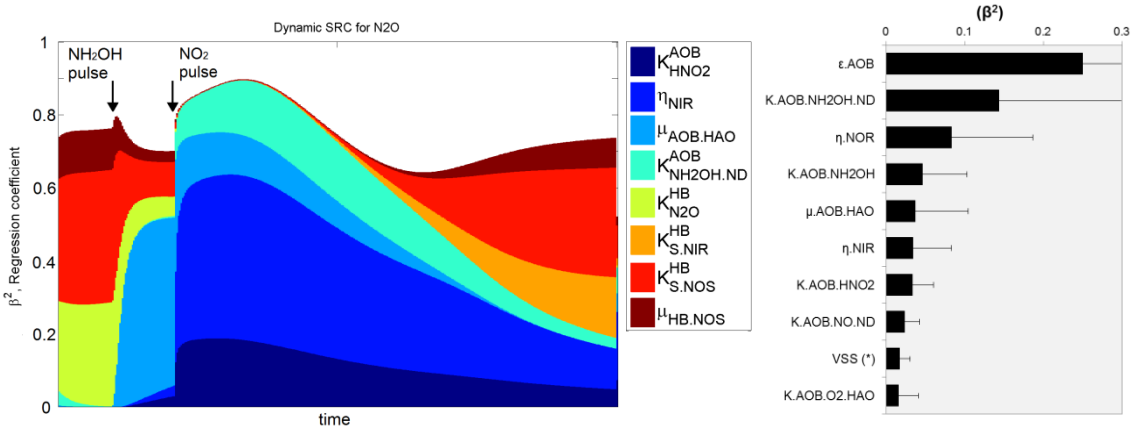


**Figure 4.6.** Global sensitivity analysis for $N_2O$, an example from Respirom_PN (**Figure 4.1**). Left: Dynamic $N_2O$ sensitivity ($\beta^2$) of an experiment targeting ND-associated parameters where $NH_2OH$ and $NO_2^-$ were spiked. The sensitivity of $\mu_{AOB.HAO}$ increases after the $NH_2OH$ pulse and the sensitivity $\eta_{NIR}$ and $K_{AOB.HNO2}$ increased after the $NO_2^-$ pulse. Right: Averaged sensitivity during an $NH_4^+$ oxidation experiment targeting NN-associated parameters. The three parameters to which liquid $N_2O$ concentrations are most sensitive to: $\varepsilon_{AOB}$, $K_{AOB.NH2OH}$ and $\eta_{NOR}$. (**Paper III**).

## Parameter estimation

The objective function for the minimization problem is defined as:

$$\mathrm{RMNSE} = \sum_{k}^{m}\sum_{j}^{n}\frac{\mathrm{RMSE_j}}{\bar{y}_{obs,j}}; \qquad \mathrm{RMSE_j} = \sqrt{\frac{\sum_i^p\left(y_{sim,i} - y_{obs,i}\right)^2}{p}}$$

Where *m* is the number of experiments in one scenario (e.g. 2 $NH_4^+$ experiments in Scenario (C)), *n* the number of data series in one experiment (e.g. NO, $N_2O$), *p* experimental points of each data series, $y_{sim,i}$ the model prediction and $y_{obs,i}$ the experimental data at time *i*. As the dimensions of the minimization problem increase (i.e. number of parameters) the convergence of the algorithm to a minimum becomes more computationally demanding. Additionally, single search algorithms might not find the global minimum among multiple minima (Nelder and Mead, 1965). Thus, to avoid finding a local minimum, global and multiple largely-bounded local optimization algorithms are used (Wágner *et al.*, 2016).

### Validation of model response

Previous $N_2O$ models describe the overall fit and capabilities based on the visual inspection or regression of model simulations and experimental data (Lang *et al.*, 2017; Pan *et al.*, 2015; Ding *et al.*, 2016). For example, the performance of two models cannot be compared via visual inspection (Ni *et al.*, 2014) or regression coefficients ($R^2$), which do not identify structural deficiencies unless combined with quantitative metrics such as RMSE (Haefner, 2005). A more rigorous analysis of residuals (e.g. Gaussian distributions, autocorrelation functions (ACF), F-test, etc.) is required to validate the model response (Bennett *et al.*, 2013). In this study the F-test is used as it can identify a deficient model fit despite a visually good fit and high degree of correlation ($R^2 > 0.99$).

### Validation of parameter values

By addressing the practical identifiability of newly estimated parameters model calibrations and experimental designs can be compared to discriminate between $N_2O$ models. What is the confidence in the reported best-fit parameter values? Approximate confidence regions can be calculated with different methods. Based on the error function and the size of the parameter subset and dataset (Beale, 1960), or considering the Fisher Information Matrix (FIM) as a lower bound for the variance matrix (Dochain and Vanrolleghem, 2001). The FIM summarises the information concerning the model parameters gained from an experiment:

$$\mathrm{FIM} = \sum_{i=1}^{N} Y_p\left(t_i, \underline{\theta}\right)^T \underline{Q_i} Y_p\left(t_i, \underline{\theta}\right)$$

where $Y_p$ is the output sensitivity function with respect to the parameters $\theta$ and $\underline{Q_i}$ the weighting matrix, typically selected as the inverse of the error covariance matrix. This method is widely used, but assumes a linear approximation of the state variables with respect to the parameters, which might not apply to non-linear systems. The bootstrap method analyses the system properties by using repeated simulations, like a Monte-Carlo method, and has been successfully applied in those cases (Joshi *et al.*, 2006). Hence, if the confidence intervals of the parameter estimates are determined more accurately the 95% confidence intervals of the state variables will be calculated more precisely.

In $N_2O$ model evaluation studies the parameter variance and correlation matrix, indicators of the confidence that can be given to a value, are not typically reported, which complicates the comparison between studies (Spérandio *et al.*, 2016; Ding *et al.*, 2016; Pocquet *et al.*, 2016; Kim *et al.*, 2017) (**Paper I**). Sometimes overlooked, methods used to calculate confidence intervals for parameter estimates often rely on structural assumption of the residuals. Here, to improve these limitations the gaussian distribution (Kolmogorov-Smirnov test 95%) and the interdependency of residuals at different lag times are analysed and minimized when possible (Lilliefors, 1967; Cierkens *et al.*, 2012) (**Figure 4.7**). The autocorrelation of residuals is minimized by reducing the data acquisition frequency, which increased the confidence interval of the estimated parameters (**Figure 4.7**). Testing the model response can avoid over interpretation of the dataset and uncertainty underestimation (variance/mean ≪ 0.001% (Peng *et al.*, 2015)).

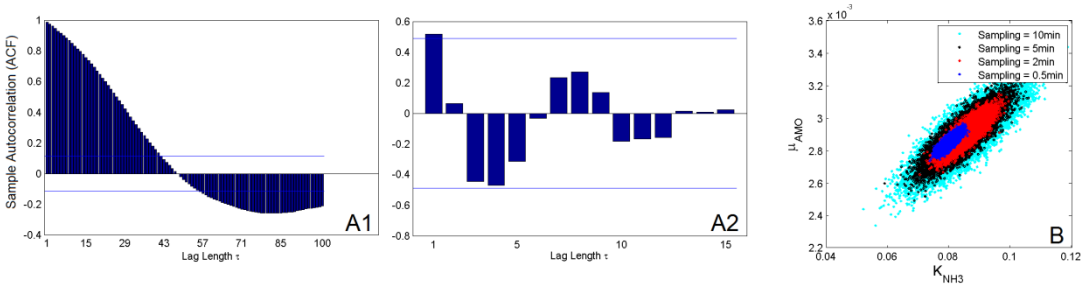


**Figure 4.7.** Autocorrelation of DO residuals for increasing time lags (τ) from an experiment used to estimate parameters associated with $NH_4^+$ oxidation ($K_{AOB.NH3}$, $\mu_{AOB.AMO}$). A1: Residuals from the original dataset. A2: residuals from the downsampled dataset. B: Pairwise samples from the estimated multivariate normal distribution for $K_{AOB.NH3}$ (mgN/L) and $\mu_{AOB.AMO}$ ($min^{-1}$) for sampling rates of 0.5 (blue), 2 (red), 5 (black) and 10 (cyan) minutes. (**Paper III**).

### Uncertainty propagation

The uncertainty obtained during parameter estimation can be used to build confidence intervals in model predictions (Neumann and Gujer, 2008; Belia *et al.*, 2009).

The precision, or width of the confidence interval, associated to $N_2O$ emissions will be a key factor to consider when comparing the performance of $N_2O$ models during the development of mitigation strategies. Specifically, the carbon footprint of wastewater systems is very sensitive to $N_2O$ emissions (Gustavsson and Tumlin, 2013) and precise predictions are desired. Yet, the

uncertainty of $N_2O$ emissions associated to parameter estimation has never been studied.

Here, the uncertainty from the parameter estimation results is evaluated via Monte-Carlo simulations. The reliability of predictive distributions (95% confidence intervals) is used to validate the model response as suggested by (Jin *et al.*, 2010). Parameter values were sampled via Latin Hypercube Sampling (LHS, n = 500) for two cases: (1) from literature following (Sin *et al.*, 2009), and (2), compared to the distributions obtained after parameter estimation. As an example, in **Paper IV**, the uncertainty of $N_2O$ and NO emissions during excess $NH_4^+$ oxidation at two different DO levels (0.5, 2.0 mg/L) is described. The calibrated NDHA model predicts for low and high DO, an $N_2O$ emission factor of 4.6 ± 0.6 % and 1.2 ± 0.1% (case (2)), which corresponds to low coefficients of variation (9 and 12%). However, when the uncertainty is propagated based on the reference case (1) the confidence intervals are 360% larger. These results highlight the importance of evaluating the uncertainty of parameter estimates in $N_2O$ emissions, but unfortunately cannot be compared to other $N_2O$ modelling studies.

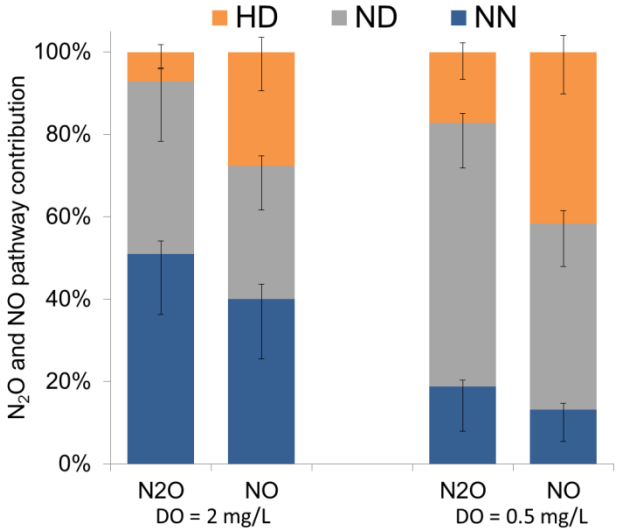


**Figure 4.8.** Nitrous oxide ($N_2O$) and nitric oxide (NO) pathway contribution during $NH_4^+$ oxidation at low and high DO for the calibrated NDHA model for mixed liquor biomass. The standard deviations correspond to uncertainty from estimated parameters: (top) from Respirom_ML, (bottom) default by classes following (Sin *et al.*, 2009) (n = 500). (**Paper IV**).

In this work, mathematical models and calculations were implemented in the Matlab-Simulink environment (The MathWorks, Natick, MA) (**Paper III**, **IV** and **V**) and in Aquasim (Reichert, 1998) (**Paper I**).

# 5 Model evaluation

## 5.1 Case 1: AOB-enriched biomass

A novel experimental design to calibrate $N_2O$ models through extant respirometry is evaluated on an AOB-enriched biomass.

**Nitrous oxide production: Experimental and modelling results**

Aerobic $NH_4^+$-oxidation products, $NH_2OH$ and $NO_2^-$ are responsible for the higher $N_2O$ production rate at the onset of anoxia and not $NH_4^+$ itself, which requires molecular $O_2$ for its oxidation (Sayavedra-Soto *et al.*, 1996). The higher $N_2O$ yield of nitrifying biomass and pure cultures fed on $NH_2OH$ compared to $NH_4^+$ observed has been already reported (de Bruijn *et al.*, 1995; Kim *et al.*, 2010; Kozlowski *et al.*, 2016). However, even under anoxic conditions the sole presence of $NH_2OH$ also yields a large amount of $N_2O$, recently suggested as a new $N_2O$ producing pathway by (cyt) P460 (Caranto *et al.*, 2016). The addition of an electron donor like $NO_2^-$ further increases $N_2O$ production, highlighting the role of the primary N-substrates on $N_2O$ dynamics, especially of $NH_2OH$ (**Figure 5.1**). Based on the model structure of other two-pathway models for AOB none can predict the observed $N_2O$ dynamics: while in certain models $NH_2OH$ does not react under anoxic conditions (Ding *et al.*, 2016; Pocquet *et al.*, 2016), in other $NH_2OH$ reacts producing both $N_2O$ and $HNO_2$ (Ni *et al.*, 2014).

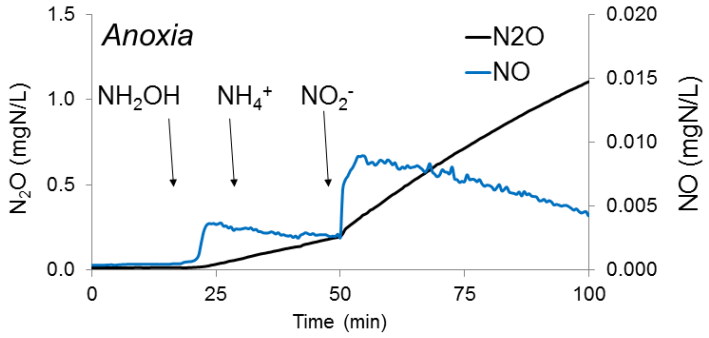


**Figure 5.1.** Experimental $N_2O$ (black) and NO (blue) liquid concentrations after $NH_2OH$, $NH_4^+$ and $NO_2^-$ pulses added under anoxia for the AOB-enriched biomass. (Unpublished data).

Parameter estimation to fit the $N_2O$ datasets is performed after the NDHA model showed a good fit for DO and hence for the main N-substrates ($NH_4^+$,

$NO_2^-$, $NO_3^-$). The sequence in which the $N_2O$-associated parameters are estimated targeted each $N_2O$ production pathway as follows: under anoxia and no electron donors for AOB (e.g. $NH_2OH$) the contributions of NN and ND are null and hence HD-associated parameters can be estimated independently, and the new estimated parameters fixed. During $NH_4^+$ oxidation experiments at high DO levels the ND and HD contributions are minimal, as both are inhibited by DO, and NN-associated parameters can be estimated and fixed. Finally, the ND contribution is estimated from $NH_4^+$ and $NH_2OH$ oxidation experiments at low DO.

Specifically for the AOB contribution, $N_2O$ production observed from $NH_4^+$ oxidation at high DO is used to calibrate the NN pathway. Then, experiments designed to reach anoxia at varying $HNO_2$ concentrations are used to estimate parameters associated to the ND pathway, as they are the most sensitive. After parameter estimation the NDHA model describes the $N_2O$ production dynamics and yield observed in the calibration datasets (F-test = 1). After parameter estimation the 95% predictive distribution for liquid $N_2O$ narrows by 58% from the reference uncertainty scenario (Sin *et al.*, 2009). The model is then validated on three batches with lower $HNO_2$ and with higher $NH_2OH$ pulses. The average Janus coefficient is 1.57 and $R^2$ is 0.985, indicating a good validation (**Figure 5.2**, bottom). Hence, the NDHA model can describe the $N_2O$ production rates at a range of DO and $HNO_2$ concentrations. For more details see **Paper III**.

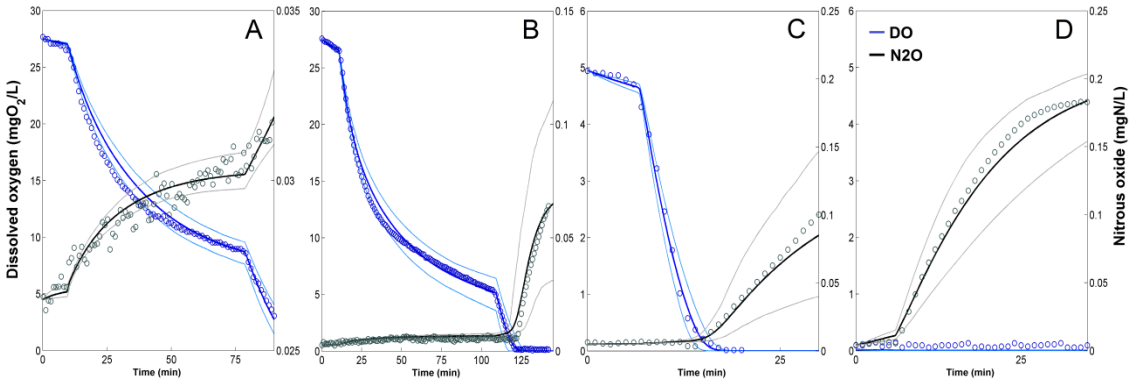


**Figure 5.2.** Experimental (markers) and model predictions (dark lines – best-fit, light lines - 95% CI) for the experiments from Respirom_PN. From left to right: (A) Aerobic $NH_4^+$ pulses, (B) Aerobic → anoxic $NH_4^+$ pulses, (C) Aerobic $NH_4^+$ pulse, (D) Anoxic $NH_2OH$ pulse. (**Paper III**).

## Model evaluation

Evaluations of the NDHA model at varying DO and $HNO_2$ concentrations at pH = 7.5 are performed to study the variability of $N_2O$ emissions at a wider range of operating conditions (**Figure 5.3**). The model predicts the largest $N_2O$ emission at the lowest DO and high $HNO_2$; and the lowest $N_2O$ emission at the highest DO and lowest $HNO_2$. This relationship has been described by other two-pathway models, where ND was the main contributor to the $N_2O$ emission factor during $NH_4^+$ oxidation (Pocquet *et al.*, 2016; Ni *et al.*, 2014). The contribution of the NN pathway is maximal when $HNO_2$ is not present and decreased with increasing $HNO_2$. On the other hand, the ND contribution follows opposite trends, indicating a shift between autotrophic pathways driven by $HNO_2$ and DO. The HD contribution is maximal at low DO and high $HNO_2$ but at low levels.

The uncertainty of the $N_2O$ emission factor is, in average, only 25% of that predicted with the reference case. Taken together, the $N_2O$ production observed in all the scenarios can only be potentially described by the NDHA model structure compared to other $N_2O$ models (Ni *et al.*, 2014; Pocquet *et al.*, 2016; Ding *et al.*, 2016) (**Paper II**) (**Figure 3.6**). Additionally, the estimated parameters from respirometric assays decrease significantly the uncertainty of $N_2O$ emissions.

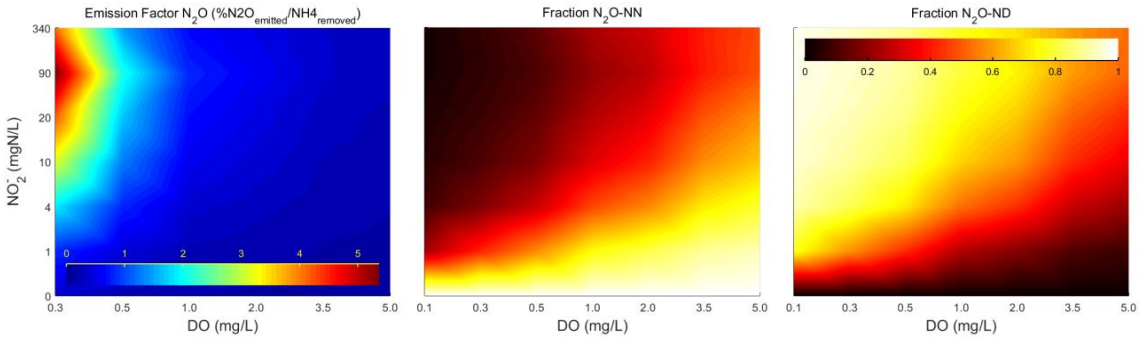


**Figure 5.3.** NDHA model simulations with best-fit parameters: $N_2O$ emissions (% $N_2O_{emitted}/NH_4^+{}_{removed}$) and NN (middle) and ND (right) pathway contributions. The contribution of the HD pathway is not shown, maximum 0.02. $NH_4^+$ oxidation by AOB-enriched biomass at constant DO (0.1 - 0.3 - 0.5 - 1.0 - 2.0 - 3.5 - 5.0 mg/L), and $NO_2^-$ (0 – 1 – 4 – 10 – 20 – 90 – 340 mgN/L). (**Paper III**).

## 5.2 Case 2: Mixed liquor biomass

A nitrification/denitrification case study is used to investigate, with default parameter values, the main processes driving $N_2O$ production and sources of uncertainty during aerobic $NH_4^+$ removal. The majority of $N_2O$ is emitted during the aerobic part of the cycle, when $NH_4^+$ oxidation occurs. The GSA ranking shows that up to four of the ten most sensitive parameters for $N_2O$ and NO liquid concentrations correspond to AOB, and the rest to NOB and HB. These results highlight the importance of NOB and HB together with AOB on the $N_2O$ production from a mixed culture biomass during $NH_4^+$ oxidation. The experimental design developed that targets sources of uncertainty for $N_2O$ emission predictions should include NOB and HB processes.

**Nitrous oxide production: Experimental and modelling results**

Irrespectively of the N-substrate being oxidized, at the onset of anoxia NO and $N_2O$ concentrations increase. First NO, and then $N_2O$, reach a maximum followed by a steady decrease, indicating net $N_2O$ consumption.

In this study, the HD contribution is estimated first as no electron donors for AOB are present (addition of $N_2O$, $NO_2^-$, $NO_3^-$ or soluble organic carbon). Hence, ten parameters associated to hydrolysis of particulates, heterotrophic denitrification and organic carbon removal are estimated. Of special interest, three parameters associated to $N_2O$ consumption: two describing the pH dependence of the maximum reduction rate ($w_{nosZ}$, $pH_{opt.nosZ}$) and the substrate affinity for $N_2O$ ($K_{HB.N2O}$) (**Figure 5.4**, **Table 5.1**). Similarly to **Paper III**, the contribution of the NN pathway is estimated next during $NH_4^+$ oxidation at high DO, followed by the ND.

**Table 5.1.** Selected NDHA model parameters estimated from $N_2O$ and NO datasets. (**Paper III, IV**).

**Respirom_PN**

| Parameter | Unit | Value |
|---|---|---|
| $\varepsilon_{AOB}$ | ( - ) | $0.48 \pm 0.005$ ($x10^{-3}$) |
| $\eta_{NOR}$ | ( - ) | $0.16 \pm 0.005$ |
| $K_{AOB.NH2OH.ND}$ | mgN/L | $0.25 \pm 0.005$ |
| $K_{AOB.HNO2}$ | µgN/L | $0.67 \pm 0.03$ |

**Respirom_ML**

| Parameter | Unit | Value |
|---|---|---|
| $\varepsilon_{AOB}$ | ( - ) | $0.0031 \pm 0.0001$ |
| $\eta_{NOR}$ | ( - ) | $0.36 \pm 0.02$ |
| $\eta_{NIR}$ | ( - ) | $0.22 \pm 0.01$ |
| $pH_{opt.nosZ}$ | ( - ) | $7.9 \pm 0.1$ |
| $w_{nosZ}$ | ( - ) | $2.2 \pm 0.2$ |
| $K_{HB.N2O}$ | mgN/L | $0.078 \pm 0.020$ |

Based on the overall good fit of model predictions and experimental data the NDHA model describes the dynamics of the measured DO and N-species ($R^2 \geq 0.94$). A total of 17 parameters are estimated with bounded approximate

confidence regions indicating good identifiability (CV < 25%). For more details see **Paper IV**.

The predictive ability of the calibrated NDHA model is evaluated on a set of batch experiments when mixed liquor biomass from the same WWTP had been subject to varying N pulses at constant aeration (For details see **Paper I**).

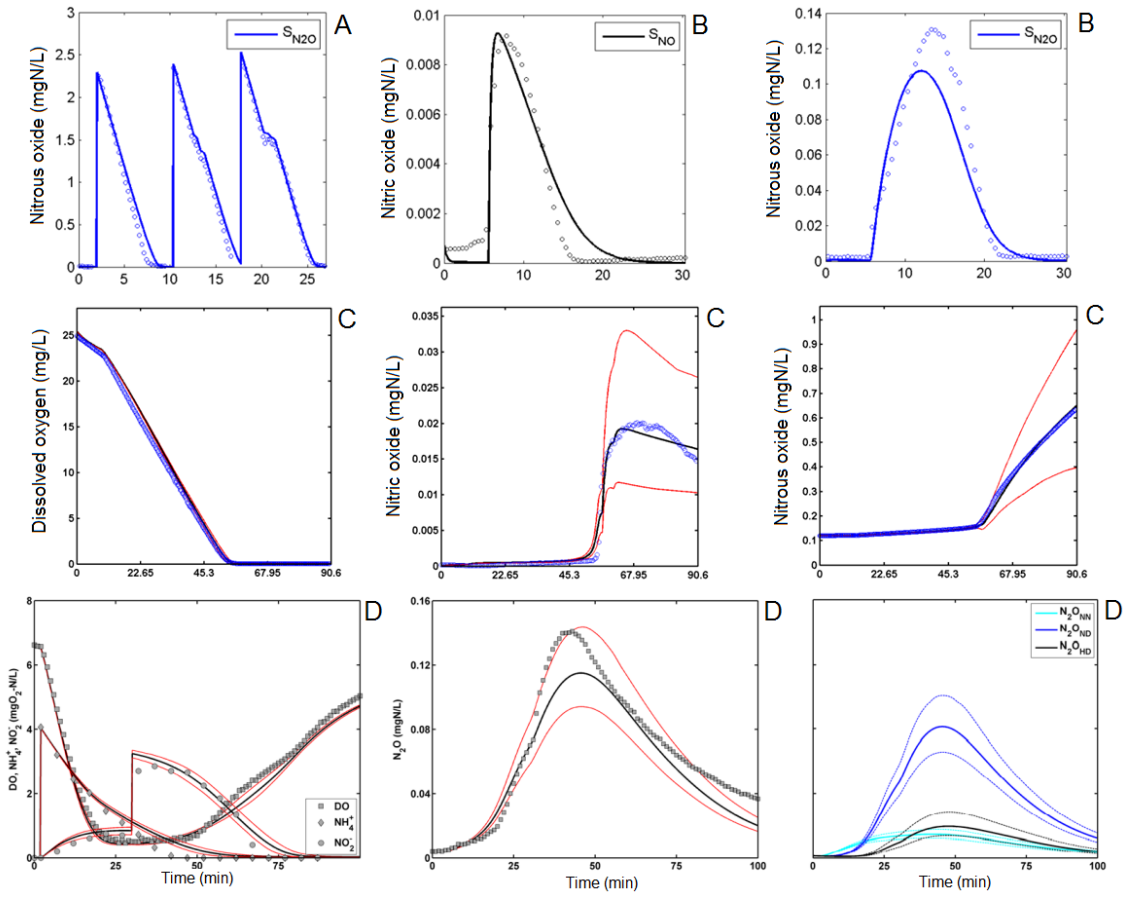


**Figure 5.4.** Experimental and modelling results obtained during parameter estimation. $N_2O$ consumption profile after DO pulses (t = 13, 21 min) (A). NO and $N_2O$ production after anoxic $NO_2^-$ pulse under endogenous conditions (B). Oxygen consumption, NO and $N_2O$ accumulation rates after $NH_4^+$ pulse addition (t = 10 min) (C). Model evaluation results for mixed liquor biomass: Effect of $NO_2^-$ pulse ($t_{pulse}$ = 30 min) (D). (**Paper IV**).

Overall, the model captures the trends of DO, main N-substrates and liquid $N_2O$ without any parameter modification ($R^2_{avg}$ for DO = 0.98; $NH_4^+$ = 0.99; $NO_2^-$ = 0.84; $N_2O$ = 0.80). Higher $NH_4^+$ pulses yield more $N_2O$ as more $NH_4^+$ oxidation occurs at low DO, thus promoting the contribution of denitrifica-

tion pathways. Addition of a $NO_2^-$ pulse increases the fraction of $N_2O$ produced compared to a $NO_3^-$ pulse or no pulse (**Figure 5.4, D**).

## Model evaluation

$NH_4^+$ oxidation simulations with best-fit estimate parameters are run for a wider range of DO (0.2 – 4 mg/L) and $NO_2^-$ (0 – 1.4 mgN/L), representative of full-scale system where the biomass originates. The $N_2O$ emission factor and individual pathway contributions to the total $N_2O$ pool at pseudo-steady state are shown in **Figure 5.5**. The simulated $NH_4^+$ oxidation at low DO yields a higher $N_2O$ emission factor as compared to that at higher DO (4.6 and 1.2% respectively), in agreement with other nitrification/denitrification systems (Hu *et al.*, 2010; Tallec *et al.*, 2006) and comparable with those reported by (Wunderlin *et al.*, 2012). The NN pathway contributes most at the lowest $NO_2^-$ and highest DO (98%), and the least at high $NO_2^-$ and low DO (3%). The ND and HD pathways show similar trends with maximum contributions of 72% and 43% respectively, but opposite compared to the NN pathway.

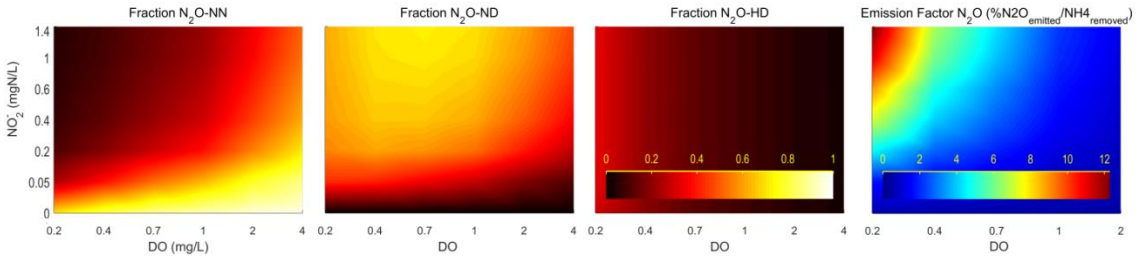


**Figure 5.5.** Model evaluation at varying $NO_2^-$ and DO concentrations during excess $NH_4^+$ removal (pH = 7.2). From left to right: Pathway contributions to total $N_2O$ pool NN, ND, HD; $N_2O$ emission factor. (**Paper IV**).

The different microbial community composition between AOB-enriched and mixed liquor biomass poses a significant effect on the associated $N_2O$ production during $NH_4^+$ removal. In the mixed liquor biomass the $NO_2^-$ sink is much larger due to a higher NOB biomass fraction, and hence, a higher $N_2O$ emission factor is expected from the AOB-enriched biomass. If $N_2O$ is produced during anoxic periods, or transiency into anoxia, it accumulates in the liquid phase and can be stripped at the onset of aeration. In this scenario the mixed liquor biomass also offers an advantage with respect to the AOB-enriched biomass as the heterotrophic fraction of the biomass will act as an

$N_2O$ sink even in the absence of additional organic carbon (**Figure 5.7**). Assuming a constant autotrophic $N_2O$ production, the observed or net $N_2O$ production from mixed liquor biomass is expected to be lower as the heterotrophic biomass can mask autotrophically-driven $N_2O$ production (**Figure 5.7**).

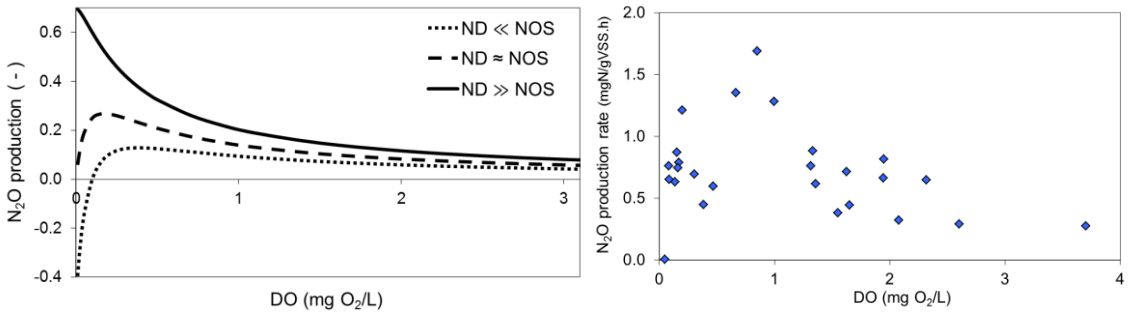


**Figure 5.7.** Left: Theoretical model evaluations for mixed microbial communities: AOB ≫ HB (solid line), AOB ≈ HB (dashed line), and AOB ≪ HB (dotted line). Right: net $N_2O$ production rates observed during $NH_4^+$ oxidation at constant DO. Mixed liquor biomass from Respirom_ML_aer (**Figure 4.2.**).

### Role of hydroxylamine on nitrous oxide models

Low $NH_2OH$ bulk concentrations were reported for AOB pure cultures and nitrifying systems ($NH_2OH$ < 0.1mgN/L) (Soler-Jofra *et al.*, 2016; Yu and Chandran, 2010), indicating a quick turnover of $NH_2OH$. However, $NH_2OH$ predictions from $N_2O$ models are not verified and would overestimate $NH_2OH$ equilibrium concentrations during $NH_4^+$ oxidation ($\mu_{AMO} \geq \mu_{HAO}$, $K_{AOB.NH2OH} \approx K_{AOB.NH4}$ = 0.7 – 2.4mgN/L) (Pocquet *et al.*, 2016; Ding *et al.*, 2016; Ni *et al.*, 2011, 2013b, 2014). Here, a faster HAO process compared to AMO prevents high $NH_2OH$ accumulations and is therefore necessary for more accurate $NH_2OH$ predictions. This is in agreement with the calibrated NDHA model where $\mu_{AMO} < \mu_{HAO}$ and $K_{AOB.NH2OH} < K_{AOB.NH4}$, being $K_{AOB.NH2OH}$ = 0.2 mgN/L the lowest value reported in $N_2O$ models. Simulation results of a biofilm system also calculated overestimation of $NH_2OH$ release from other $N_2O$ models, where 27% of the $NH_3$ oxidized accumulated as $NH_2OH$ (Todt and Dörsch, 2016).

Experimental and modelling results suggest that $N_2O$ pathways such as the associated to cyt P460, could be responsible for the high $N_2O$ production observed during aerobic $NH_2OH$ oxidation (Kozlowski *et al.*, 2016). The NDHA model might not individually describe all the co-occurring $N_2O$ pathways in the AOB metabolism. However, $N_2O$ production associated to

wastewater treatment conditions is successfully captured by lumping pathways into the NN and ND processes.

**Role of nitric oxide on nitrous oxide models**

NO and $N_2O$ production from $NH_4^+$ oxidation under aerobic conditions is significantly lower than at low oxygen tension, as reported for AOB pure cultures (Kozlowski *et al.*, 2016). In nitrifying systems NO and $N_2O$ production was also triggered by $NO_2^-$ and anoxic conditions (Kampschreur *et al.*, 2008b; Wunderlin *et al.*, 2012). Modelling results show that the higher anoxic rates can be explained by the transient accumulation of $NH_2OH$ which, under anoxia, has been suggested to act as electron donor for $NO_2^-$ reduction to $N_2O$ in a two-step process over NO (de Bruijn *et al.*, 1995; Poth and Focht, 1985; Yu and Chandran, 2010; Kester, 1997).

The ratio between the substrate affinity of NO reductases, $K_{AOB.NO}$ / $K_{HB.NO}$, is an important parameter of $N_2O$ models as it can shift the contributions of the ND and HD pathways for the same overall $N_2O$ fit (**Paper I**). However, direct estimation of NO affinity is difficult due to its toxicity (Schulthess and Gujer, 1996). In $N_2O$ models $K_{NO}$ values are typically assumed (Pan *et al.*, 2013; Hiatt and Grady, 2008) and highly variable ($K_{HB.NO}$ = 0.00015-0.05 mgN/L and $K_{AOB.NO}$, 0.004-0.1mgN/L, $K_{AOB.NO}$ / $K_{HB.NO}$ = 1 - 56) (Wang *et al.*, 2016a; Hiatt and Grady, 2008; Spérandio *et al.*, 2016; Schreiber *et al.*, 2009; Ni *et al.*, 2011). For example, in the study by (Wang *et al.*, 2016a) the HD pathway has an NO affinity over 50 times higher than the NN pathway. The HD pathway could, in theory, uptake NO produced by the NN pathway at a much higher rate and underestimate the NN contribution to the total $N_2O$ pool. Hence, based on current knowledge and to avoid a preferential NO-consumption/$N_2O$-production pathway the NO affinity ratio between AOB and HB is set to one (**Figure 4.8**).

# 6 Conclusions

The main findings of this thesis are:

- In microbial communities from conventional biological nitrogen removal systems heterotrophs are more abundant than autotrophs and heterotrophic activity should not be neglected even under very low carbon-to-nitrogen conditions. Hence, in mixed microbial communities the heterotrophic contribution to $N_2O$ production should always be considered.
- A consilient mathematical model structure that describes $N_2O$ production during biological nitrogen removal is proposed. Three biological pathways, two autotrophic and one heterotrophic, are coupled with abiotic processes. Consistent with experimental studies, the model considers NO as the direct precursor of $N_2O$ in three biologically-driven pathways. This model can describe all relevant NO and $N_2O$ production pathways with fewer parameters than other proposed models.
- An experimental design to estimate $N_2O$ model parameters through extant respirometry is developed and applied to two different biomass types: AOB-enriched and Activated Sludge mixed liquor communities. The experimental design allowed the isolation of individual process rates and the estimation of parameters associated with oxygen consumption (endogenous, nitrite and ammonium oxidation) and $N_2O$ production (NN, ND and HD pathway contributions). In respirometric and batch assays $N_2O$ and NO production increased during ammonium oxidation under low dissolved oxygen concentrations and the presence of nitrite.
- The model predicted the NO and $N_2O$ dynamics at varying ammonium, nitrite and dissolved oxygen levels from two independent systems: (a) an AOB-enriched biomass and (b) Activated Sluge mixed liquor biomass. A total of ten (a) and seventeen (b) parameters were identified with high accuracy (coefficients of variation < 25%).
- A rigorous procedure to estimate parameters associated to $N_2O$ models is presented. Moreover, the critical validation of the model response and the estimated parameter values will benefit $N_2O$ model discrimination procedures.
- As an end-product in the metabolism of aerobic ammonium oxidizers and obligate intermediate of heterotrophic denitrifiers, the uncertainty of nitrogenous substrates (e.g. ammonium, nitrite, etc.) propagates to $N_2O$

predictions. Hence, $N_2O$ model predictions should be described by best-fit $N_2O$ predictions together with uncertainty metrics (e.g. confidence intervals).

- A model describing organic carbon oxidation and four-step denitrification through electron competition using fewer parameters than other models is proposed. The model describes reaction rates as analogy to current intensity through resistors in electric circuits. The model describes the electron competition during the reduction rates of single and most of the combined nitrogen oxides for four different carbon sources. Further validation under different carbon and nitrogen loadings needs to be explored.

# 7 Future perspectives

In this study $N_2O$ datasets for parameter estimation relied on online sensors for bulk measurements. The model can then predict the contribution of each pathway to the total $N_2O$ pool. Other analytical techniques such as stable isotope labelling ($^{15}N$, $^{18}O$ or isotopic signatures) could be performed simultaneously to validate or correct predictions regarding pathway contributions.

The applicability of the proposed model could be extended to continuous or full-scale systems. However, for the purpose of model discrimination and model development lab-scale systems with defined controlled environments are preferred. For example, biochemical gradients exist along the bioaggregates in biofilm configurations where pH changes from the bulk to the inner layer of the aggregate. Hence, biofilm models should consider explicit pH calculations as $N_2O$ formation ($K_{AOB.HNO2}$) and consumption ($pH_{opt.nosZ}$) are pH-dependent. It was shown that heterotrophs are ubiquitous, even if supported by biomass decay products and thus, should always be considered in $N_2O$ models.

The role of $NH_2OH$ as electron donor in the AOB metabolism remains to be untangled as new $N_2O$ producing pathways are discovered (Caranto *et al.*, 2016). $NH_2OH$ might not be the direct electron donor for $NO_2^-$ and NO reduction (cytochromes) and the simplification of our assumption vs the use of lumped set of electron carriers (Ni *et al.*, 2014) deserves further examination.

As more datasets are being retrieved, direct comparison of the benefits of more complex mechanistic models compared to empirical approaches could be studied (Leix *et al.*, 2017).

Another suite of questions are: How marginal is the benefit of including more species that share function but differ in their kinetic parameters? (e.g. *Nitrospira spp.*, *Nitrobacter spp.*). How complex do $N_2O$ models need to be to capture $N_2O$ emissions with a given accuracy and precision? Mechanistic models have focused on *accuracy*; and the *precision* example shown in this study can be considered as a reference for further comparisons.

Additionally, it is recommended for $N_2O$ modelling studies to recognize and quantify uncertainties associated to $N_2O$ emissions together with best-fit simulations and parameter identifiability metrics. If the uncertainty of $N_2O$ predictions from parameter variance is identified (i.e. certain parameters carry most of the uncertainty) then Optimal Experimental Design (OED) tech-

niques can help reducing it (Munack and Posten, 1989). OED criteria have been successfully applied to batch experiments with important improvements in parameter confidences.

In this work an example methodology is proposed, but other modelling frameworks such as a Bayesian hierarchical approach that considers a probabilistic parameter estimation could be used. It provides identifiability and sensitivity metrics and has also been applied for the estimation of activated sludge process parameters (Sharifi *et al.*, 2014; Cox, 2004). A substantial limitation compared to the method presented here is the higher computational cost (number of simulations). On the other hand, if the parameter subset to consider for estimation could be minimized, the complexity of the multidimensional problem would decrease significantly.

Finally, in the next step the model is ready to be used for plant-wide applications. While some parameters will certainly need to be estimated (after the mass balance for solids the maximum growth rates will probably differ), the parameter set reported here should describe the kinetics of full-scale systems.

# 8 References


Ahn JH, Kim S, Park H, Rahm B, Pagilla K, Chandran K. (2010). N2O emissions from activated sludge processes, 2008-2009: results of a national monitoring survey in the United States. *Environ Sci Technol* **44**: 4505–11.

Ahn JH, Kwan T, Chandran K. (2011). Comparison of partial and full nitrification processes applied for treating high-strength nitrogen wastewaters: microbial ecology through nitrous oxide production. *Environ Sci Technol* **45**: 2734–40.

Alefounder PR, Greenfield AJ, Mccarthy JEG, Ferguson SJ. (1983). Selection and organisation of denitrifying electron-transfer pathways in Paracoccus Denitrificans. *Biochim Biophys Acta* **724**: 20–39.

Almeida JS, Reis MAM, Carrondo MJT. (1997). A Unifying Kinetic Model of Denitrification. *J Theor Biol* **186**: 241–249.

Beale EML. (1960). Confidence Regions in Non-Linear Estimation. *J R Stat Soc Ser B-statistical Methodol* **22**: 41–88.

Belia E, Amerlinck Y, Benedetti L, Johnson B, Sin G, Vanrolleghem PA, *et al.* (2009). Wastewater treatment modelling: Dealing with uncertainties. *Water Sci Technol* **60**: 1929–1941.

Bennett ND, Croke BFW, Guariso G, Guillaume JHA, Hamilton SH, Jakeman AJ, *et al.* (2013). Characterising performance of environmental models. *Environ Model Softw* **40**: 1–20.

Berks BC, Ferguson SJ, Moir JWB, Richardson DJ. (1995). Enzymes and associated electron transport systems that catalyse the respiratory reduction of nitrogen oxides and oxyanions. *Biochim Biophys Acta - Bioenerg* **1232**: 97–173.

Betlach MR, Tiedje JM. (1981). Kinetic explanation for accumulation of nitrite, nitric oxide, and nitrous oxide during bacterial denitrification. *Appl Environ Microbiol* **42**: 1074–1084.

Boiocchi R, Gernaey K V., Sin G. (2016). Control of wastewater N2O emissions by balancing the microbial communities using a fuzzy-logic approach. *IFAC-PapersOnLine* **49**: 1157–1162.

Boiocchi R, Gernaey K V., Sin G. (2017). Understanding N 2 O formation mechanisms through sensitivity analyses using a plant-wide benchmark simulation model. *Chem Eng J* **317**: 935–951.

Böttcher B, Koops HP. (1994). Growth of lithotrophic ammonia-oxidizing bacteria on hydroxylamine. *FEMS Microbiol Lett* **122**: 263–266.

Brockmann D, Rosenwinkel K-H, Morgenroth E. (2008). Practical

identifiability of biokinetic parameters of a model describing two-step nitrification in biofilms. *Biotechnol Bioeng* **101**: 497–514.

Broda E. (1977). Two kinds of lithotrophs missing in nature. *Z Allg Mikrobiol* **17**: 491–493.

Brotto AC, Li H, Dumit M, Gabarró J, Colprim J, Murthy S, *et al.* (2015). Characterization and mitigation of nitrous oxide (N 2 O) emissions from partial and full-nitrification BNR processes based on post-anoxic aeration control. *Biotechnol Bioeng* **112**: 2241–2247.

de Bruijn P, van de Graaf AA, Jetten MSM, Robertson LA, Kuenen JG. (1995). Growth of Nitrosomonas europaea on hydroxylamine. *FEMS Microbiol Lett* **125**: 179–184.

Brun R, Kühni M, Siegrist H, Gujer W, Reichert P. (2002). Practical identifiability of ASM2d parameters--systematic selection and tuning of parameter subsets. *Water Res* **36**: 4113–27.

Brun R, Reichert P, Kfinsch HR. (2001). Practical identifiability analysis of large environmental simulation models. *Water Resour Res* **37**: 1015–1030.

Burgess JE, Colliver BB, Stuetz RM, Stephenson T. (2002). Dinitrogen oxide production by a mixed culture of nitrifying bacteria during ammonia shock loading and aeration failure. *J Ind Microbiol Biotechnol* **29**: 309–313.

Caranto JD, Vilbert AC, Lancaster KM. (2016). Nitrosomonas europaea cytochrome P460 is a direct link between nitrification and nitrous oxide emission. *Proc Natl Acad Sci* **113**: 14704–14709.

Chandran K. (2011). Protocol for the measurement of nitrous oxide fluxes from biological wastewater treatment plants. *Methods Enzymol* **486**: 369–85.

Chandran K, Hu Z, Smets BF. (2008). A critical comparison of extant batch respirometric and substrate depletion assays for estimation of nitrification biokinetics. *Biotechnol Bioeng* **101**: 62–72.

Chandran K, Smets BF. (2005). Optimizing experimental design to estimate ammonia and nitrite oxidation biokinetic parameters from batch respirograms. *Water Res* **39**: 4969–78.

Chandran K, Stein LY, Klotz MG, van Loosdrecht MCM. (2011). Nitrous oxide production by lithotrophic ammonia-oxidizing bacteria and implications for engineered nitrogen-removal systems. *Biochem Soc Trans* **39**: 1832–7.

Chao Y, Mao Y, Yu K, Zhang T. (2016). Novel nitrifiers and comammox in a full-scale hybrid biofilm and activated sludge reactor revealed by metagenomic approach. *Appl Microbiol Biotechnol* **100**: 8225–8237.

Cierkens K, Plano S, Benedetti L, Weijers S, de Jonge J, Nopens I. (2012). Impact of influent data frequency and model structure on the quality of WWTP model calibration and uncertainty. *Water Sci Technol* **65**: 233–42.

Costa E, Pérez J, Kreft J-U. (2006). Why is metabolic labour divided in nitrification? *Trends Microbiol* **14**: 213–219.

Cox CD. (2004). Statistical distributions of uncertainty and variability in activated sludge model parameters. *Water Environ Res* **76**: 2672–2685.

Daelman MRJ, van Voorthuizen EM, van Dongen LGJM, Volcke EIP, van Loosdrecht MCM. (2013). Methane and nitrous oxide emissions from municipal wastewater treatment - results from a long-term study. *Water Sci Technol* **67**: 2350–5.

Daims H, Lebedeva E V., Pjevac P, Han P, Herbold C, Albertsen M, *et al.* (2015). Complete nitrification by Nitrospira bacteria. *Nature* **528**: 504–509.

Daims H, Wagner M. (2010). The microbiology of nitrogen removal. In: *Microbiology of Activated Sludge*. IWA Publishing: London, UK.

Desloover J, De Clippeleir H, Boeckx P, Du Laing G, Colsen J, Verstraete W, *et al.* (2011). Floc-based sequential partial nitritation and anammox at full scale with contrasting N2O emissions. *Water Res* **45**: 2811–21.

Desloover J, Vlaeminck SE, Clauwaert P, Verstraete W, Boon N. (2012). Strategies to mitigate N2O emissions from biological nitrogen removal systems. *Curr Opin Biotechnol* **23**: 474–82.

Ding X, Zhao J, Hu B, Chen Y, Ge G, Li X, *et al.* (2016). Mathematical modeling of nitrous oxide production in an anaerobic/oxic/anoxic process. *Bioresour Technol* **222**: 39–48.

Dochain D, Vanrolleghem PA. (2001). Dynamic Modelling and Estimation in Wastewater Treatment Processes. IWA Publishing: London, UK.

Domeignoz-Horta LA, Putz M, Spor A, Bru D, Breuil MC, Hallin S, *et al.* (2016). Non-denitrifying nitrous oxide-reducing bacteria - An effective N2O sink in soil. *Soil Biol Biochem* **103**: 376–379.

Domingo-Félez C, Mutlu AG, Jensen MM, Smets BF. (2014). Aeration Strategies To Mitigate Nitrous Oxide Emissions from Single-Stage Nitritation/Anammox Reactors. *Environ Sci Technol* **48**: 8679–8687.

Döring C, Gehlen H. (1961). Über die Kinetik der Reaktion zwischen Hydroxylamin und Salpetriger Säure. *Zeitschrift für Anorg und Allg Chemie* **312**: 32–44.

Ekama GA, Wentzel C. (1999). Denitrification kinetics in biologicl N and P removal ctivated sludge systems treating municipal wastewaters. *Water Sci*

*Technol* **39**: 69–77.

Ellis TG, Barbeau DS, Smets BF, Grady CPL. (1996). Respirometric technique for determination of extant kinetic parameters describing biodegradation. *Water Environ Res* **68**: 917–926.

Feelisch M, Stamler JS. (1996). Donors of Nitrogen Oxides. In: Sons JW and (ed). *Methods in Nitric Oxide Research;*. Chichester, England, pp 71–115.

Foley J, de Haas D, Yuan Z, Lant P. (2010). Nitrous oxide generation in full-scale biological nutrient removal wastewater treatment plants. *Water Res* **44**: 831–44.

Frame CH, Lau E, Nolan EJ, Goepfert TJ, Lehmann MF. (2017). Acidification Enhances Hybrid N2O Production Associated with Aquatic Ammonia-Oxidizing Microorganisms. *Front Microbiol* **7**: 2104.

Ginige MP, Hugenholtz P, Daims H, Wagner M, Keller J, Blackall LL. (2004). Use of Stable-Isotope Probing, Full-Cycle rRNA Analysis, and Fluorescence In Situ Hybridization-Microautoradiography To Study a Methanol-Fed Denitrifying Microbial Community. *Appl Environ Microbiol* **70**: 588–596.

Graf DRH, Jones CM, Hallin S. (2014). Intergenomic Comparisons Highlight Modularity of the Denitrification Pathway and Underpin the Importance of Community Structure for N2O Emissions. *PLoS One* **9**: e114118.

Grant RF, Pattey E. (1999). Mathematical modeling of nitrous oxide emissions from an agricultural field during spring thaw. *Global Biogeochem Cycles* **13**: 679–694.

Guisasola A, Petzet S, Baeza J a, Carrera J, Lafuente J. (2007). Inorganic carbon limitations on nitrification: experimental assessment and modelling. *Water Res* **41**: 277–86.

Guo L, Vanrolleghem P a. (2014). Calibration and validation of an activated sludge model for greenhouse gases no. 1 (ASMG1): prediction of temperature-dependent N2O emission dynamics. *Bioprocess Biosyst Eng* **37**: 151–163.

Gustavsson DJI, Tumlin S. (2013). Carbon footprints of Scandinavian wastewater treatment plants. *Water Sci Technol* **68**: 887.

Haefner JW. (2005). Modeling Biological Systems: Principles and Applications. Second. Springer.

Hallin S, Throbäck IN, Dicksved J, Pell M. (2006). Metabolic profiles and genetic diversity of denitrifying communities in activated sludge after addition of methanol or ethanol. *Appl Environ Microbiol* **72**: 5445–5452.

Harper WF, Takeuchi Y, Riya S, Hosomi M, Terada A. (2015). Novel abiotic reactions increase nitrous oxide production during partial nitrification: Modeling and experiments. *Chem Eng J* **281**: 1017–1023.

Heil J, Wolf B, Brüggemann N, Emmenegger L, Tuzson B, Vereecken H, *et al.* (2014). Site-specific 15N isotopic signatures of abiotically produced N2O. *Geochim Cosmochim Acta* **139**: 72–82.

Henze M, Gujer W, Matsuo T, van Loosdrecht MC. (2000). Activated Sludge Models ASM1, ASM2, ASM2d and ASM3. Scientific and Technical Reports. *IWA Publ London*.

Henze M, van Loosdrecht MC, Ekama GA, Brdajanovic D. (2008). Biological wastewater treatment. Principles, modelling and design. IWA Publishing: London.

Hiatt WC, Grady CPL. (2008). An updated process model for carbon oxidation, nitrification, and denitrification. *Water Environ Res* **80**: 2145–2156.

Hooper AB, Terry KR. (1979). Hydroxylamine oxidoreductase of Nitrosomonas. Production of nitric oxide from hydroxylamine. *BBA - Enzymol* **571**: 12–20.

Hu Z, Zhang J, Li S, Xie H, Wang J, Zhang T, *et al.* (2010). Effect of aeration rate on the emission of N2O in anoxic-aerobic sequencing batch reactors (A/O SBRs). *J Biosci Bioeng* **109**: 487–91.

Hu Z, Zhang J, Xie H, Liang S, Li S. (2013). Minimization of nitrous oxide emission from anoxic-oxic biological nitrogen removal process: effect of influent COD/NH4+ ratio and feeding strategy. *J Biosci Bioeng* **115**: 272–8.

Huang D, Lai Y, Becker JG. (2014). Impact of initial conditions on extant microbial kinetic parameter estimates: application to chlorinated ethene dehalorespiration. *Appl Microbiol Biotechnol* **98**: 2279–2288.

Igarashi N, Moriyama H, Fujiwara T, Fukumuri Y, Tanaka N. (1997). he 2.8 A structure of hydroxylamine oxidoreductase from a nitrifying chemoautotrophic bacterium, Nitrosomonas europaea. *Nature* **4**: 276–284.

Jiang D, Khunjar WO, Wett B, Murthy SN, Chandran K. (2015). Characterizing the Metabolic Trade-Off in Nitrosomonas europaea in Response to Changes in Inorganic Carbon Supply. *Environ Sci Technol* **49**: 2523–31.

Jin X, Xu C-Y, Zhang Q, Singh VP. (2010). Parameter and modeling uncertainty simulated by GLUE and a formal Bayesian method for a conceptual hydrological model. *J Hydrol* **383**: 147–155.

Jones CM, Spor A, Brennan FP, Breuil M-C, Bru D, Lemanceau P, *et al.*

(2014). Recently identified microbial guild mediates soil N2O sink capacity. *Nat Clim Chang* **4**: 801–805.

Joshi M, Seidel-Morgenstern A, Kremling A. (2006). Exploiting the bootstrap method for quantifying parameter confidence intervals in dynamical systems. *Metab Eng* **8**: 447–455.

Joss A, Derlon N, Cyprien C, Burger S, Szivak I, Traber J, *et al.* (2011). Combined nitritation-anammox: advances in understanding process stability. *Environ Sci Technol* **45**: 9735–42.

Kampschreur MJ, Kleerebezem R, de Vet WWJM, van Loosdrecht MCM. (2011). Reduced iron induced nitric oxide and nitrous oxide emission. *Water Res* **45**: 5945–5952.

Kampschreur MJ, Picioreanu C, Tan N, Kleerebezem R, Jetten MS., van Loosdrecht MC. (2007). Unraveling the Source of Nitric Oxide Emission During Nitrification. *Water Environ Res* **79**: 2499–2509.

Kampschreur MJ, Poldermans R, Kleerebezem R, van der Star WRL, Haarhuis R, Abma WR, *et al.* (2009a). Emission of nitrous oxide and nitric oxide from a full-scale single-stage nitritation-anammox reactor. *Water Sci Technol* **60**: 3211–7.

Kampschreur MJ, van der Star WRL, Wielders HA, Mulder JW, Jetten MSM, van Loosdrecht MCM. (2008a). Dynamics of nitric oxide and nitrous oxide emission during full-scale reject water treatment. *Water Res* **42**: 812–26.

Kampschreur MJ, Tan NCG, Kleerebezem R, Picioreanu C, Jetten MSM, Van Loosdrecht MCM. (2008b). Effect of dynamic process conditions on nitrogen oxides emission from a nitrifying culture. *Environ Sci Technol* **42**: 429–35.

Kampschreur MJ, Temmink H, Kleerebezem R, Jetten MSM, van Loosdrecht MCM. (2009b). Nitrous oxide emission during wastewater treatment. *Water Res* **43**: 4093–103.

van Kessel MAHJ, Speth DR, Albertsen M, Nielsen PH, Op den Camp HJM, Kartal B, *et al.* (2015). Complete nitrification by a single microorganism. *Nature* **528**: 555–559.

Kester RA. (1997). Production of NO and N2O by Pure Cultures of Nitrifying and Denitrifying Bacteria during Changes in Aeration. *Appl Environ Microbiol* **63**: 3872–3877.

Kim M, Wu G, Yoo C. (2017). Quantification of nitrous oxide (N2O) emissions and soluble microbial product (SMP) production by a modified AOB-NOB-N2O-SMP model. *Bioresour Technol* **227**: 227–238.

Kim S-W, Miyahara M, Fushinobu S, Wakagi T, Shoun H. (2010). Nitrous oxide emission from nitrifying activated sludge dependent on denitrification

by ammonia-oxidizing bacteria. *Bioresour Technol* **101**: 3958–63.

Kozlowski JA, Kits KD, Stein LY. (2016). Comparison of Nitrogen Oxide Metabolism among Diverse Ammonia-Oxidizing Bacteria. *Front Microbiol* **7**: 1–9.

Kozlowski JA, Price J, Stein LY. (2014). Revision of N2O-Producing Pathways in the Ammonia-Oxidizing Bacterium Nitrosomonas europaea ATCC 19718. *Appl Environ Microbiol* **80**: 4930–4935.

Kucera I, Dadak V, Dobry R. (1983). The distribution of redox equivalents in the anaerobic respiratory chain of Paracoccus denitrificans. *Eur J Biochem* **130**: 359–364.

Lang L, Pocquet M, Ni B-J, Yuan Z, Spérandio M. (2017). Comparison of different two-pathway models for describing the combined effect of DO and nitrite on the nitrous oxide production by ammonia-oxidizing bacteria. *Water Sci Technol* **75**: 491–500.

Law Y, Ni B-J, Lant P, Yuan Z. (2012). N2O production rate of an enriched ammonia-oxidising bacteria culture exponentially correlates to its ammonia oxidation rate. *Water Res* **46**: 3409–19.

Leix C, Drewes JE, Ye L, Koch K. (2017). Strategies for enhanced deammonification performance and reduced nitrous oxide emissions. *Bioresour Technol* **236**: 174–185.

Li B, Wu G. (2014). Effects of sludge retention times on nutrient removal and nitrous oxide emission in biological nutrient removal processes. *Int J Environ Res Public Health* **11**: 3553–69.

Lide DR (ed). (2009). CRC Handbook of Chemistry and Physics. 89th ed. CRC Press/Taylor and Francis: Boca Raton, FL.

Lilliefors HW. (1967). On the Kolmogorov-Smirnov Test for Normality with Mean and Variance Unknown. *J Am Stat Assoc* **62**: 399.

Liu R-T, Wang X-H, Zhang Y, Wang M-Y, Gao M-M, Wang S-G. (2016). Optimization of operation conditions for the mitigation of nitrous oxide (N2O) emissions from aerobic nitrifying granular sludge system. *Environ Sci Pollut Res* **23**: 9518–9528.

Liu S, Vereecken H, Brüggemann N. (2014). A highly sensitive method for the determination of hydroxylamine in soils. *Geoderma* **232**–**234**: 117–122.

Liu Y, Peng L, Chen X, Ni B-J. (2015). Mathematical Modeling of Nitrous Oxide Production during Denitrifying Phosphorus Removal Process. *Environ Sci Technol* **49**: 8595–8601.

Lotito AM, Wunderlin P, Joss A, Kipf M, Siegrist H. (2012). Nitrous oxide

emissions from the oxidation tank of a pilot activated sludge plant. *Water Res* **46**: 3563–73.

Lu H, Chandran K, Stensel D. (2014). Microbial ecology of denitrification in biological wastewater treatment. *Water Res* **64**: 237–254.

Lücker S, Schwarz J, Gruber-Dorninger C, Spieck E, Wagner M, Daims H. (2015). Nitrotoga-like bacteria are previously unrecognized key nitrite oxidizers in full-scale wastewater treatment plants. *ISME J* **9**: 708–720.

Machado VC, Tapia G, Gabriel D, Lafuente J, Baeza JA. (2009). Systematic identifiability study based on the Fisher Information Matrix for reducing the number of parameters calibration of an activated sludge model. *Environ Model Softw* **24**: 1274–1284.

Madigan MT, Martinko JM, Stahl D, Clark DP. (2010). Brock Biology of Microorganisms. 13th ed. Pearson.

Mannina G, Cosenza A. (2015). Quantifying sensitivity and uncertainty analysis of a new mathematical model for the evaluation of greenhouse gas emissions from membrane bioreactors. *J Memb Sci* **475**: 80–90.

Mannina G, Ekama G, Caniani D, Cosenza A, Esposito G, Gori R, *et al.* (2016). Greenhouse gases from wastewater treatment — A review of modelling tools. *Sci Total Environ* **551**–**552**: 254–270.

Manser R, Gujer W, Siegrist H. (2005). Consequences of mass transfer effects on the kinetics of nitrifiers. *Water Res* **39**: 4633–4642.

Martin C, Ayesa E. (2010). An Integrated Monte Carlo Methodology for the calibration of water quality models. *Ecol Modell* **221**: 2656–2667.

Massara TM, Malamis S, Guisasola A, Baeza JA, Noutsopoulos C, Katsou E. (2017). A review on nitrous oxide (N 2 O) emissions during biological nutrient removal from municipal wastewater and sludge reject water. *Sci Total Environ* **596**–**597**: 106–123.

Meijer SCF. (2004). Theoretical and practical aspects of modelling activated sludge processes. Delft University of Technology. e-pub ahead of print, doi: ISBN 90-9018027-3.

Mellbye BL, Giguere A, Chaplen F, Bottomley PJ, Sayavedra-Soto LA. (2016). Steady-State Growth under Inorganic Carbon Limitation Conditions Increases Energy Consumption for Maintenance and Enhances Nitrous Oxide Production in Nitrosomonas europaea Parales RE (ed). *Appl Environ Microbiol* **82**: 3310–3318.

Mokhayeri Y, Riffat R, Murthy S, Bailey W, Takacs I, Bott C. (2009). Balancing yield, kinetics and cost for three external carbon sources used for suspended growth post-denitrification. *Water Sci Technol* **60**: 2485.

Monteith HD, Sahely HR, MacLean HL, Bagley DM. (2005). A Rational Procedure for Estimation of Greenhouse-Gas Emissions from Municipal Wastewater Treatment Plants. *Water Environ Res* **77**: 390–403.

Mosier A, Kroeze C, Nevison C, Oenema O, Sybil Seitzinger, van Cleemput O. (1999). An overview of the revised 1996 IPCC guidelines for national greenhouse gas inventory methodology for nitrous oxide from agriculture. *Environ Sci Policy* **2**: 325–333.

Munack A, Posten C. (1989). Design of optimal experiments for parameter estimation. In: Vol. 3. *Proceedings of the 1989 American Control Conference*. pp 2010–2016.

Nelder JA, Mead R. (1965). A Simplex Method for Function Minimization. *Comput J* **7**: 308–313.

Neumann MB, Gujer W. (2008). Underestimation of Uncertainty in Statistical Regression of Environmental Models: Influence of Model Structure Uncertainty. *Environ Sci Technol* **42**: 4037–4043.

Ni B-J, Peng L, Law Y, Guo J, Yuan Z. (2014). Modeling of Nitrous Oxide Production by Autotrophic Ammonia-Oxidizing Bacteria with Multiple Production Pathways. *Environ Sci Technol* **48**: 3916–24.

Ni B-J, Ruscalleda M, Pellicer-Nàcher C, Smets BF. (2011). Modeling nitrous oxide production during biological nitrogen removal via nitrification and denitrification: extensions to the general ASM models. *Environ Sci Technol* **45**: 7768–76.

Ni B-J, Ye L, Law Y, Byers C, Yuan Z. (2013a). Mathematical modeling of nitrous oxide (N2O) emissions from full-scale wastewater treatment plants. *Environ Sci Technol* **47**: 7795–803.

Ni B-J, Ye L, Law Y, Byers C, Yuan Z. (2013b). Mathematical Modeling of Nitrous Oxide (N 2 O) Emissions from Full-Scale Wastewater Treatment Plants. *Environ Sci Technol* **47**: 7795–7803.

Ni B-J, Yuan Z. (2015). Recent advances in mathematical modeling of nitrous oxides emissions from wastewater treatment processes. *Water Res* **87**: 336–346.

Ni B-J, Yuan Z, Chandran K, Vanrolleghem PA, Murthy S. (2013c). Evaluating four mathematical models for nitrous oxide production by autotrophic ammonia-oxidizing bacteria. *Biotechnol Bioeng* **110**: 153–63.

Nielsen JL, Nielsen PH. (2002). Quantification of functional groups in activated sludge by microautoradiography. *Water Sci Technol* **46**: 389–395.

Nielsen PH, Mielczarek AT, Kragelund C, Nielsen JL, Saunders AM, Kong Y, *et al.* (2010). A conceptual ecosystem model of microbial communities in

enhanced biological phosphorus removal plants. *Water Res* **44**: 5070–88.

Nowka B, Daims H, Spieck E. (2014). Comparative oxidation kinetics of nitrite-oxidizing bacteria: nitrite availability as key factor for niche differentiation. *Appl Environ Microbiol* **81**: 745–753.

Osaka T, Yoshie S, Tsuneda S, Hirata A, Iwami N, Inamori Y. (2006). Identification of Acetate- or Methanol-Assimilating Bacteria under Nitrate-Reducing Conditions by Stable-Isotope Probing. *Microb Ecol* **52**: 253–266.

Palomo A, Jane Fowler S, Gülay A, Rasmussen S, Sicheritz-Ponten T, Smets BF. (2016). Metagenomic analysis of rapid gravity sand filter microbial communities suggests novel physiology of Nitrospira spp. *ISME J* **10**: 2569–2581.

Pan Y, Ni B-J, Lu H, Chandran K, Richardson D, Yuan Z. (2015). Evaluating two concepts for the modelling of intermediates accumulation during biological denitrification in wastewater treatment. *Water Res* **71**: 21–31.

Pan Y, Ni B, Yuan Z. (2013). Modeling electron competition among nitrogen oxides reduction and N2O accumulation in denitrification. *Environ Sci Technol* **47**: 11083–91.

Panwivia S, Sirvithayapakorn S, Wantawin C, Noophan P (Lek), Munakata-Marr J. (2014). Comparison of nitrogen removal rates and nitrous oxide production from enriched anaerobic ammonium oxidizing bacteria in suspended and attached growth reactors. *J Environ Sci Heal Part A* **49**: 851–856.

Park KY, Inamori Y, Mizuochi M, Ahn KH. (2000). Emission and control of nitrous oxide from a biological wastewater treatment system with intermittent aeration. *J Biosci Bioeng* **90**: 247–252.

Park S, Bae W, Chung J, Baek S-C. (2007). Empirical model of the pH dependence of the maximum specific nitrification rate. *Process Biochem* **42**: 1671–1676.

Peng L, Ni B-J, Ye L, Yuan Z. (2015). The combined effect of dissolved oxygen and nitrite on N2O production by ammonia oxidizing bacteria in an enriched nitrifying sludge. *Water Res* **73**: 29–36.

Perez-Garcia O, Chandran K, Villas-Boas SG, Singhal N. (2016a). Assessment of nitric oxide (NO) redox reactions contribution to nitrous oxide (N2O) formation during nitrification using a multispecies metabolic network model. *Biotechnol Bioeng* **113**: 1124–1136.

Perez-Garcia O, Lear G, Singhal N. (2016b). Metabolic Network Modeling of Microbial Interactions in Natural and Engineered Environmental Systems. *Front Microbiol* **7**. e-pub ahead of print, doi: 10.3389/fmicb.2016.00673.

Perez-Garcia O, Villas-Boas SG, Swift S, Chandran K, Singhal N. (2014). Clarifying the regulation of NO/N2O production in Nitrosomonas europaea during anoxic-oxic transition via flux balance analysis of a metabolic network model. *Water Res* **60C**: 267–277.

Picioreanu C, Pérez J, van Loosdrecht MCM. (2016). Impact of cell cluster size on apparent half-saturation coefficients for oxygen in nitrifying sludge and biofilms. *Water Res* **106**: 371–382.

Pocquet M, Wu Z, Queinnec I, Spérandio M. (2016). A two pathway model for N2O emissions by ammonium oxidizing bacteria supported by the NO/N2O variation. *Water Res* **88**: 948–959.

Poth M, Focht DD. (1985). 15N Kinetic Analysis of N20 Production by Nitrosomonas europaea: an Examination of Nitrifier Denitrification. *Appl Environ Microbiol* **49**: 1134–1141.

Purkhold U, Pommerening-Roser A, Juretschko S, Schmid MC, Koops H-P, Wagner M. (2000). Phylogeny of All Recognized Species of Ammonia Oxidizers Based on Comparative 16S rRNA and amoA Sequence Analysis: Implications for Molecular Diversity Surveys. *Appl Environ Microbiol* **66**: 5368–5382.

Ravishankara AR, Daniel JS, Portmann RW. (2009). Nitrous Oxide (N2O): The Dominant Ozone-Depleting Substance Emitted in the 21st Century. *Science (80- )* **326**: 123–125.

Reichert P. (1998). AQUASIM 2.0 - User Manual. Computer Program for the Identification and Simulation of Aquatic Systems.

Richardson D, Felgate H, Watmough N, Thomson A, Baggs E. (2009). Mitigating release of the potent greenhouse gas N(2)O from the nitrogen cycle - could enzymic regulation hold the key? *Trends Biotechnol* **27**: 388–97.

Rodriguez-Caballero A, Pijuan M. (2013). N2O and NO emissions from a partial nitrification sequencing batch reactor: exploring dynamics, sources and minimization mechanisms. *Water Res* **47**: 3131–40.

Sanford RA, Wagner DD, Wu Q, Chee-Sanford JC, Thomas SH, Cruz-García C, *et al.* (2012). Unexpected nondenitrifier nitrous oxide reductase gene diversity and abundance in soils. *Proc Natl Acad Sci U S A* **109**: 19709–14.

Sayavedra-Soto LA, Hommes NG, Russell SA, Arp DJ. (1996). Induction of ammonia monooxygenase and hydroxylamine oxidoreductase mRNAs by ammonium in Nitrosomonas europaea. *Mol Microbiol* **20**: 541–548.

Schramm A, Santegoeds CM, Nielsen HK, Ploug H, Wagner M, Pribyl M, *et al.* (1999). On the occurrence of anoxic microniches, denitrification, and sulfate reduction in aerated activated sludge. *Appl Environ Microbiol* **65**:

4189–4196.

Schreiber F. (2009). Mechanisms_SI of Transient Nitric Oxide and Nitrous Oxide Production in a Complex Biofilm. *ISME J* 1–8.

Schreiber F, Loeffler B, Polerecky L, Kuypers MM, de Beer D. (2009). Mechanisms of transient nitric oxide and nitrous oxide production in a complex biofilm. *ISME J* **3**: 1301–1313.

Schulthess R, Gujer W. (1996). Release of nitrous oxide (N2O) from denitrifying activated sludge: Verification and application of a mathematical model. *Water Res* **30**: 521–530.

Schulthess R, Kühni M, Gujer W. (1995). Release of nitric and nitrous oxide from denitrifying activated sludge. *Water Res* **29**: 215–226.

Sharifi S, Murthy S, Takács I, Massoudieh A. (2014). Probabilistic parameter estimation of activated sludge processes using Markov Chain Monte Carlo. *Water Res* **50**: 254–66.

Sin G, Gernaey K V, Neumann MB, van Loosdrecht MCM, Gujer W. (2009). Uncertainty analysis in WWTP model applications: a critical discussion using an example from design. *Water Res* **43**: 2894–906.

Sin G, Van Hulle SWH, De Pauw DJW, van Griensven A, Vanrolleghem P a. (2005). A critical comparison of systematic calibration protocols for activated sludge models: a SWOT analysis. *Water Res* **39**: 2459–74.

Snip LJP, Boiocchi R, Flores-Alsina X, Jeppsson U, Gernaey K V. (2014). Challenges encountered when expanding activated sludge models: a case study based on N2O production. *Water Sci Technol* **70**: 1251–60.

Soler-Jofra A, Stevens B, Hoekstra M, Picioreanu C, Sorokin D, van Loosdrecht MCM, *et al.* (2016). Importance of abiotic hydroxylamine conversion on nitrous oxide emissions during nitritation of reject water. *Chem Eng J* **287**: 720–726.

Sorokin DY, Lücker S, Vejmelkova D, Kostrikina NA, Kleerebezem R, Rijpstra WIC, *et al.* (2012). Nitrification expanded: discovery, physiology and genomics of a nitrite-oxidizing bacterium from the phylum Chloroflexi. *ISME J* **6**: 2245–2256.

Spérandio M, Pocquet M, Guo L, Ni B-J, Vanrolleghem PA, Yuan Z. (2016). Evaluation of different nitrous oxide production models with four continuous long-term wastewater treatment process data series. *Bioprocess Biosyst Eng* **39**: 493–510.

Spott O, Russow R, Stange CF. (2011). Formation of hybrid N2O and hybrid N2 due to codenitrification: First review of a barely considered process of microbially mediated N-nitrosation. *Soil Biol Biochem* **43**: 1995–2011.

Stocker TF, Qin D, Plattner G-K, Tignor M, Allen SK, Boschung J, *et al.* (2013). IPCC Fifth Assessment Report - The physical science basis. Cambridge University Press: Cambridge, United Kingdom and New York, NY, USA.

Strous M, Heijnen J. (1998). The sequencing batch reactor as a powerful tool for the study of slowly growing anaerobic ammonium-oxidizing microorganisms. *Appl Microbiol Biotechnol* **50**: 589–596.

Sun S, Bao Z, Sun D. (2015). Study on emission characteristics and reduction strategy of nitrous oxide during wastewater treatment by different processes. *Environ Sci Pollut Res* **22**: 4222–4229.

Sweetapple C, Fu G, Butler D. (2013). Identifying key sources of uncertainty in the modelling of greenhouse gas emissions from wastewater treatment. *Water Res* **47**: 4652–65.

Tallec G, Garnier J, Billen G, Gousailles M. (2006). Nitrous oxide emissions from secondary activated sludge in nitrifying conditions of urban wastewater treatment plants: effect of oxygenation level. *Water Res* **40**: 2972–80.

Terada A, Lackner S, Kristensen K, Smets BF. (2010). Inoculum effects on community composition and nitritation performance of autotrophic nitrifying biofilm reactors with counter-diffusion geometry. *Environ Microbiol* **12**: 2858–2872.

Terada A, Sugawara S, Hojo K, Takeuchi Y, Riya S, Harper WF, *et al.* (2017). Hybrid Nitrous Oxide Production from a Partial Nitrifying Bioreactor: Hydroxylamine Interactions with Nitrite. *Environ Sci Technol* **51**: 2748–2756.

Terada A, Sugawara S, Yamamoto T, Zhou S, Koba K, Hosomi M. (2013). Physiological characteristics of predominant ammonia-oxidizing bacteria enriched from bioreactors with different influent supply regimes. *Biochem Eng J* **79**: 153–161.

Thomsen JK, Geest T, Cox RP. (1994). Mass spectrometric studies of the effect of pH on the accumulation of intermediates in denitrification by Paracoccus denitrificans. *Appl Environ Microbiol* **60**: 536–541.

Todt D, Dörsch P. (2016). Mechanism leading to N2O production in wastewater treating biofilm systems. *Rev Environ Sci Bio/Technology* **15**: 355–378.

Udert KM, Larsen TA, Gujer W. (2005). Chemical nitrite oxidation in acid solutions as a consequence of microbial ammonium oxidation. *Environ Sci Technol* **39**: 4066–4075.

Upadhyay AK, Hooper AB, Hendrich MP. (2006). NO reductase activity of the tetraheme cytochrome C554 of Nitrosomonas europaea. *J Am Chem Soc*

**128**: 4330–7.

Vajrala N, Martens-Habbena W, Sayavedra-Soto L a, Schauer A, Bottomley PJ, Stahl D a, *et al.* (2013). Hydroxylamine as an intermediate in ammonia oxidation by globally abundant marine archaea. *Proc Natl Acad Sci* **110**: 1006–1011.

Vanrolleghem P, Spanjers H, Petersen B, Ginesteft P, Takacs I. (1999). Estimating (combinations of) Activated Sludge Model No. 1 parameters and components by respirometry. *Water Sci Technol* **39**: 195–214.

Wágner DS, Valverde-Pérez B, Sæbø M, Bregua de la Sotilla M, Van Wagenen J, Smets BF, *et al.* (2016). Towards a consensus-based biokinetic model for green microalgae – The ASM-A. *Water Res* **103**: 485–499.

Wang Q, Ni B-J, Lemaire R, Hao X, Yuan Z. (2016a). Modeling of Nitrous Oxide Production from Nitritation Reactors Treating Real Anaerobic Digestion Liquor. *Sci Rep* **6**: 25336.

Wang X, Yang X, Zhang Z, Ye X, Kao CM, Chen S. (2014). Long-term effect of temperature on N2O emission from the denitrifying activated sludge. *J Biosci Bioeng* **117**: 298–304.

Wang Y, Lin X, Zhou D, Ye L, Han H, Song C. (2016b). Nitric oxide and nitrous oxide emissions from a full-scale activated sludge anaerobic/anoxic/oxic process. *Chem Eng J* **289**: 330–340.

Wild D, Schulthess R Von, Gujer W. (1994). Synthesis of denitrification enzymes in activated sludge: Modelling with structured biomass. *Water Sci Technol* **30**: 113–122.

Wunderlin P, Mohn J, Joss A, Emmenegger L, Siegrist H. (2012). Mechanisms of N2O production in biological wastewater treatment under nitrifying and denitrifying conditions. *Water Res* **46**: 1027–37.

Yan P, Qin R, Guo J, Yu Q, Li Z, Chen Y, *et al.* (2017). Net-Zero-Energy Model for Sustainable Wastewater Treatment. *Environ Sci Technol* **51**: 1017–1023.

Yang Q, Liu X, Peng C, Wang S, Sun H, Peng Y. (2009). N 2 O Production during Nitrogen Removal via Nitrite from Domestic Wastewater: Main Sources and Control Method. *Environ Sci Technol* **43**: 9400–9406.

Ye L, Ni B-J, Law Y, Byers C, Yuan Z. (2014). A novel methodology to quantify nitrous oxide emissions from full-scale wastewater treatment systems with surface aerators. *Water Res* **48**: 257–68.

Yu R, Chandran K. (2010). Strategies of Nitrosomonas europaea 19718 to counter low dissolved oxygen and high nitrite concentrations. *BMC Microbiol* **10**: 70.

Yu R, Kampschreur MJ, van Loosdrecht MCM, Chandran K. (2010). Mechanisms and specific directionality of autotrophic nitrous oxide and nitric oxide generation during transient anoxia. *Environ Sci Technol* **44**: 1313–9.

Zhang L, Narita Y, Gao L, Ali M, Oshiki M, Okabe S. (2017). Maximum specific growth rate of anammox bacteria revisited. *Water Res* **116**: 296–303.

Zheng J, Doskey P V. (2015). Modeling nitrous oxide production and reduction in soil through explicit representation of denitrification enzyme kinetics. *Environ Sci Technol* **49**: 2132–9.

Zhu-Barker X, Cavazos AR, Ostrom NE, Horwath WR, Glass JB. (2015). The importance of abiotic reactions for nitrous oxide production. *Biogeochemistry* **126**: 251–267.

Zhu X, Burger M, Doane TA, Horwath WR. (2013). Ammonia oxidation pathways and nitrifier denitrification are significant sources of N2O and NO under low oxygen availability. *Proc Natl Acad Sci* **110**: 6328–6333.

# 9 Papers

**I** **Domingo-Félez, C.**, Pellicer-Nàcher, C., Petersen, M. S., Jensen, M. M., Plósz, B. G., Smets, B.F. 2017. Heterotrophs are key contributors to nitrous oxide production in activated sludge under low C-to-N ratios during nitrification – Batch experiments and modeling. *Biotechnology and Bioengineering*, **114**, 132-140.

**II** **Domingo-Félez, C.**, Smets, B.F. 2016. A consilience model to describe N2O production during biological N removal. *Environmental Science: Water Research and Technology*, **6**, 923-930.

**III** **Domingo-Félez, C.**, Calderó-Pascual, M., Sin, G., Plósz, B. G., Smets, B.F. 2017. Calibration of the comprehensive NDHA-N2O dynamics model for nitrifier-enriched biomass using targeted respirometric assays. *Submitted*

**IV** **Domingo-Félez, C.**, Smets, B.F. 2017. Application of the NDHA model to describe N2O dynamics in activated sludge mixed culture biomass. *Manuscript in preparation*.

**V** **Domingo-Félez, C.**, Smets, B.F. 2017. Modelling electron competition in a mixed denitrifying microbial community with different carbon sources through an electric circuit analogy. *Manuscript in preparation*.